AN ABSTRACT OF THE THESIS OF

MICHAEL HIRAKAMI for the M. S. (Degree) in Electrical and Electronics Engineering

Date thesis is presented Augn. 29, 1966

Title ALTERNATING CURRENT AND VOLTAGE PROFILES ON COMPENSATED HIGH-VOLTAGE UNDERGROUND POWER CABLES

Abstract approved Redacted for Privacy
(Major professor)

The utilization of extra-high-voltage underground power cables over distances greater than 100 miles presents serious problems relative to the voltage and current limits of such cables. These problems are directly associated with the fixed amount of capacitance inherent in long cable lines. As a result, large charging currents are characteristic with long cable line operation when energized under steady-state conditions.

A possible means of handling this problem is realized in the use of shunt inductive reactors as charging-current compensating elements. These reactors have a definite effect on the voltage and current magnitudes depending upon the mode of compensation. Without compensation, maximum voltage and current magnitudes well exceed the cable limits of voltage and current. With compensation,

these maximum amplitudes are reduced in magnitude depending upon the number and degree of compensating units. This thesis presents a quantitative evaluation of the voltage and current profiles of long cable lines with various modes of compensation.

ALTERNATING CURRENT AND VOLTAGE PROFILES ON COMPENSATED HIGH-VOLTAGE UNDERGROUND POWER CABLES

by

MICHAEL HIRAKAMI

A THESIS

submitted to

OREGON STATE UNIVERSITY

in partial fulfillment of
the requirements for the
degree of

MASTER OF SCIENCE

June 1967

APPROVED:

Redacted for Privacy

Associate Professor of Electrical and Electronics Engineering
In Charge of Major

Redacted for Privacy

Head of Department of Electrical and Electronics Engineering

Redacted for Privacy

Dean of Graduate School

Date thesis is presented August 29, 1966

Typed by Donna Olson

ACKNOWLEDGEMENT

The author wishes to express his gratitude to Professor J. F. Engle for his suggestions, guidance, and assistance in the preparation of this thesis.

He would also like to thank Professor G. C. Alexander for the use of several computer programs for plotting the data presented in this thesis.

Appreciation is also given to Mr. L. O. Barthold in the Electric Utility Engineering Department of the General Electric Company for his helpful suggestions and assistance in data verification and literary research.

TABLE OF CONTENTS

LIST OF FIGURES

LIST OF TABLES

ALTERNATING CURRENT AND VOLTAGE PROFILES ON COMPENSATED HIGH-VOLTAGE UNDERGROUND POWER CABLES

I. INTRODUCTION

With the advent of new high-voltage cable technology, an entirely new field in power transmission has emerged as a possible means of coping with today's increasing demand for transporting larger blocks of power. Present trends toward higher system voltages, larger generating capacity, and greater transmission distances all dictate a need for more advanced research on extra-high-voltage (EHV) underground cable systems as a possible option that electric utilities may utilize. This move toward such an option has been initiated by the vanishing availability of rights-of-way as well as the rapidly expanding suburban areas.

A significant problem confronting the system planning engineer is the limitation imposed by the capacitance of long cable lines upon their power transmission capabilities. This fixed amount of capacitance inherent in these cables gives rise to large charging currents which exceed the maximum allowable current-carrying capacity of high-voltage cables under most operating conditions. However, a possible solution to this problem may exist in the use of shunt inductive reactors as charging-current compensating elements on long EHV underground cables. Thus, this thesis will concern itself with

the fundamental aspects of voltage and current on long compensated cable lines under steady-state operation. Graphs and tabulations obtained from the computer results of the power cable simulation outline the basic analysis to follow.

II. SYSTEM DESCRIPTION

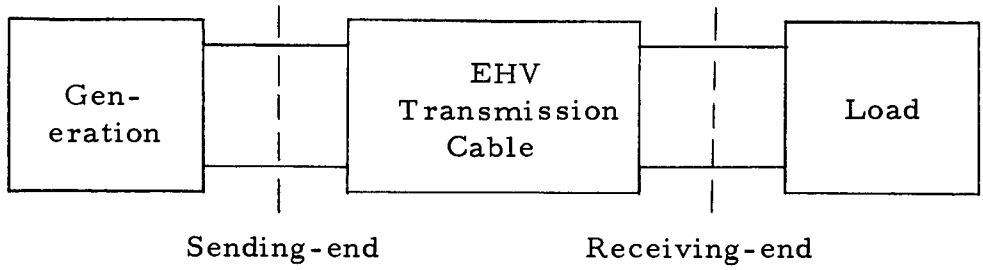

Figure 1. Block diagram of EHV transmission cable system.

The general cable system is shown in Figure 1. This system represents one of a number of possible interconnecting links between a generating station and a system substation as a means of transporting large blocks of power over long distances. The system assumes no load tapping at any point between the sending end and the receiving end. This analysis will pertain to the transmission cable and its characteristics.

Basic Line Length

For purposes of analysis only, a basic system line length of 120 miles was chosen because of its various numerical factors. This greatly faciliated the locations of compensating units at equal increments along the line. This particular length of line may disagree in some respects with the system engineer's definition of the term "long" cable lines. However, this represents a substantial

transmission distance, which has had only a limited amount of attention, and is within those lengths of high-voltage aerial lines now in operation.

Modes of Compensation

In investigating the effects of shunt inductive reactors, there are several variables which may lead to numerous solutions. Among these variables are the amount (percentage) of compensation and the number of compensating units. Investigation of each and every one of these variables over a wide range would be impractical in this thesis. Only those cases used in specific examples will be analyzed.

The term "full compensation" or "100% compensation" will designate the arrangement in which the total line capacitive reactance is exactly equal to the shunt compensating inductive reactance (see Appendix IV). Under-compensation will correspond to less shunt compensating inductive reactance than total line capacitive reactance. These will be designated on the basis of percentages such as 75% and 50% compensation. All uncompensated portions of the charging current must be absorbed at either or both ends of the cable line.

Location of compensating units will be placed at equal intervals along the cable line. These units will be symmetrically located primarily to account for power transfer in either direction. No compensating unit will be placed at either the receiving or the sending end.

Bypassing economic consideration, the number of compensating units will vary from no units to a possible five units at 20 mile increments. Additional units may be considered on longer lines if the critical length (1, 2, 4) of the line is less than the compensating increment spacing. The various circuit arrangements have been outlined in Figure 2 for a base length of 120 miles.

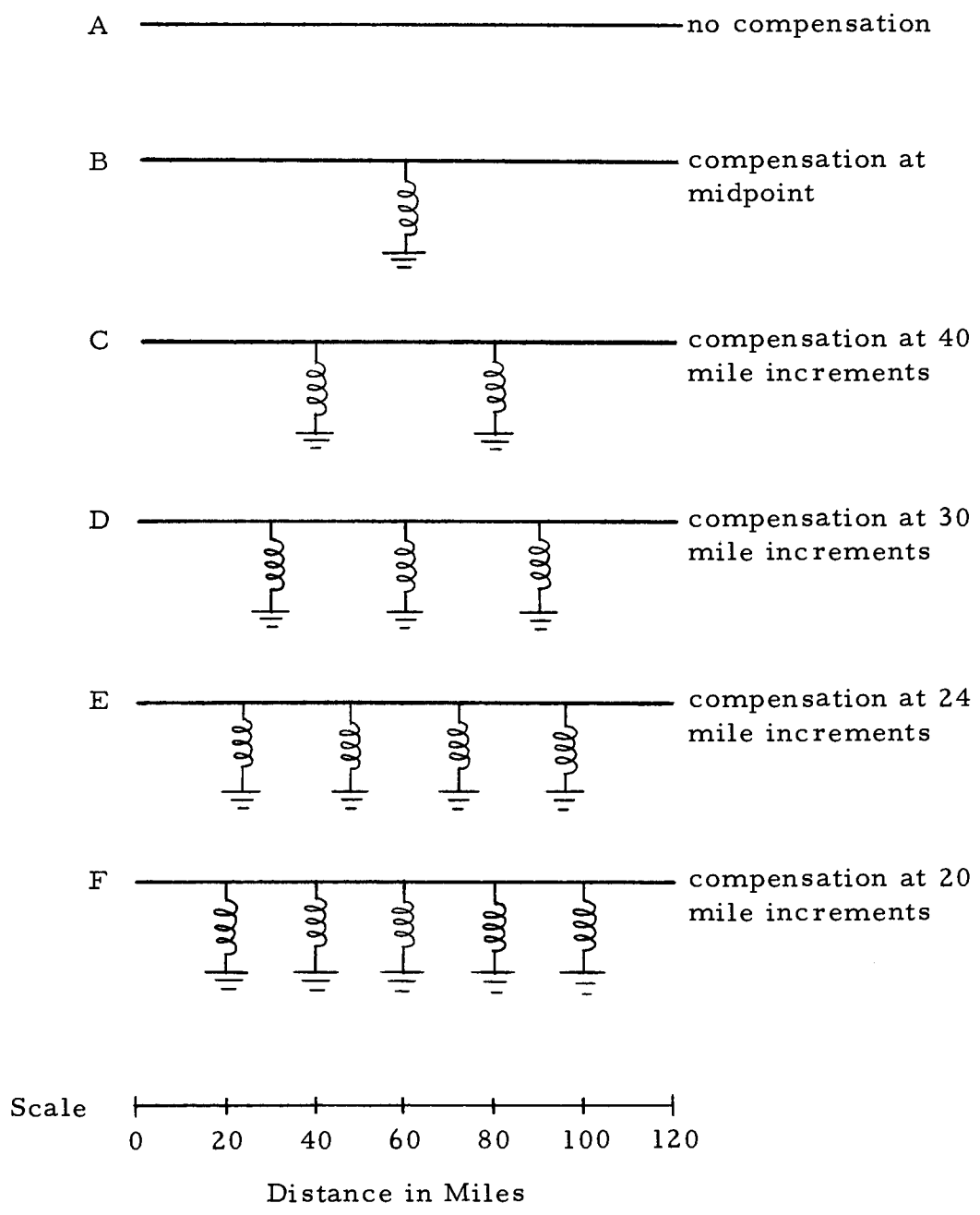

Figure 2. Circuit arrangements of compensating reactors.

III. METHOD OF ANALYSIS

The basic characteristics of a cable line longer than 100 miles may be expected to cause a rise in voltage at the receiving end above that at the sending end when the cable is energized under most loading conditions. This rise in voltage may be of such a magnitude as to exceed the maximum voltage limit of the cable at any point or section along the line. It is hoped that with shunt inductive compensation the tendency of the voltage magnitude to rise along the cable will be suppressed.

The intent of this thesis will be to illustrate and discuss the voltage and current profiles of long underground power cables, both compensated and uncompensated. The data for these profiles were obtained from a computer program using the IBM 1620 digital computer. Simulation of the cable was done by generalized circuit constants discussed in Appendix II for two-mile section lengths. The method of calculation using 12 significant digits by the computer program is listed in Appendix V.

Table I illustrates the greater degree of accuracy obtained by using 12 significant digits in numerical calculations performed by the computer. The usual eight digit accuracy resulted in an error in the sixth significant digit, whereas identical voltage magnitudes were calculated with 12 significant digits for various section lengths. Truncation error is the cause of the discrepancy between the two

modes of accuracy.

Table I. Effect on increased word length on calculation accuracy

Number of Sections	Miles Represented by Each Section	Pu Receiving-end Voltage with 1.0 Pu Load, Unity Power Factor	
		Eight-Digit Word Length	Twelve-Digit Word Length
1	120	1.2412271	1.2412402366
2	60	1.2412274	1.2412402366
3	40	1.2412272	1.2412402366
60	2	1.2412311	1.2412402366
120	1	1.2412290	1.2412402366

The process of cable simulation using two-mile section lengths was accomplished by matrix multiplication. The ABCD constants for 60 two-mile sections in series were successively combined to obtain the total ABCD constants. Verification of this method has been analytically proved in Appendix II.

The voltage and current profiles have been calculated on a per-unit (pu) basis. Calculations are founded on general equations for voltage and current of two-terminal-pair networks as explained in Appendix I. The power factor (pf) of the load has been assumed to be unity for all cases. Full load is equivalent to one pu receiving-end power. Input variables include the percentage and number of

compensations as well as the pu load power. The following three-phase base values have been adopted for this analysis.

Base power = 400 megavolt-amperes (mva)

Base voltage = 230 kilovolts (kv)

Figures of voltage and current profiles have been plotted from the sending to the receiving end. Hence, 120 miles indicates the receiving end of the cable while zero miles indicates the sending end. Quantitative analysis of these figures will always proceed from the receiving end to the sending end unless indicated otherwise. Wherever applicable, the vertical axis has been offset from zero by the amount indicated on each figure.

IV. DISCUSSION OF PROFILES

Cable voltage and current profiles have been drawn using the IBM 1627-II Plotter. Total variations of voltage and current magnitudes for the no-load and full-load cases have been drawn on the basis of two per figure as shown in Figures 4 and 5. Individual profiles have been drawn on separate figures with suppressed zeroes where discussion justifies an enlargement of the vertical scale size. Two-mile sections have been used in all cases as the calculating increment in obtaining the voltage and current profiles. The cable line used in the analysis is described in Appendix III.

Uncompensated Cable Line

For the uncompensated line, the absolute voltage magnitude exhibits a non-linear rise as a function of the distance along the cable. This effect is illustrated in Figure 6 and is primarily attributed to the large shunt capacitive reactances distributed along the line.

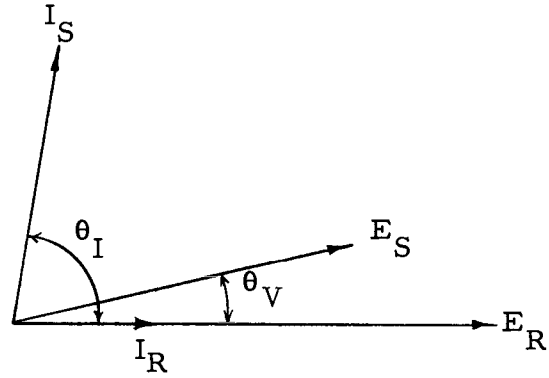

Figure 3. Phasor diagram of receiving-end and sending-end voltage and current for uncompensated cable line.

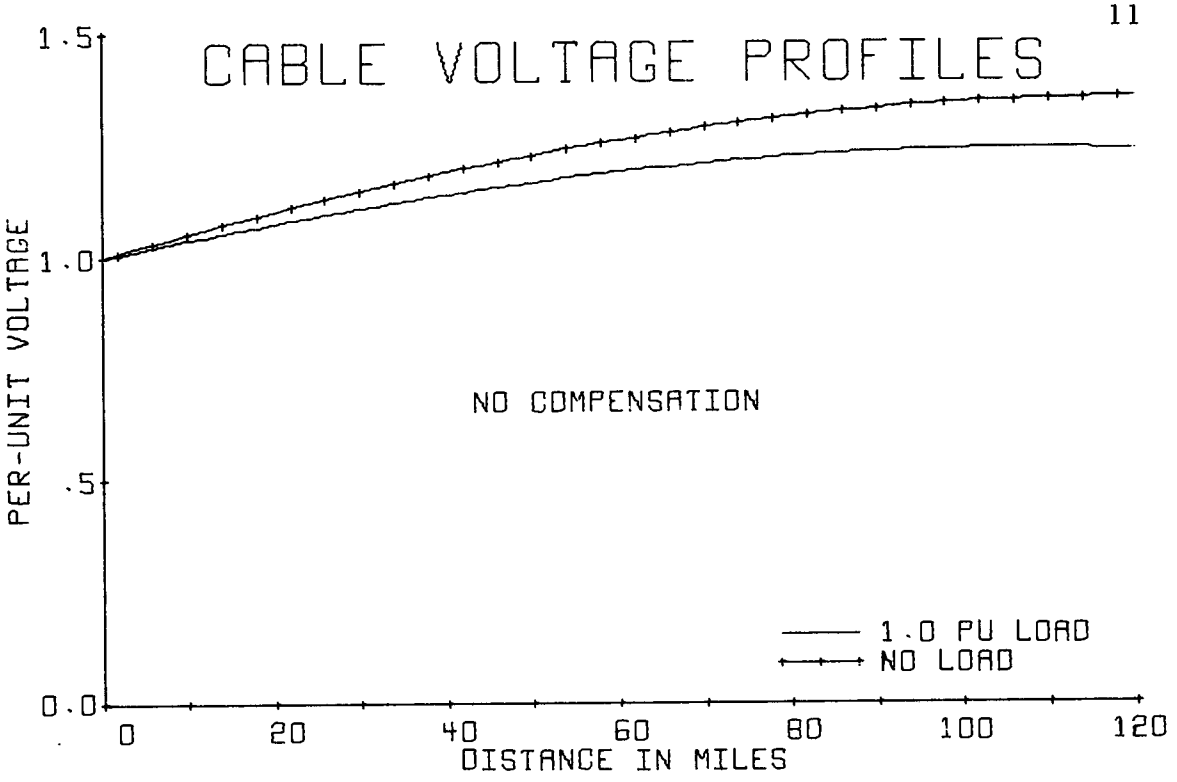

FIGURE 4. PER-UNIT VOLTAGE MAGNITUDES VERSUS DISTANCE FROM THE CABLE SENDING END FOR A UNITY PF LOAD.

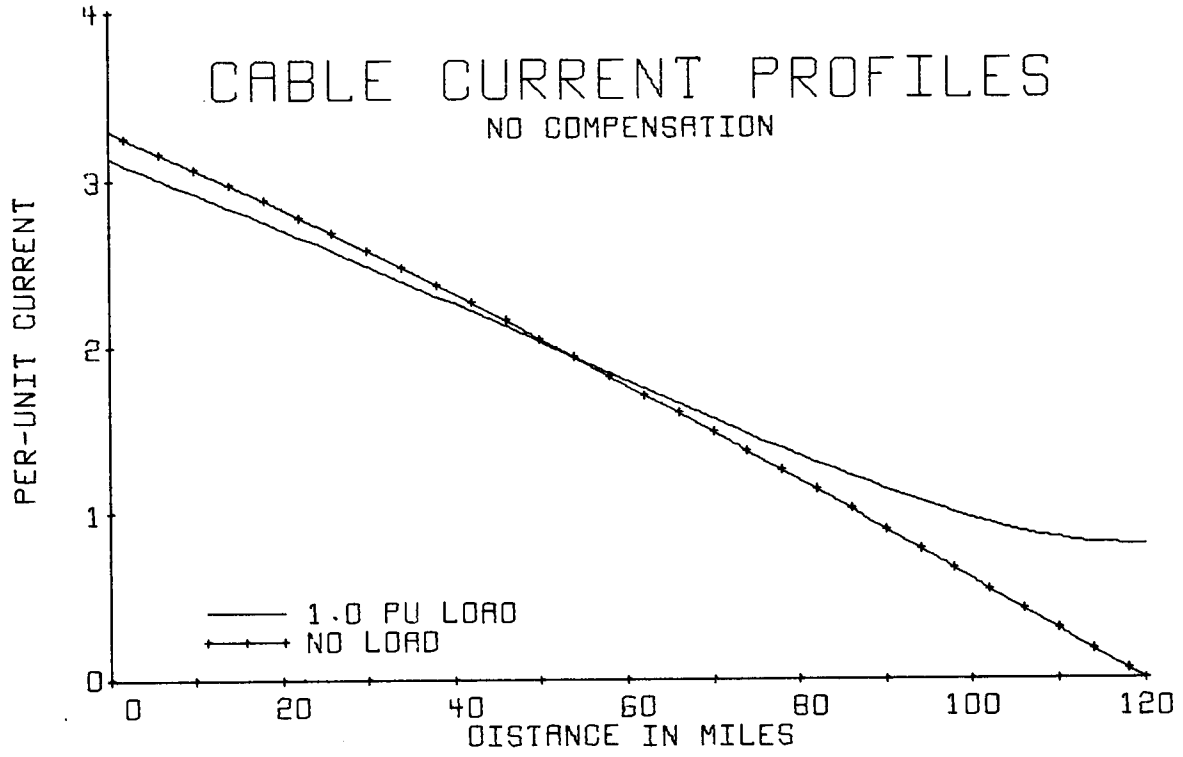

FIGURE 5. PER-UNIT CURRENT MAGNITUDES VERSUS DISTANCE FROM THE CABLE SENDING END FOR A UNITY PF LOAD.

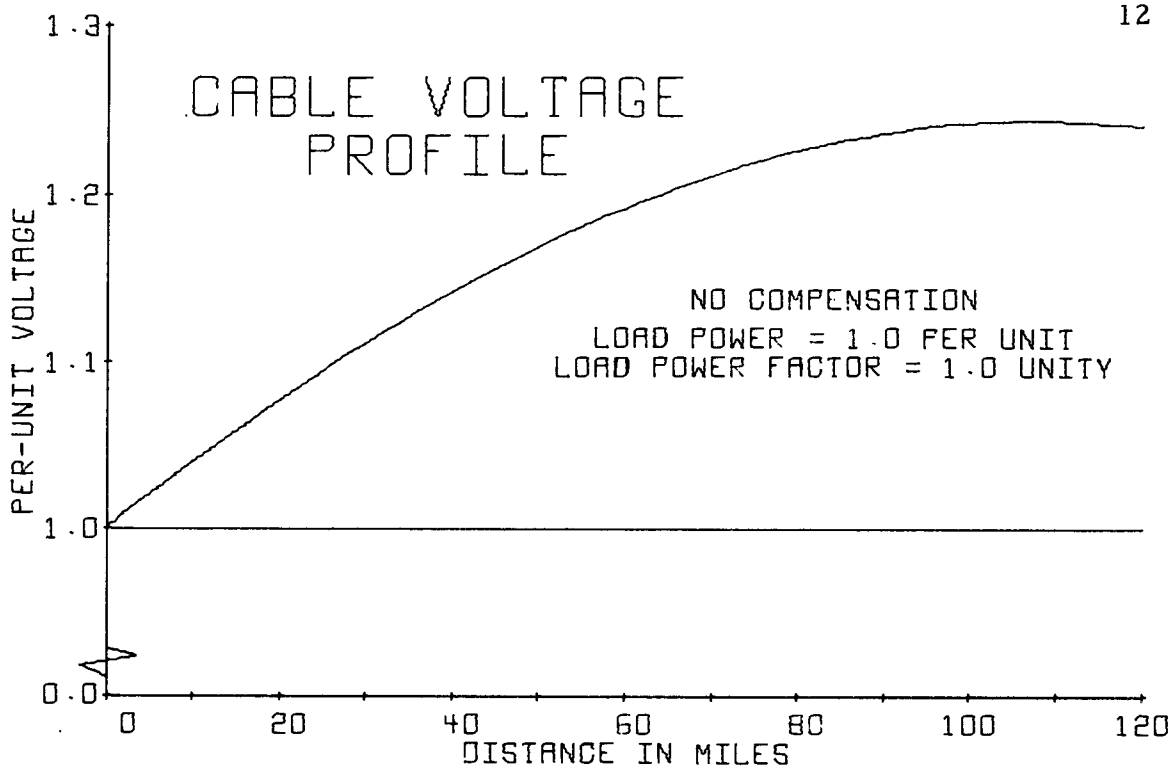

FIGURE 6. PER-UNIT VOLTAGE MAGNITUDE VERSUS DISTANCE FROM THE CABLE SENDING END.

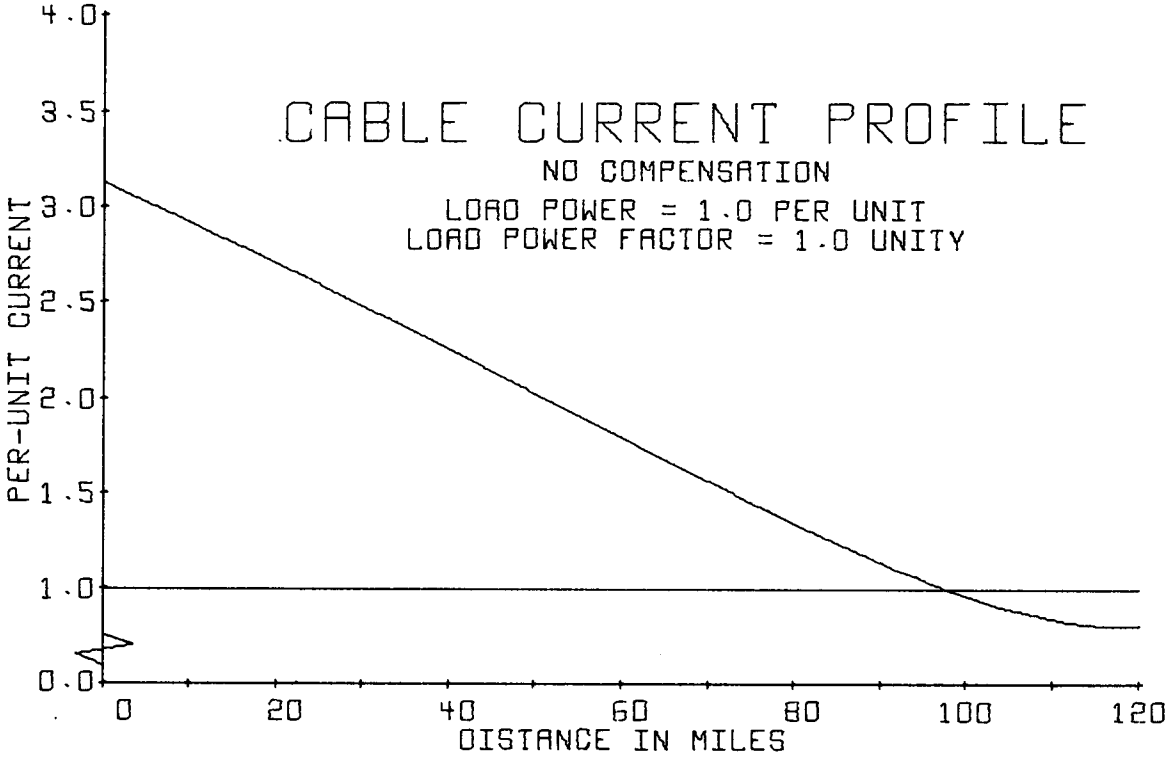

FIGURE 7. PER-UNIT CURRENT MAGNITUDE VERSUS DISTANCE FROM THE CABLE SENDING END.

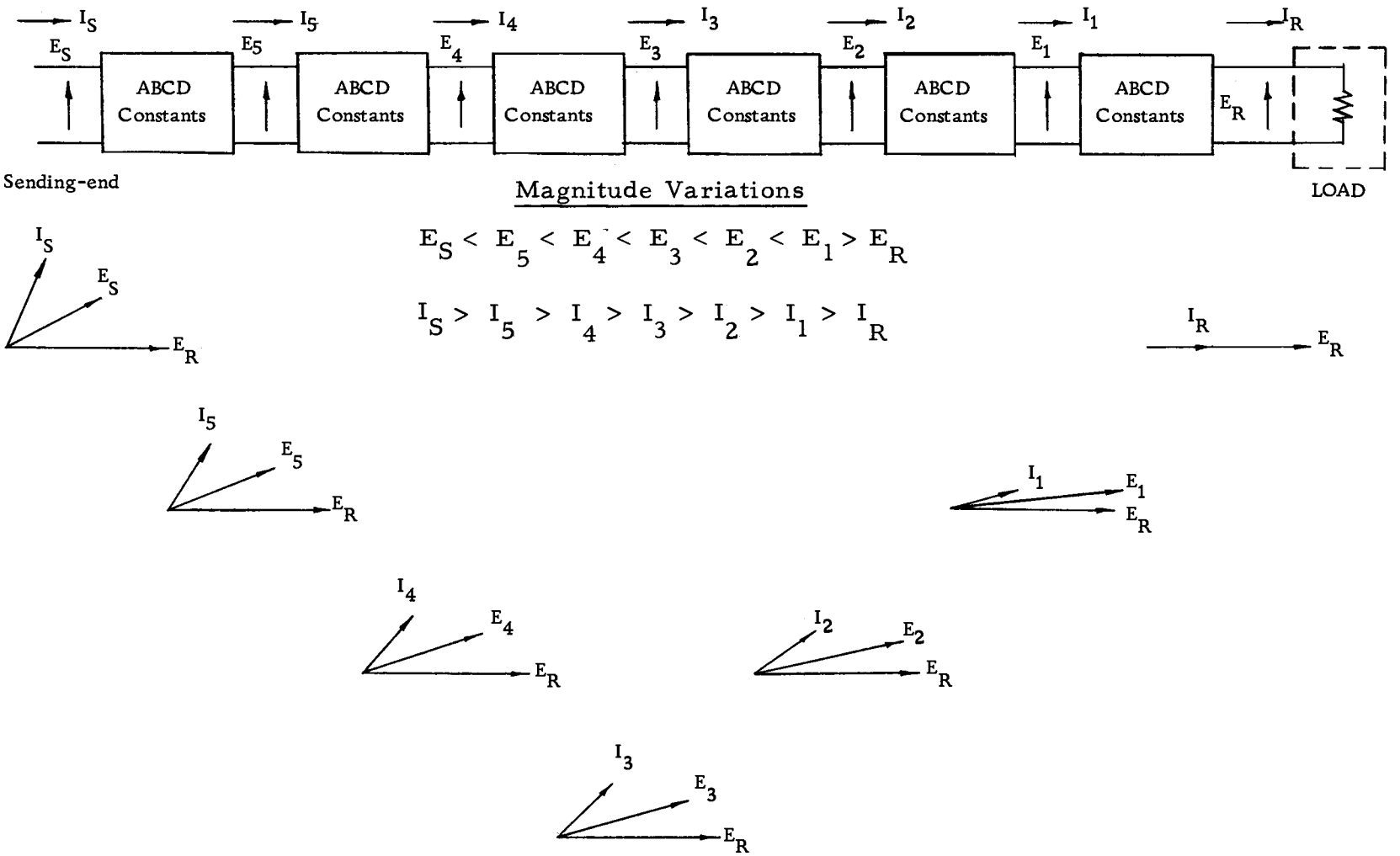

Figure 8. Equivalent circuit and phasor diagram representation of an uncompensated cable model.

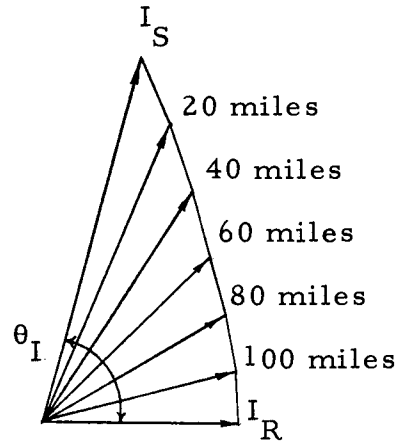

Figure 9. Phasor diagram describing the loci of the phasor current at 20 mile increments on the uncompensated cable line.

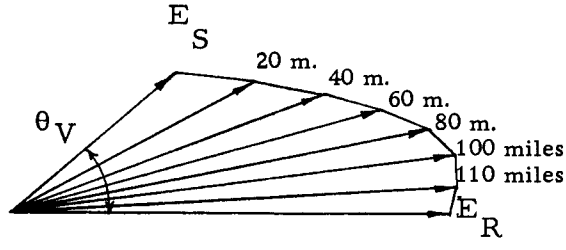

Figure 10. Phasor diagram describing the loci of the phasor voltage at various increments on the uncompensated cable line.

Meticulous inspection of the voltage profile indicates a maximum peak voltage prior to the receiving-end termination of the cable line under full load operation. This is followed by a slight decrease in magnitude at the receiving-end termination. Initially, this seems contrary to normal expectations. However, a more thorough investigation will show this phenomenon to be related to the effect

produced by the cable charging current distributed along the line.

With a unity load power factor, the receiving-end phasor current, I_R, is in phase with the receiving-end phasor voltage, E_R, as shown in Figure 3. Using these phasor quantities, a step-by-step quantitative analysis can be used to determine the voltage and current at the sending end as discussed in Appendix I. As the process of determining the voltage and current along the line progresses from the receiving end to the sending end, the magnitude of the phasor current increases due to an increase in charging current. Correspondingly, the equivalent series voltage drop associated with each section of the line increases although the equivalent series impedance Z of each section remains the same.

Figure 8 illustrates these variations in phasor voltage and phasor current at each section along the model of the cable line. With a small phase angle associated with I_1, the line voltage E_1 is greater than E_R. Consideration of the next section results in an increase in line current I_2 both in phase angle and in magnitude. With a larger leading current phase angle, the resulting line voltage E_2 is less than E_1. Thus, E_1 becomes the maximum peak voltage on the cable line. Once this peak is reached, the voltage at each point on the line decreases when working towards the sending end since the line current leads the voltage at every point on the line.

The relative angle shown in Figure 11 between the line current

and voltage at each section is small at first but becomes increasingly larger when working towards the sending end. As shown in Figures 9 and 10, the phase angle associated with the phasor current increases at a greater rate than the phase angle of the phasor voltage. It is this change in relative angle that determines or controls the magnitude of the voltage and current along the line.

θ = relative phase angle

I' = phasor current for one section

E' = phasor voltage for one section

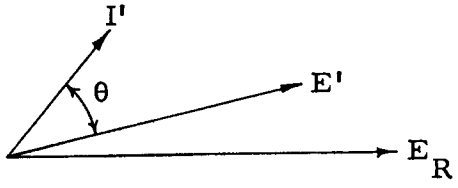

Figure 11. Phasor diagram describing the relative angle at a typical section on the uncompensated cable line.

Open-Circuit Termination

With an open-circuit (no-load) termination on an uncompensated line, no maximum peak voltage is present prior to the receiving-end terminals as shown in Figure 12. This is due to the fact that no current exists at the receiving-end terminals. The current profile in Figure 13 exhibits a nearly linear change in amplitude. Considering the approximated circuit shown in Figure 32 with $I_R = 0$ and for a short section length at the cable receiving end, the phase shift in

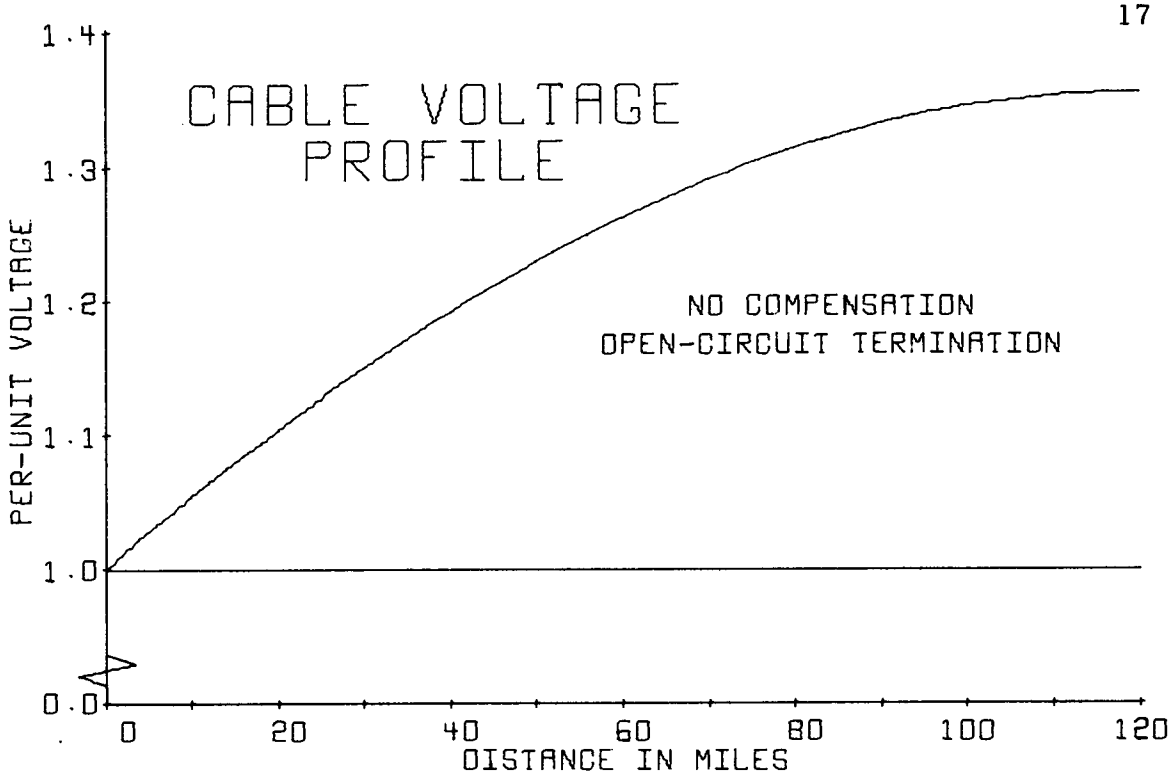

FIGURE 12. PER-UNIT VOLTAGE MAGNITUDE VERSUS DISTANCE FROM THE CABLE SENDING END.

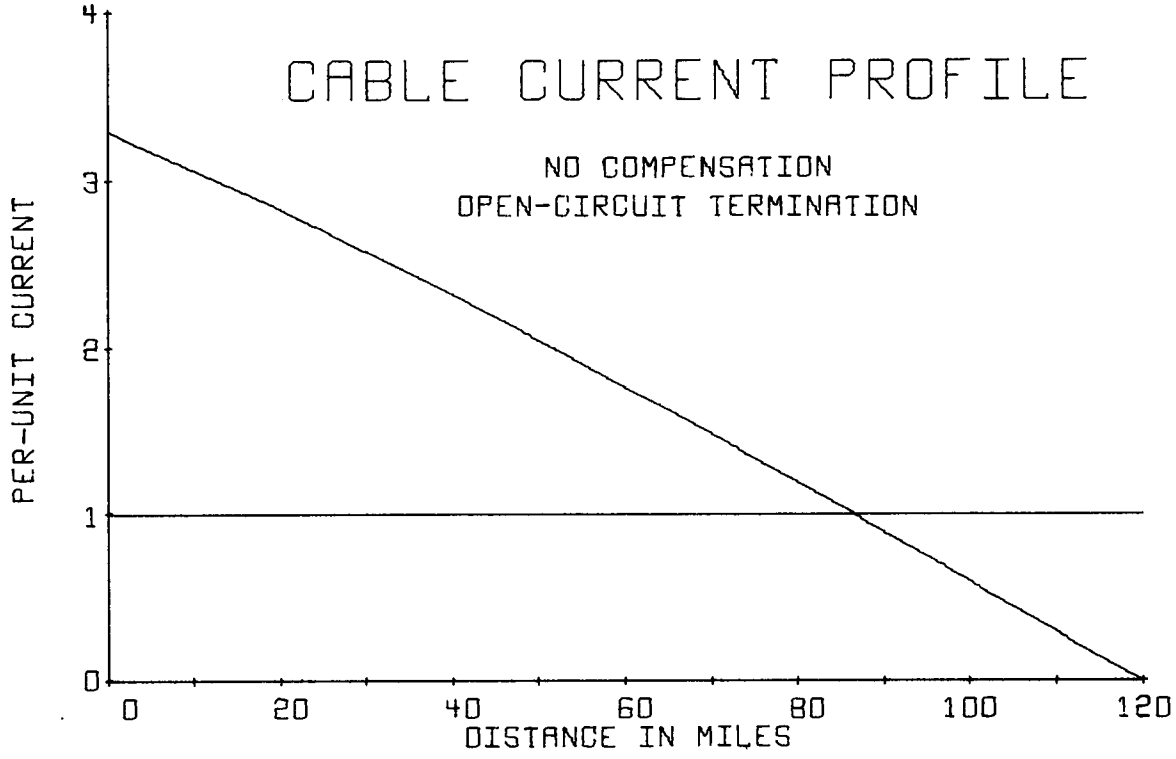

FIGURE 13. PER-UNIT CURRENT MAGNITUDE VERSUS DISTANCE FROM THE CABLE SENDING END.

voltage across Z is small. Therefore, I_S, the sending-end current, is almost in phase with I for that section. Since the cable line can be approximated by a series of these sections, a similar phase shift in voltage for each section across the series impedance would occur. The voltage drop increases for each of these sections when working towards the sending end. The resulting change in slope of the current magnitude decreases slightly.

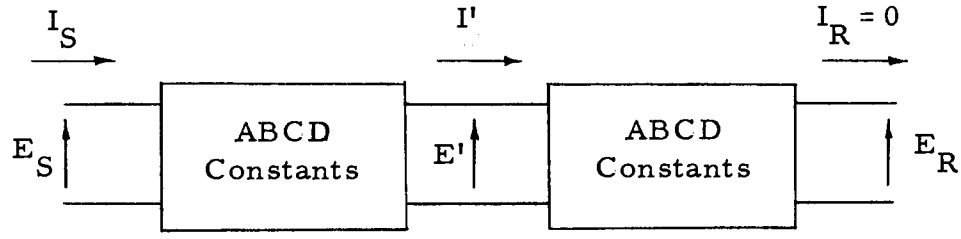

Figure 14a. Equivalent representation for an open-circuit uncompensated cable line with ABCD constants.

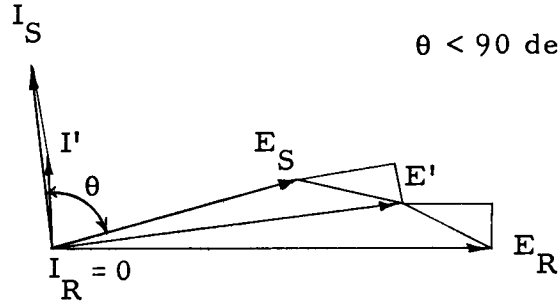

Figure 14b. Phasor diagram for an open-circuit uncompensated cable line.

Analytical results have indicated that a negative real current is obtained at the sending end. Initially, this would seem to imply that power is flowing out of the cable sending-end terminals. With successive additions of charging currents, the resulting line current at the input is located in the second quadrant when E_R is used as reference. However, the relative angle between the sending-end voltage and sending-end current is less than 90 degrees as shown in Figure 14b. Thus, no power actually flows out of the sending-end terminals.

The analytical results for the uncompensated cable line substantiate the voltage rise phenomenon characteristic of underground power cables. Due to the inherent shunt capacitance, neither the full-load nor the no-load case of cable line operation is possible within the limitation of specified cable operating conditions.[1] Overvoltages of as much as 36% above the base voltage for the open-circuit case and 25% for the full-load case have been calculated for the uncompensated cable line under normal, steady-stage, operating conditions. Currents in excess of 200% of the rated current have also been calculated for the line. Most of these currents are reactive currents with the ratio of the magnitude of reactive current to real current being 30 to 5 for the full-load case and 33 to 1 for the open-circuit case.

---

[1] See footnote, Table III, p. 39.

Compensated Cable Line

With compensation present in the transmission system, the concept of relative angles becomes important when considering the voltage and current characteristics on the cable line. Numerous configurations of compensating networks are possible. However, only those circuit arrangements shown in Figure 2 will be analyzed. Voltage and current profiles combining the no-load and full-load cases with various degrees of compensation are shown in Appendix VI as well as in Figures 15 and 16.

Single-Compensation Cable Line

Figures 17 and 18 illustrate the full-load voltage and current profiles, respectively, for 100% compensation using arrangement B shown in Figure 2. A load power of one pu corresponds to the load power of arrangement A discussed previously for the uncompensated cable line. Hence, comparisons can be made between these two circuit arrangements.

The voltage profile in Figure 17 exhibits a different profile as compared to the uncompensated case in Figure 6. Unlike the previous case, no distinct voltage rise appears at any point along the line. Also, the sending-end voltage is much greater than the receiving-end voltage. A change in slope in the voltage profile occurring

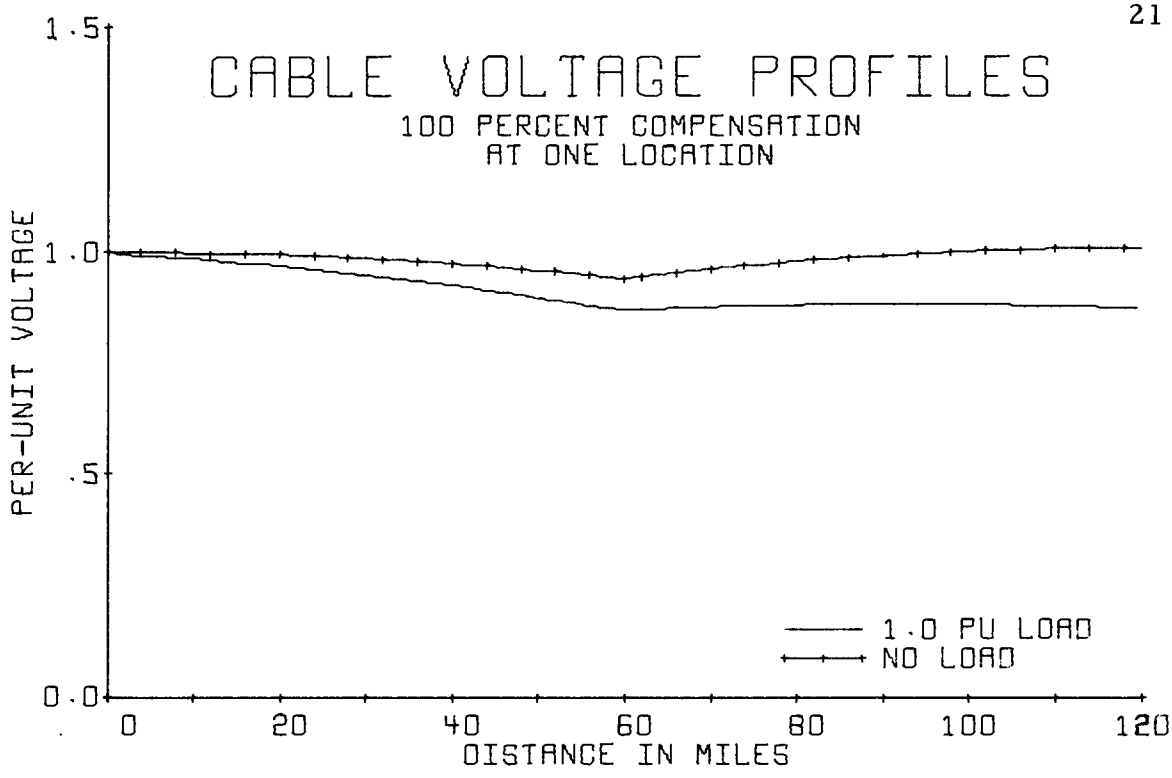

FIGURE 15. PER-UNIT VOLTAGE MAGNITUDES VERSUS DISTANCE FROM THE CABLE SENDING END FOR A UNITY PF LOAD.

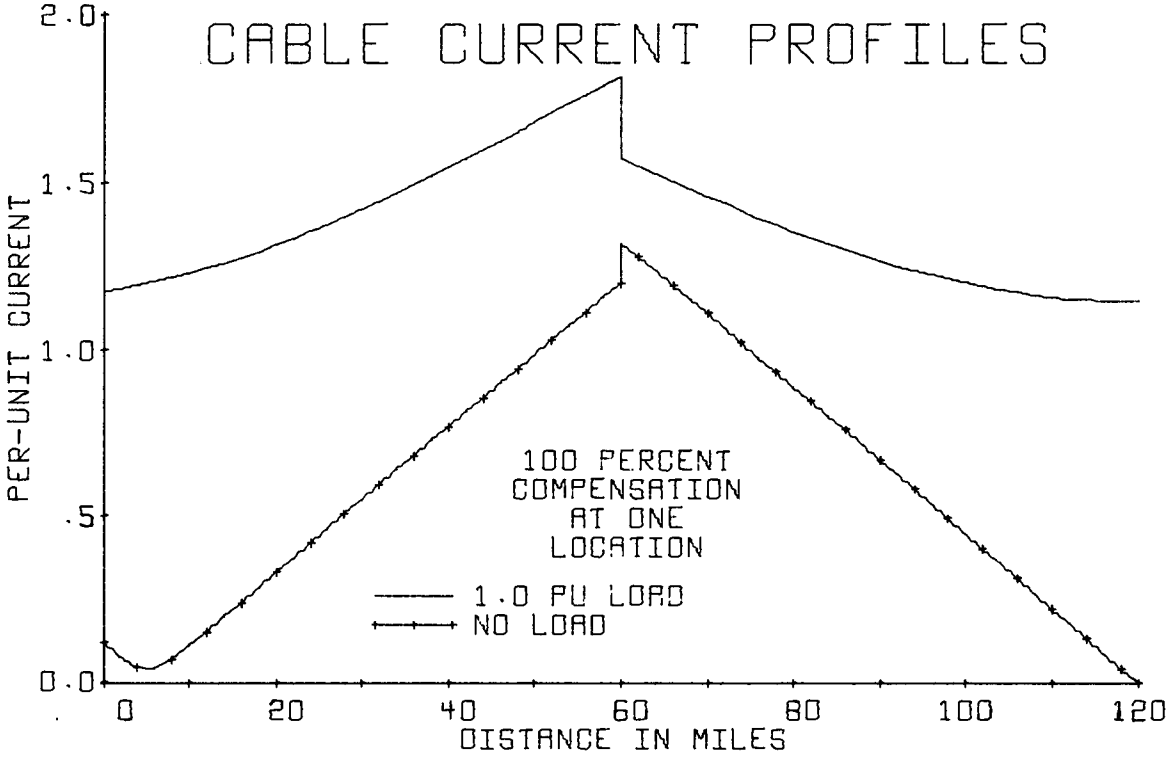

FIGURE 16. PER-UNIT CURRENT MAGNITUDES VERSUS DISTANCE FROM THE CABLE SENDING END FOR A UNITY PF LOAD.

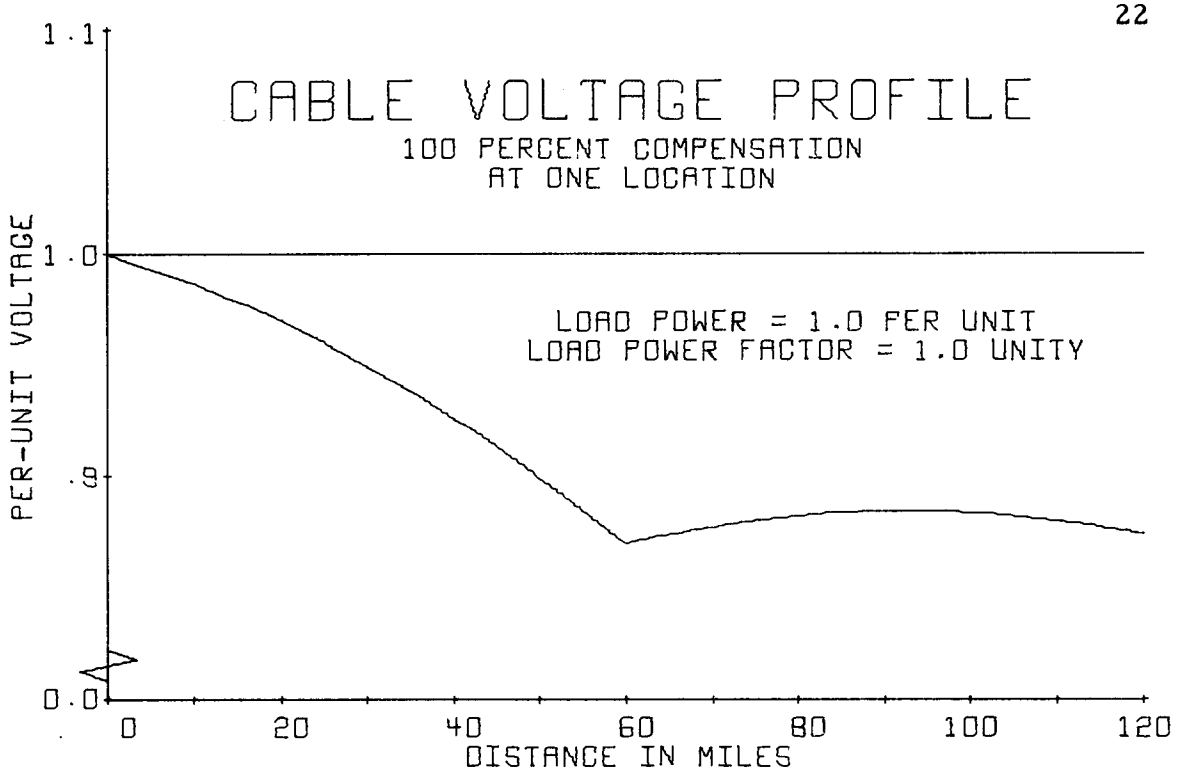

FIGURE 17. PER-UNIT VOLTAGE MAGNITUDE VERSUS DISTANCE FROM THE CABLE SENDING END.

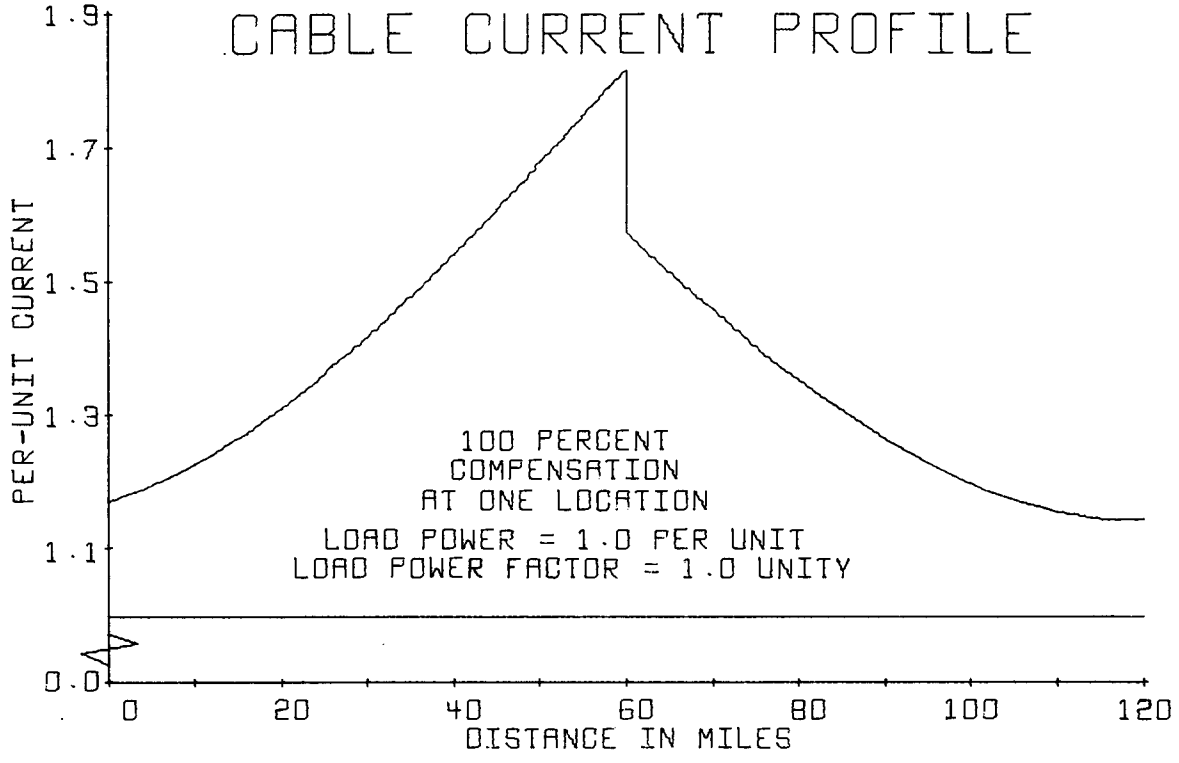

FIGURE 18. PER-UNIT CURRENT MAGNITUDE VERSUS DISTANCE FROM THE CABLE SENDING END.

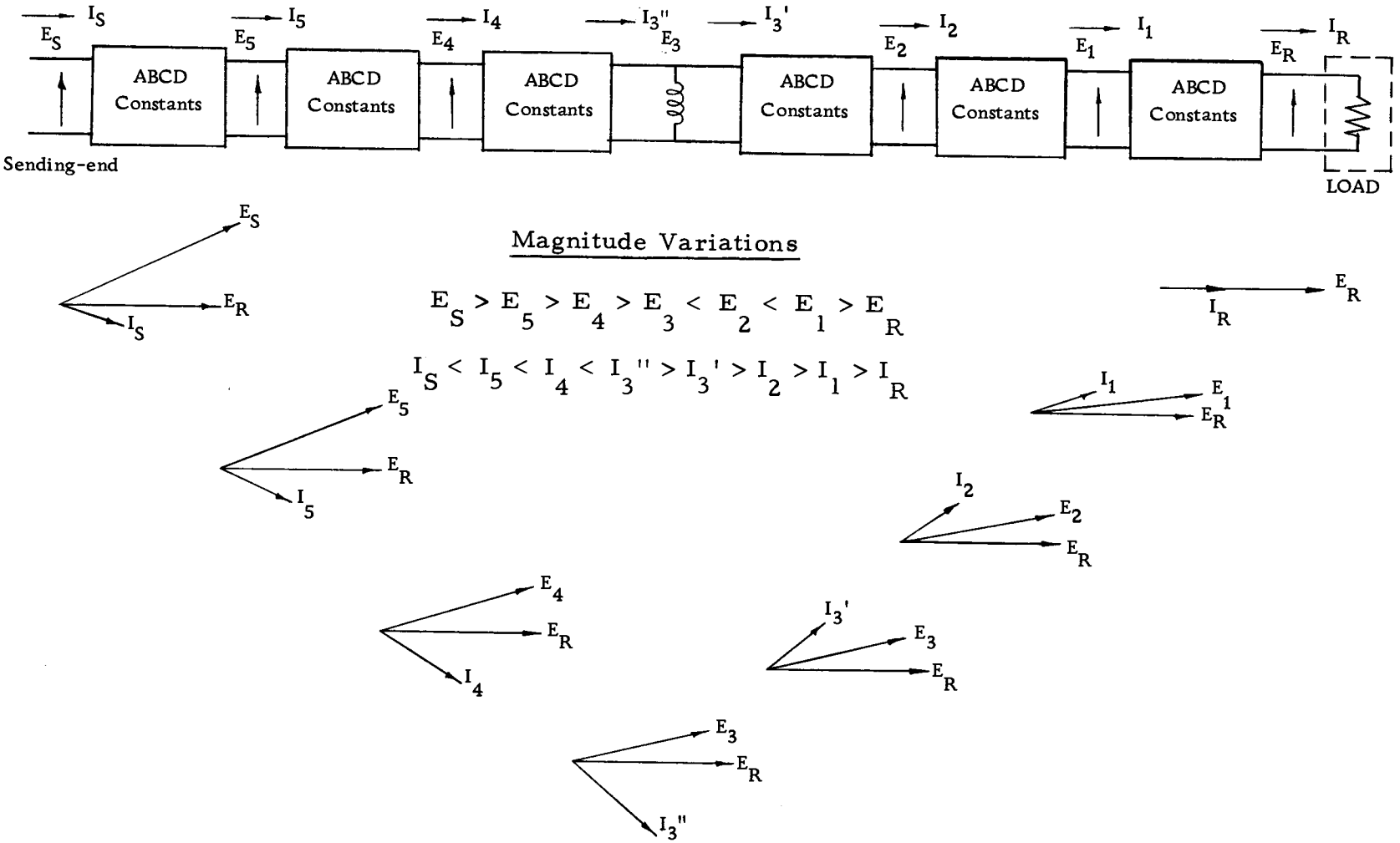

Figure 19. Equivalent circuit and phasor diagram representation of 100% compensated cable model.

at a distance of 60 miles is the most noticeable difference. This change in slope is the result of a lumped shunt inductive impedance located at 60 miles. Its effect on the cable line is not like the distributed shunt capacitance inherent in the cable. Because of the nature of this compensating network, the location of the reactor does not limit the amount of vars contributed by the lumped impedance; since distribution of vars can occur in either direction from the reactor as shown in Figure 20.

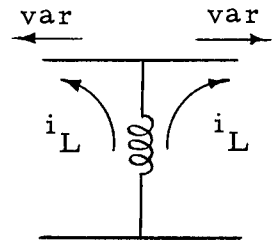

Figure 20. Var flow from shunt reactor.

A slight similarity in voltage profile between Figure 6 and Figure 17 exists on the cable line from 60 to 120 miles. Within this distance, the shape of the voltage profile in Figure 17 is analogous to that in Figure 6. Both curves show a peak voltage prior to the receiving-end terminal. However, because of the difference in terminal conditions, the voltage peak in Figure 17 occurs at 94 miles while it occurs at 108 miles in Figure 6. The cause of this peak in voltage is the same for both cases and is attributed to the

change in relative angle between the phasor voltage and current at each point along the line.

The compensating reactor causes a decrease in the receiving-end voltage below that of the sending-end voltage, as shown by the series of phasor diagrams in Figure 19. Figure 21 summarizes the results of Figure 19 for 100% compensation located at the middle of the cable line. The cable line as viewed at the sending end appears to be inductive in nature for the amount of compensation used.

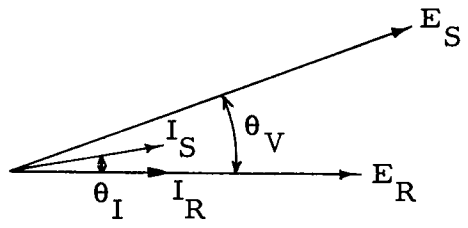

θ_V = 15 degrees

θ_I = 5.5 degrees

Figure 21. Phasor diagram of a 100% compensated cable line compensated at one location.

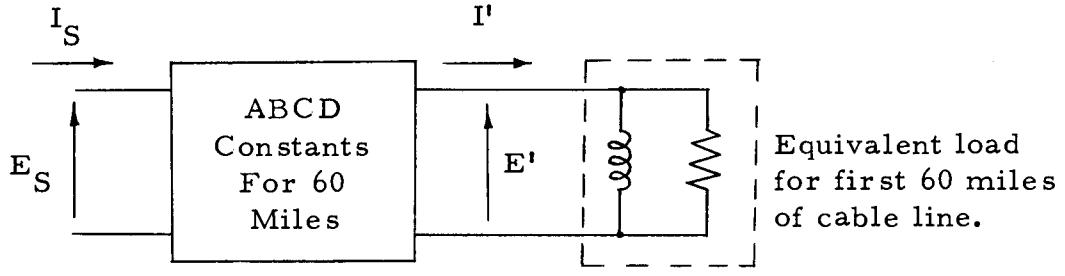

Figure 22. Equivalent representation of compensated cable line with the last 60 miles of cable line simulated by a lagging load.

At the point of compensation, a large inductive current i_L will add to the leading line current I_3' resulting in a lagging line current I_3'' as shown in the phasor diagrams of Figure 19. Depending upon the magnitude of this inductive current, an effective lagging load is seen by the first 60 miles of cable line as shown in Figure 22. This effective load is a composite of the last 60 miles of cable line as well as the compensating reactor. With this effective load for the first 60 miles of cable line, the voltage profile over this distance reacts as if the line were inductive in nature. Thus, an increase in voltage magnitude occurs from the compensating point to the sending end. Figure 19 illustrates graphically the various reactions that take place along the cable line.

Using the same type of analysis presented earlier, the current profile shown in Figure 18 can be examined for the compensated cable line. Initially, the magnitude of the current tends to rise from the receiving end as in Figure 7 up to the compensation network. At this point, a sharp break in the current profile with an increase in magnitude is a result of the large inductive current. This compensating current effectively increases the magnitude of the line current due to the orientation of the current phasor with respect to the voltage phasor immediately prior to the compensating network.

$I'' > I'$

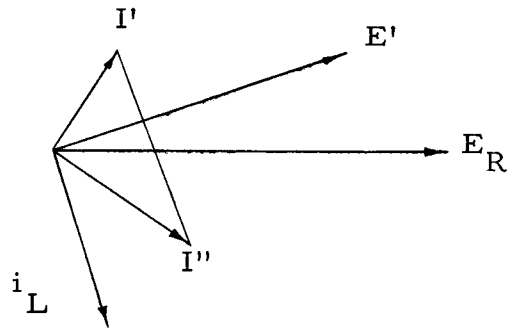

I' = line current before compensation network

I'' = line current after compensation network

i_L = inductive current associated with the compensating network

Figure 23. Phasor diagram at the point of compensation on the cable line.

As shown in Figure 23, the new line current I'' at the point of compensation is definitely greater than the line current prior to the compensation network when working from the receiving end. However, this may not always be the case since the magnitude of the inductive current i_L could possibly be small enough so that the resulting line current may be smaller than the current just prior to the compensating network.

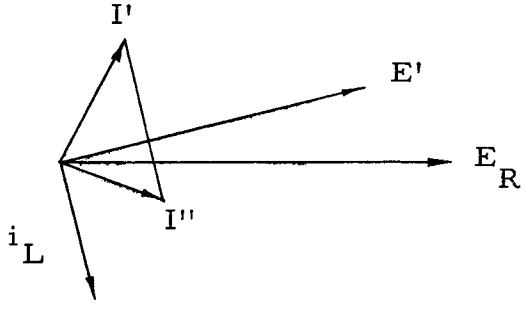

$I'' < I'$

Figure 24. Phasor diagram at the point of a small compensation network on a cable line.

The effect of reducing i_L with all the parameters unchanged can be observed by comparing Figures 23 and 24. The starting value of the load pf will also affect these relative magnitudes at the point of compensation.

Further examination of Figure 18 indicates a decrease in the magnitude of the line current after the compensating network. This is accounted for by the fact that the charging currents for each section add in such a manner so as to reduce the magnitude of the current until a critical point where further addition of charging currents causes a rise once again in the magnitude of the line current.

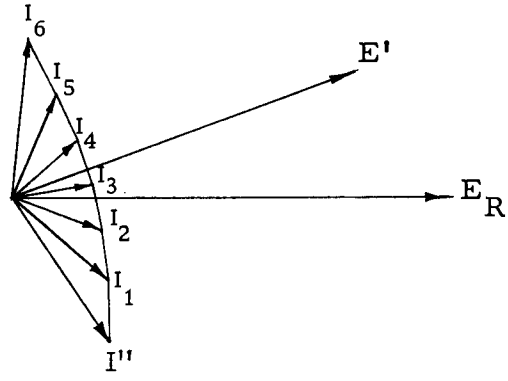

$$I'' > I_1 > I_2 > I_3 < I_4 < I_5 < I_6$$

Figure 25. Accumulative addition of current phasors on the cable line.

In general, whenever the angle of the line current is negative with respect to the line voltage at that point on the cable, further additions of charging currents for the next few successive sections will result in a decrease in line current. The opposite might hold true whenever the relative angle becomes positive at any point on the line.

Open-Circuit Termination

With compensation on the cable line, the open-circuit case exhibits different profiles than for the uncompensated line. For 100% compensation, the compensating inductive reactance is set equal to the total shunt distributed capacitive reactance of the cable; i.e., $X_L = X_C$. The value taken for X_C when finding X_L is a lumped quantity obtained through static measurements. This choice of X_C does not account for the distributed effects of the series impedance and shunt reactance present in the cable. Therefore, the use of a lumped compensating network in the middle of the line does not entirely cancel the effect of the distributed shunt capacitance inherent in the cable. Figure 26 illustrates an approximate representation of the singly-compensated cable line using two equivalent π circuits of 60 miles each. From this circuit approximation, it is observed that I_S would be zero with I_R equal to zero if Z were zero. With Z equal to zero, no sending-end current flows at no load ($I_R = 0$), and it could be said that the line charging current is fully compensated. However, the choice of $X_L = X_C$ for the real cable, for which Z is not zero, cannot produce zero input current at no load; even though it simplifies setting up the calculations.

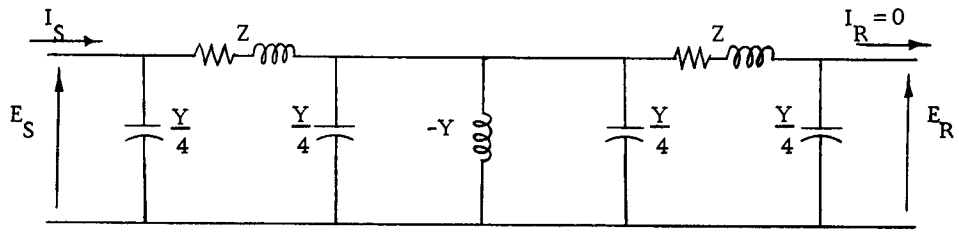

Figure 26. Approximate representation of a 100% compensated cable line with an open-circuit termination.

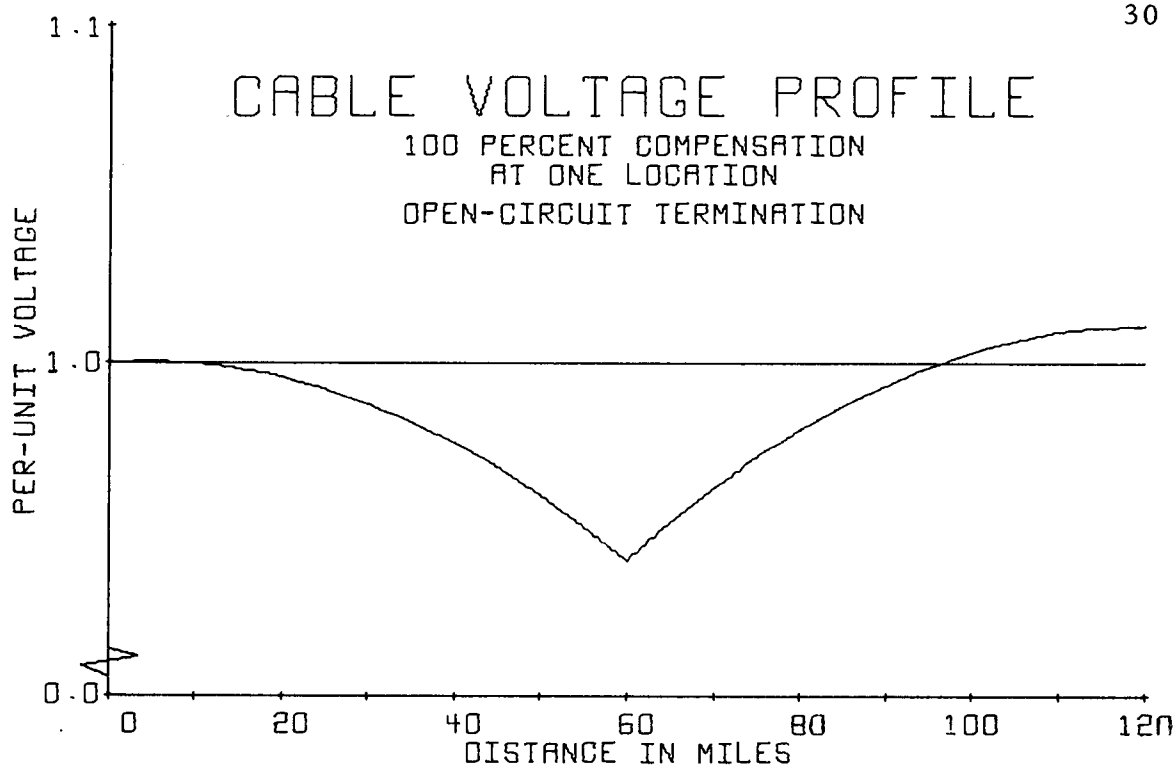

FIGURE 27. PER-UNIT VOLTAGE MAGNITUDE VERSUS DISTANCE FROM THE CABLE SENDING END.

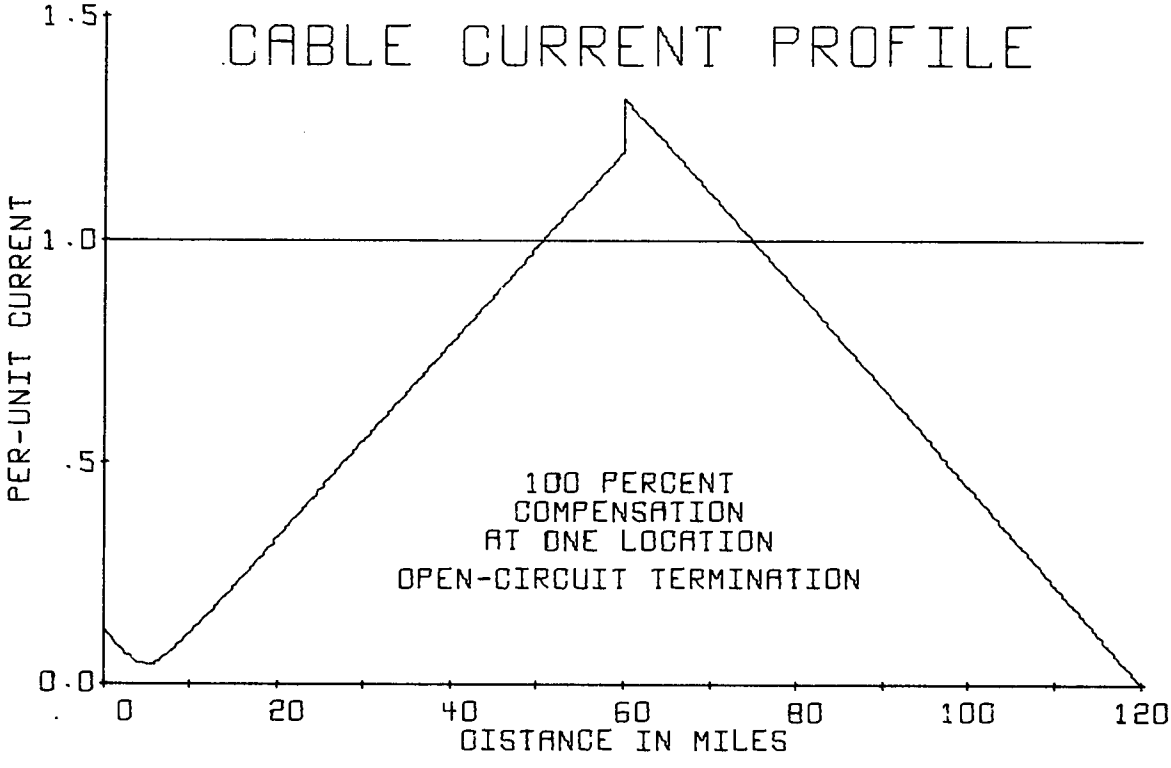

FIGURE 28. PER-UNIT CURRENT MAGNITUDE VERSUS DISTANCE FROM THE CABLE SENDING END.

As shown in Figure 28, line currents near the middle of the line are considerably larger than at either terminal. These line currents are mainly reactive currents associated with the vars from the shunt reactor being absorbed by the distributed shunt capacitance along the line. On the basis of the approximate model in Figure 26, the discontinuity in the current profile at the point of compensation arises from the effect of the equivalent series impedance in the cable. If there were no series impedance in the cable, a continuous current profile would be obtained for the open-circuit case because the line voltage would not vary and the shunt susceptance would change from $+\frac{Y}{2}$ to $-\frac{Y}{2}$ at the point of compensation. However, with series impedance present, the compensating reactance necessary for current magnitude continuity at the point of compensation depends on the change in voltage phase and amplitude introduced by the series impedance. Since the series impedance was neglected in choosing X_L for 100% compensation, it is expected that some discontinuity in the line current magnitude will occur at the point of compensation.

The phasor diagram of a compensated cable system with an open-circuit termination will shift its current phasor from a leading one to a lagging one when taken across a compensating network as shown in Figures 29a and 29b. Therefore, the voltage amplitude along the line may decrease or increase depending upon the phase current encountered at each point, whether lagging or leading.

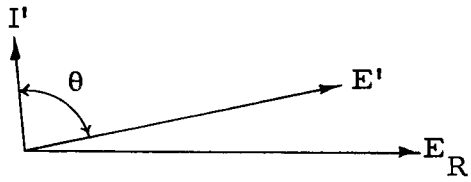

θ < 90 degrees

Figure 29a. Phasor diagram of the open-circuit, compensated cable system at a point prior to the compensation network from the receiving end.

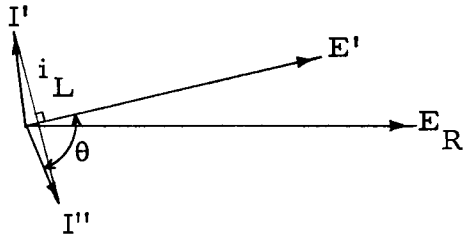

θ < 90 degrees

Figure 29b. Phasor diagram of the open-circuit, compensated cable system at the point of compensation.

The current profiles for circuit arrangements with two or more compensating networks are shown in Appendix VI for the open-circuit case. These profiles exhibit sharp changes in magnitude at various points on the line. These changes are a similar result of the accumulative addition of current phasors as shown in Figure 25. The great advantage of compensating networks is realized when comparing the voltage and current profiles for the uncompensated and compensated cable line with an open-circuit termination.

In summarizing the foregoing analysis, the compensated cable line limits, and sometimes suppresses, the amount of voltage rise on power cables. The effect of the compensating reactor is to retard the

accumulation of large charging currents along the line. Analytical results verify these effects of the compensating reactor by allowing no overvoltage to occur for the full-load case and a maximum of one percent overvoltage for the no-load case for a single, 100% compensated cable line. A maximum line current of 82% above rated current was calculated for the full-load case and 32% for the no-load case. These examples represent a substantial reduction in the percentage of line current above rated current as compared to the uncompensated line.

Multiple and Partially Compensated Cable Lines

Much of the foregoing analysis can be applied to cable lines with two or more compensating networks. The use of multiple reactors distributed at various intervals along the cable line creates a more effective means of controlling the excessive charging currents. Hence, the large accumulation of these charging currents are held in check by the various reactors placed at equal increments.

Studies of partially compensated lines reveal overall effects similar to those found for the fully compensated cable lines. With the degrees of compensation of 75% and 50%, investigation of these cases shows a fair amount of regulation of both voltage and current when compared to the fully compensated case. Maximum overvoltages as well as the percentage of line current above rated current have been reduced to a greater degree in some instances than the case with 100% compensation. Since only a part of the total shunt

capacitance distributed along the line is compensated for by these reactors, large magnitudes of reactive power are created on the line. This reactive power must be absorbed by the system at one or both ends of the cable line. Consequently, in dealing with partially compensated cable lines, some consideration must be given to the system at the cable line terminals to absorb the large magnitudes of reactive power. However, because of its ability to regulate voltage and current magnitudes effectively at lower compensating degrees, the partially compensated cable lines warrant careful evaluation as a system's option in comparison with the fully compensated lines.

Several curves have been plotted for the full-load and no-load conditions of cable operation. Some of these curves have already been discussed earlier while others are shown in Appendix VI. All the curves for the various compensation arrangements are based on a unity pf load. The maximum pu voltage and current magnitudes at any point along the cable line for each arrangement have been tabulated in Table II. These results indicate a general decrease in the magnitude of maximum current as the number of compensations increases. This is expected since the progressive accumulation of charging currents do not have the opportunity to reach large proportions with more compensating units. Further examination indicates that 75% compensation yields more favorable results than does 100% compensation. At each point of compensation, a

Table II. 230 KV cable, 400 MVA thermal rating

Circuit Arrangement	Percent Compensation	Maximum Pu Voltage and Current Magnitudes for Various Load Conditions			
		Full Load Unity Power Factor		No Load	
		Voltage	Current	Voltage	Current
A	none	1.24	3.13	1.36	3.30
B	100	1.00	1.82	1.01	1.32
	75	1.00	1.60	1.08	1.41
	50	1.04	1.64	1.16	1.52
C	100	1.00	1.56	1.00	0.89
	75	1.00	1.33	1.08	0.95
	50	1.04	1.58	1.16	1.47
D	100	1.00	1.44	1.00	0.66
	75	1.00	1.21	1.08	0.71
	50	1.04	1.58	1.16	1.46
E	100	1.00	1.36	1.00	0.53
	75	1.00	1.17	1.08	0.70
	50	1.05	1.58	1.16	1.47
F	100	1.00	1.31	1.00	0.44
	75	1.00	1.17	1.07	0.70
	50	1.05	1.58	1.16	1.47

large lagging current is attributed to the large compensating reactance of the shunt reactor as shown in Figure 23. Hence, an increase in line current at this point is a result of excessive compensating current. This increase, however, defeats the purpose of compensation on cable lines.

The voltage profiles between compensating points display a non-linear variation in magnitude depending upon the relative angle between the phasor voltage and current. At each compensating point on the cable line, the relative angle decreases because of the addition of an inductive current. The resulting angle can either be positive or negative depending upon the magnitude of the inductive current and also the orientation of the phasor current with respect to the voltage prior to the point of compensation.

The relative angle determines the general decrease or increase in voltage magnitude between compensating units. Whenever this relative angle is greater than a critical angle of approximately 20 degrees, a decrease in voltage magnitude occurs with the successive additions of charging current for each section between compensating units. Similarly, an increase in voltage magnitude occurs whenever the relative angle is less than the critical angle.

For multiple-compensated lines, the effect of each compensating unit on the relative angle is accumulative. Since the magnitude of each compensating unit is only a fraction of the total compensation, the relative angle at a compensating point near the receiving end of the cable could result in an angle greater than the critical angle. A relative angle less than the critical angle could also occur at a compensating point near the sending end of the same cable. The effects of these two phenomena are illustrated in Figures 42, 46, 50,

and 54 in Appendix VI.

The various current profiles shown in Appendix VI for the full load case exhibit magnitudes above rated current (i. e., 1. 0 pu current) at the receiving end. This is the result of the receiving-end voltage magnitude being respectively lower than one pu. Large current magnitudes at other points along the line are due to the cable charging currents.

The cable current profiles for multiple compensated lines with open-circuit terminations substantiate some of the hypotheses stated earlier. With 100% compensation, very little, if any, line current appears at the sending-end terminals. These line currents are largely reactive currents, and with several compensations, one or more points along the cable line will exhibit no current flow. For both the full-load and no-load cases, an increase in line current at various compensating points is observed as well as a decrease in line current at other points along the same cable line. This increase or decrease in line current at each compensating point depends upon the degree of compensation as well as the total accumulation of charging current up to the compensating point.

The variations in voltage and current along the cable line may dictate the maximum amount of pu power delivered to a unity pf load. Maximum limits of both voltage and current can determine the maximum real-power transmission capabilities without overloading the

cables. Thus, with those maximum limits specified for the 230 kv cable, Table III illustrates the maximum pu power delivered to a unity pf load for the various circuit arrangements.

Of particular interest in Table III is the equal and sometimes better ability of those arrangements with 75% as compared to 100% compensation to deliver maximum pu power to a unity pf load. This lesser degree of compensation represents a substantial economic savings in reactor size.

In general, whenever a unity pf load is supplied by a long cable line of given thermal ratings, maximum power transmission capabilities are increased with an increasing degree of compensation and extent of distributed compensation along the line.

Table III. Maximum per-unit power transmission* for 120 mile cable line with unity power-factor load

Circuit Arrangement	Percent Compensation	Maximum Pu Receiving-End Power
A	none	--
B	100	--
	75	--
	50	--
C	100	0.44
	75	0.43
	50	--
D	100	0.64
	75	0.76
	50	--
E	100	0.72
	75	0.81
	50	--
F	100	0.76
	75	0.81
	50	--

*The following criteria were chosen for maximum pu power transmission:

1) The maximum voltage limit at any point on the cable line was taken as 5% above base voltage.

2) The maximum current limit at any point on the cable line was taken as rated current, or 1004 amperes.

V. FUTURE AREAS OF INVESTIGATION

The analysis presented in this paper has dealt with one phase of EHV cable systems. However, within this phase there are several divisions which have not been considered and consequently can be marked for future investigation.

In the area of voltage and current compensation on long cable lines, further emphasis on the number and location of these compensating reactors is required in order to fully understand the operation of compensation on cable lines. The possibility of reactors at both terminal ends of the cable as well as unequal spacing of compensating units along the line requires more research. If power transfer is to be limited in one direction, a single compensating unit two-thirds of the distance from the cable sending-end may be all that is needed for satisfactory operation. However, the system planning engineer should keep in mind that the location of compensating units will in all probability depend upon the locations available as well as the operating characteristics of the line. Interruptions of cable lines to insert compensating reactors will involve additional cost of reactor installation, potheads, high-voltage terminal connections, and additional land area. Such added cost would be a detriment to cable systems to the point where an alternate transmission system such as the DC line would be more advantageous and economical.

The proper choice of reactor size depends upon the operation of the cable line for a particular system. Load pf, line length, the number and location of compensating reactors, and the system to which the cable is connected must all be considered in determining the optimum compensation for feasible cable operation. Consideration must also be given to the probabilities of load growth over a span of five to ten years or more as well as any other future changes in system size of operation.

The amount of flexibility afforded by switched or variable reactors demands more analysis for future cable systems. Since it is impractical to change reactor size and location, switched or variable reactor would provide better cable operation under almost any condition. Switched or variable reactor compensation could possibly be accomplished by parallel combinations of smaller reactors, by the use of variable tap-changing reactors, or by changing the amount of iron in the magnetic circuit of an iron-core reactor (1). A possible optimum cable system would be the automatic control of these variable reactors by digital computer techniques which would change the amount of compensation for unit step increases in load requirements as well as to provide some measure of insuring transient and steady-state system stability.

The term "full" or 100% compensation has been defined to be the case where the compensating shunt inductive reactance X_L is

equal to the shunt capacitive reactance X_C of the cable. Such is the criterion for 60-cycle resonance. Thus, a careful evaluation of series or parallel resonance is required by system planning engineers when considering a possible mode of compensation. Third harmonic resonance would also create adverse effects and additional problems which cannot be neglected.

VI. CONCLUSION

The utilization of shunt reactor compensation on long, high-voltage cable lines cannot be fully appreciated without considering the voltage and current profiles. Maximum current and voltage magnitudes along the line can exceed the ratings of the cable with or without compensation. Without compensation, virtually no power transmission is possible under any operating conditions on long lines. With compensation, only limited cases of various cable arrangements can be feasibly operated within the thermal limits. However, even these cases are subject to certain operating conditions.

The need for more comprehensive research of EHV a-c cable system, with or without reactor compensation, and its related problems confronting system planning engineers can only be emphasized with the rewarding justification of its own results. Needless to say, research will not always eliminate problems. However, a problem well defined becomes the index to its own solution.

BIBLIOGRAPHY

1. Dougherty, J. J. and C. S. Schifreen. Long cable lines - - alternating current with reactor compensation or direct current. AIEE Transactions on Power Apparatus and Systems 81:169-182. 1962.

2. Marble, W. C. and C. S. Schifreen. Charging current limitations in operation of high-voltage cable lines. AIEE Transactions on Power Apparatus and Systems 75: 803-817. 1956.

3. Rittenhouse, Joseph W. and John Zaborszky. Electric power transmission. New York, Ronald, 1954. 676 p.

4. Schifreen, Clement S. Extra-high-voltage cable research - - challenge of the future. AIEE Transactions on Power Apparatus and Systems 78:515-526. 1959.

5. Selby, Samuel M. Standard mathematical tables. 14th ed. Cleveland, Chemical Rubber, 1965. 632 p.

6. Stevenson, William D., Jr. Elements of power system analysis. 2nd ed. New York, McGraw-Hill, 1962. 388 p.

7. Westinghouse Electric and Manufacturing Company. Central Station Engineers. Electrical transmission and distribution reference book. East Pittsburgh, 1942. 570 p.

APPENDICES

APPENDIX I

TRANSMISSION LINE VOLTAGE AND CURRENT EQUATIONS

The expressions relating the current and voltage for one phase of a transmission line having uniformly distributed parameters are formulated as second-order differential equations. Their derivation may be found in any standard textbook on transmission line theory (6, p. 100-2). Exponential forms of these expressions relating voltages and currents at the terminals of each section are

$$E_S = \frac{E_R + I_R \cdot Z_c}{2} \epsilon^{\gamma \ell} + \frac{E_R - I_R \cdot Z_c}{2} \epsilon^{\gamma \ell} \text{ , phasor voltage (1)}$$

$$I_S = \frac{E_R/Z_c + I_R}{2} \epsilon^{\gamma \ell} + \frac{E_R/Z_c - I_R}{2} \epsilon^{\gamma \ell} \text{ , phasor current (2)}$$

These expressions give the rms phasor quantities of voltage and current and their respective phase angles at the terminals of each section of the cable line.

In long transmission line analysis, these equations for computing voltage and current of a power line can be put in a more convenient form by introducing hyperbolic functions. By rearranging equations (1) and (2) and substituting the hyperbolic functions for the exponential terms, a new set of equations can be found describing the voltages and currents at the terminals of each section. These are

$$E_S = [\cosh \gamma\ell] \cdot E_R + [Z_c \sinh \gamma\ell] \cdot I_R \quad \text{, phasor voltage} \qquad (3)$$

$$I_S = [\frac{1}{Z_c} \sinh \gamma\ell] \cdot E_R + [\cosh \gamma\ell] \cdot I_R \text{, phasor current} \qquad (4)$$

The propagation constant γ is a complex quantity composed of a real part, the attenuation constant α, and an imaginary part, the phase constant β.

$$\gamma = \alpha + j\beta$$

Since γ is complex, the argument $\gamma\ell$ of the hyperbolic function is also complex. The evaluation of these hyperbolic functions cannot be found directly from ordinary mathematical tables. However, expansion of these functions with complex arguments can simplify their evaluation by the following equations in terms of real arguments (5, p. 533).

$$\cosh (\alpha\ell + j\beta\ell) = \cosh \alpha\ell \cdot \cos \beta\ell + j \sinh \alpha\ell \cdot \sin \beta\ell \qquad (5)$$

$$\sinh (\alpha\ell + j\beta\ell) = \sinh \alpha\ell \cdot \cos \beta\ell + j \cosh \alpha\ell \cdot \sin \beta\ell \qquad (6)$$

For hand calculations, evaluation of the hyperbolic functions can be found directly from standard tables using equations (5) and (6). For automatic computing machines, a more convenient method of evaluating hyperbolic functions is to expand them in a Maclaurin power series (5, p. 531).

$$\cosh \alpha\ell = 1 + \frac{(\alpha\ell)^2}{2!} + \frac{(\alpha\ell)^4}{4!} + \frac{(\alpha\ell)^6}{6!} + \cdots\cdots$$

$$\sinh \alpha\ell = \alpha\ell + \frac{(\alpha\ell)^3}{3!} + \frac{(\alpha\ell)^5}{5!} + \frac{(\alpha\ell)^7}{7!} + \ldots\ldots$$

These series converge rapidly, and sufficient accuracy can be obtained by evaluating only the first few terms.

For several sections in tandem, the receiving-end quantities for one section become the sending-end quantities for the next section, etc. Successive iterations will yield the sending- and receiving-end quantities for a particular cable line as well as the voltage and current profiles.

In this analysis, it is assumed that

1. The sending-end voltage E_S has a constant magnitude equal to the system voltage, and is the base voltage.
2. The phase angle of the receiving-end voltage E_R is zero and is used as a reference from which all other phase angles of complex quantities are measured.
3. The base current is 1004 amperes and is the maximum allowable current.

Using those values shown in Appendix VI and a section length of two miles, the following quantities were calculated:

$\alpha\ell$ = 0.00338 nepers

$\beta\ell$ = 0.01270 radians

Z_c = 37.82 - j7.15 ohms

= 0.285 - j0.05384 per unit.

APPENDIX II

GENERALIZED CIRCUIT CONSTANTS

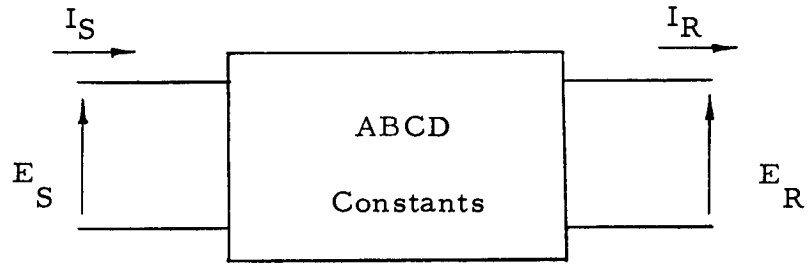

Figure 30. Two-terminal-pair network with generalized circuit constants.

Equations (3) and (4) in Appendix I represent the relationship between the sending-end and receiving-end quantities for a two-terminal-pair network such as shown in Figure 30. The coefficients of these quantities are functions of the distributed line parameters per unit length as well as the length of a cable section. Consequently, they are found to be constant for a specific section length. Hence, these constant coefficients can be related by the following notation:

$$A = \cosh \gamma\ell$$

$$B = Z_c \cdot \sinh \gamma\ell \quad , \text{ ohms per section}$$

$$C = (1/Z_c) \cdot \sinh \gamma\ell \quad , \text{ mhos per section}$$

$$D = A^2$$

---

[2] True only for a symmetrical system.

The terms A, B, C, and D are called the generalized circuit constants or the ABCD constants of any two-terminal-pair network with passive, linear, and bilateral elements. The constant D is equal to the constant A for a symmetrical network since such a network is the same when viewed from either end. With these constants a new set of equations relating the terminal quantities is given as

$$E_S = A \cdot E_R + B \cdot I_R \quad \text{, phasor voltage} \tag{7}$$

$$I_S = C \cdot E_R + D \cdot I_R \quad \text{, phasor current} \tag{8}$$

Solving simultaneously for E_R and I_R,

$$E_R = A \cdot E_S - B \cdot I_S \quad \text{, phasor voltage} \tag{9}$$

$$I_R = - C \cdot E_S + D \cdot I_S \quad \text{, phasor current} \tag{10}$$

The same coefficients for equations (9) and (10) appear in equations (7) and (8) because the determinant of equations (7) and (8) equals one or

$$A \cdot D - B \cdot C = 1$$

since $\cosh^2 \gamma\ell - \sinh^2 \gamma\ell = 1$.

Each particular section of the cable is represented by a set of generalized circuit constants. These sections can be combined in tandem to form a long transmission line, and likewise, numerical manipulation of each set of constants can be performed by matrix

multiplication to obtain the overall set of constants. The matrix multiplication for the ABCD constants of combined networks is illustrated below for two networks in series.

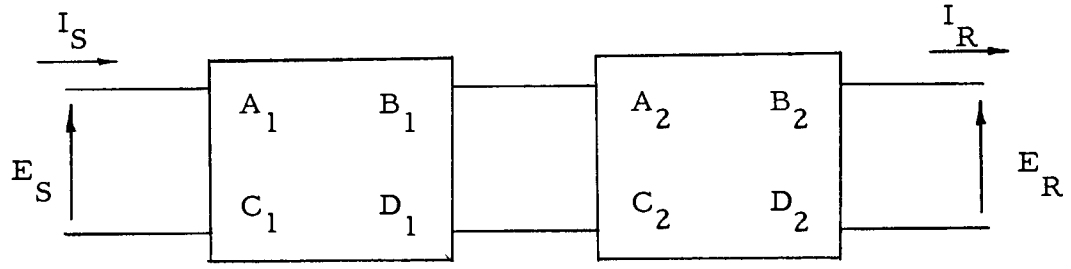

Figure 31. Two two-terminal-pair networks in series.

$$A_3 = A_1 \cdot A_2 + B_1 \cdot C_2$$

$$B_3 = A_1 \cdot B_2 + B_1 \cdot D_2$$

$$C_3 = A_2 \cdot C_1 + C_2 \cdot D_1$$

$$D_3 = B_2 \cdot C_1 + D_1 \cdot D_2$$

The generalized circuit constants A_3, B_3, C_3, and D_3 represent the ABCD constants for the combined networks in series as shown in Figure 31.

The method of cable simulation requires the successive calculations of like sections to obtain the total ABCD constants. This method can be analytically verified by considering Figure 31. Letting

$A_1B_1C_1D_1$ be the constants of three unit sections or 3ℓ and $A_2B_2C_2D_2$ be the constants of a unit section or ℓ, the constant A_3 can be equated to the constant for four sections by substituting the hyperbolic functions for the respective notations.

$$A_3 = A_1 \cdot A_2 + B_1 \cdot C_2$$

$$A_3 = (\cosh \gamma \cdot 3\ell)(\cosh \gamma \cdot \ell) + (Z_c \sinh \gamma \cdot 3\ell)(\frac{1}{Z_c} \sinh \gamma \cdot \ell)$$

$$A_3 = (\cosh \gamma \cdot 3\ell)(\cosh \gamma \cdot \ell) + (\sinh \gamma \cdot 3\ell)(\sinh \gamma \cdot \ell)$$

By a mathematical identity (5, p. 533),

$$A_3 = \cosh (\gamma \cdot 3\ell + \gamma \cdot \ell)$$

$$A_3 = \cosh \gamma \cdot (3\ell + \ell)$$

$$A_3 = \cosh \gamma \cdot 4\ell$$

The constants B_3, C_3, and D_3 can be verified in a similar manner.

APPENDIX III

LUMPED TRANSMISSION CABLE REPRESENTATION

Nomenclature

α	attenuation constant, neper per unit length.
β	phase constant, radians per unit length.
$\gamma=\sqrt{z \cdot y}$	propagation function, numeric per unit length.
ϕ	circuit phase of three phase voltage system.
A	(complex) generalized circuit constant for two-terminal-pair network
B	(complex) generalized circuit constant for two-terminal-pair network, ohms.
C	(complex) generalized circuit constant for two-terminal-pair network, mhos.
D	(complex) generalized circuit constant for two-terminal-pair network.
D_{ab}	center-to-center flat spacing between the aϕ and bϕ cables.
D_{ac}	center-to-center flat spacing between the aϕ and cϕ cables.
D_{bc}	center-to-center flat spacing between the bϕ and cϕ cables.
E_B	base voltage or system voltage, line-to-line, volts.
E_R	phasor rms voltage, line-to-neutral, at receiving end, phasor volts.
GMD	geometric mean distance, inches.
I	rms current through series impedance per unit section length of cable, phasor amperes per unit section length.

I' rms current through shunt compensating inductance, phasor amperes.

I_R phasor rms current at receiving end of line, phasor amperes.

I'_R rms current through the receiving-end shunt admittance to neutral per unit section length of cable, phasor amperes per unit section length.

I_S phasor rms current at sending end of line, phasor amperes.

I'_S rms current through sending-end shunt admittance to neutral per unit section length of cable, phasor amperes per unit section length.

ℓ unit section length of cable, miles.

R_a a-c resistance of one conductor, ohms per phase per mile.

R_s a-c resistance of the sheath of one cable, ohms per phase per mile.

X_a inductive reactance at 12 inch spacing, ohms per phase per mile.

X_c shunt capacitive reactance, ohm-miles per phase.

X_d inductive reactance spacing factor, ohms per phase per mile.

X_s inductive reactance of the sheath of one cable, ohms per phase per mile.

y shunt admittance per unit length, per phase, mhos per mile.

$Y = y \cdot \ell$ shunt admittance per phase-to-neutral, mhos per section of cable.

z series impedance per unit length, per phase, ohms per mile

$Z = z \cdot \ell$ series impedance per phase, ohms per section of cable.

$Z_c = \sqrt{z/y}$ characteristic impedance, ohms.

Z_L inductive reactance of shunt compensating reactor, ohms per phase.

Z_1 positive sequence impedance per section of cable, ohms per phase per section.

Z_2 negative sequence impedance per section of cable, ohms per phase per section.

Equivalent Circuit

The inherent characteristics of an electric cable which affect its suitability for use as a transmission link in an integrated electric system are its series impedance Z and shunt admittance Y. These characteristics are uniformly distributed along the length of the cable. Individual sections representing short lengths of the cable can be approximated by an equivalent π circuit as shown in Figure 32. However, the series consideration of several equivalent π sections may result in some inaccuracy due to approximate values of Z and Y for each section.

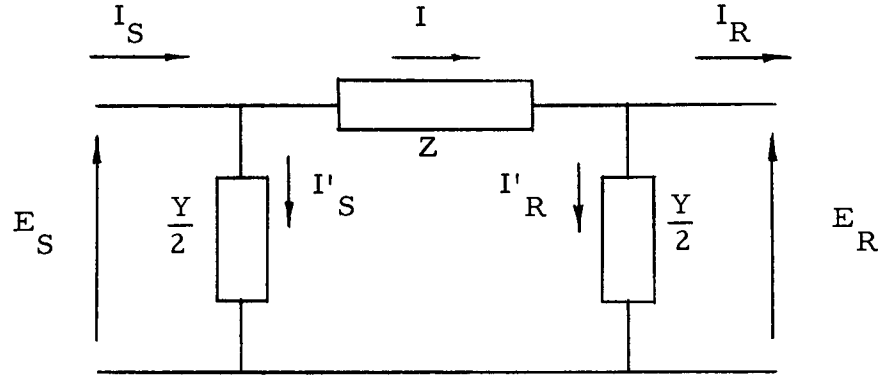

Figure 32. Equivalent π circuit for a unit section length of cable.

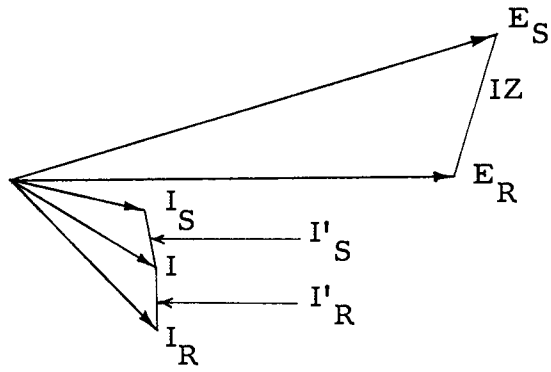

Figure 33. Phasor diagram of equivalent π circuit for a unit section length of cable.

Series Impedance

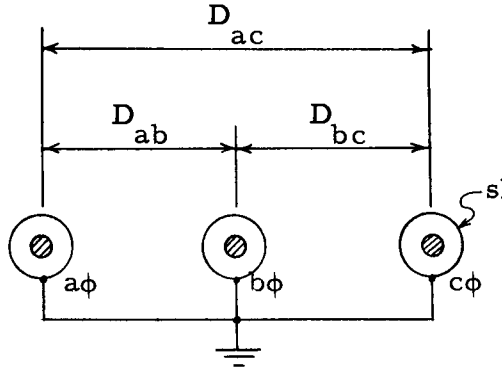

D_{ac} = 10 inches

$D_{ab} = D_{bc}$ = 5 inches

Note: The interconnection of shields to ground is done at both ends of the cable.

Figure 34. Three-phase cable system configuration used in the calculation of profiles.

With the three-phase cable system shown above, induced voltages are created in each cable sheath due to current flowing in the conductor of each cable. These voltages create sheath currents when the sheaths are solidly bonded. This represents additional losses to the system through the series impedance of the cable. Hence, the general expression for the positive or negative sequence

impedance includes sheath resistance and reactance as well as the conductor resistance and reactance. The development of this expression can be obtained from a standard transmission line book (7, p. 112-115) and is cited as

$$Z_1 = Z_2 = R_a + \frac{R_s (X_s + X_d)^2}{R_s^2 + (X_s + X_d)^2} +$$

$$j \left[X_a + X_d - \frac{(X_s + X_d)^3}{R_s^2 + (X_s + X_d)^2} \right] \text{, ohms/phase/mile}$$

where,

$$X_d = 0.2794 \log_{10} (GMD/12) \text{, ohms/phase/mile}$$

$$GMD = \sqrt[3]{D_{ab} \cdot D_{bc} \cdot D_{ac}} \text{, inches}$$

Shunt Admittance

The common characteristic of single-conductor cables is that every conductor is surrounded by a separate grounded sheath or shield. This separate shielding of each conductor eliminates all mutual capacity effects between phases making the charging current of each conductor independent of the other cables. This represents a very substantial simplification in the charging current calculations as compared to the case of the overhead lines. Values of the shunt capacitive reactance per mile of standard cables are listed in tables

from the transmission line books (3, p. 646-7, 7, p. 124).

The shunt conductance has been neglected in the calculations of voltage and current along the cable line.

Calculated Quantities for the Lumped π-equivalent

With reference to Appendix I, the calculated quantities of GMD, X_d, Z_l, and X_C are listed below:

GMD = 6.3 inches

X_d = -0.07816 ohms/phase/mile

Z_l = 0.09048 + j 0.2326 ohms/phase/mile

= 0.0006814 + j 0.001752 per unit

X_C = 5960 ohm-mile/phase

= 45.09 per unit

Table IV. Per-unit ABCD constants for two mile sections

Constants	Lumped π Equivalent Circuit	Generalized Circuit Constants
A	0.9999219443 +j0.0000607245	0.9999219452 +j0.0000303615
B	0.0013627374 +j0.0035033374	0.0013626666 +j0.00350326
C	- 0.0000006764 +j0.0445624773	- 0.0000004497 +j0.044595788

APPENDIX IV

SHUNT REACTOR COMPENSATION

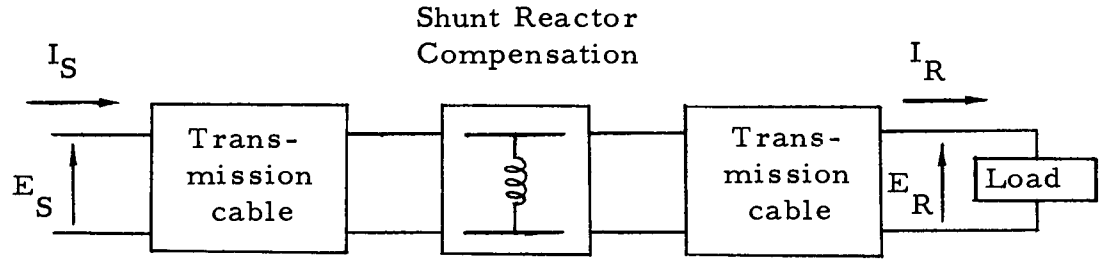

Figure 35. Block diagram of a typical shunt compensated cable system.

Shunt reactor compensation is represented by a lumped compensating network as shown in Figure 35. It is discontinous in that actual compensation occurs at one or various intervals along the length of the cable. The amount of compensation for a particular system is a function of the length ℓ of the cable, the capacitive reactance X_c, the number of compensations, and the percentage of compensation. Thus, 100 percent compensation is an inductive reactance equal to the distributed line capacitance of a cable line. The following expression gives the amount of required compensation for each unit.

Amount of compensation for each unit =

$$- \frac{(\text{length of cable})}{(X_c)\,(\text{number of compensations})} \times (\text{percent compensation}) \quad (11)$$

Shunt reactor compensation at various intervals along the length of cable can also be represented by generalized circuit constants.

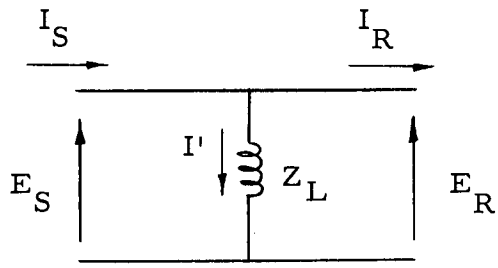

Figure 36. Equivalent circuit of the shunt reactor compensation.

$$A = \frac{E_S}{E_R}\Bigg|_{I_R = 0} = 1$$

$$B = \frac{E_S}{I_R}\Bigg|_{E_R = 0} = 0 \text{ , ohms}$$

$$C = \frac{I_S}{E_R}\Bigg|_{I_R = 0} = \frac{1}{Z_L} \text{ , mhos}$$

$$D = \frac{I_S}{I_R}\Bigg|_{E_R = 0} = 1$$

The set of ABCD constants for the compensating network can be obtained by the process shown above. The fact that each compensating network is a symmetrical network is verified with the constants A and D being equal. The imaginary part of the circuit constant C for the compensation section can be numerically calculated by equation (11). The shunt reactor compensation represents a lumped quantity and does not exhibit uniformly distributed effects as does the electrical parameters of the cable.

APPENDIX V

COMPUTER ANALYSIS AND FLOW CHARTS

The use of a digital computer in analytical studies provides a quick and efficient method of obtaining numerical results over a wide range of given conditions. The IBM 1620 Data Processing System exemplifies this fact and is the major instrument in the profile calculations for this thesis.

The flow charts shown in Figures 37, 38, and 39 describe generally the computer program used to determine the voltage and current characteristics of the cable system. The final version of the entire program included the grouping of various subprograms together as well as manipulating the matrix operations in correct order. These subprograms are categorized as follows:

1. Computation of the square root of a complex number.
2. A hyperbolic cosine and sine subroutine for complex arguments.
3. An iterative solution of the output voltage.

An iterative method was adopted based on the limited given conditions. Knowing only the load and the magnitude of the input voltage, a simple simultaneous solution is no longer possible. Thus, by initially assuming a receiving-end voltage E_R and applying assumption (2) in Appendix I, a sending-end voltage E_S can be

calculated and compared to the given quantity. If the comparison results in a difference greater than a specified tolerance, steps are taken to reduce the error. Past association with this method has indicated that a satisfactory starting value of E_R equal to E_S is an acceptable first approximation.

The following list describes the basic areas of calculations by the computer program.

1. Calculation of the series impedance and shunt admittance of the cable.

2. Calculation of the generalized circuit constants for a unit section length and for compensation units.

3. Calculation of total ABCD constants of the cable line.

4. Calculation of terminal conditions by an iterative process.

5. Calculation of voltage and current profiles starting at the receiving end and working towards the sending end.

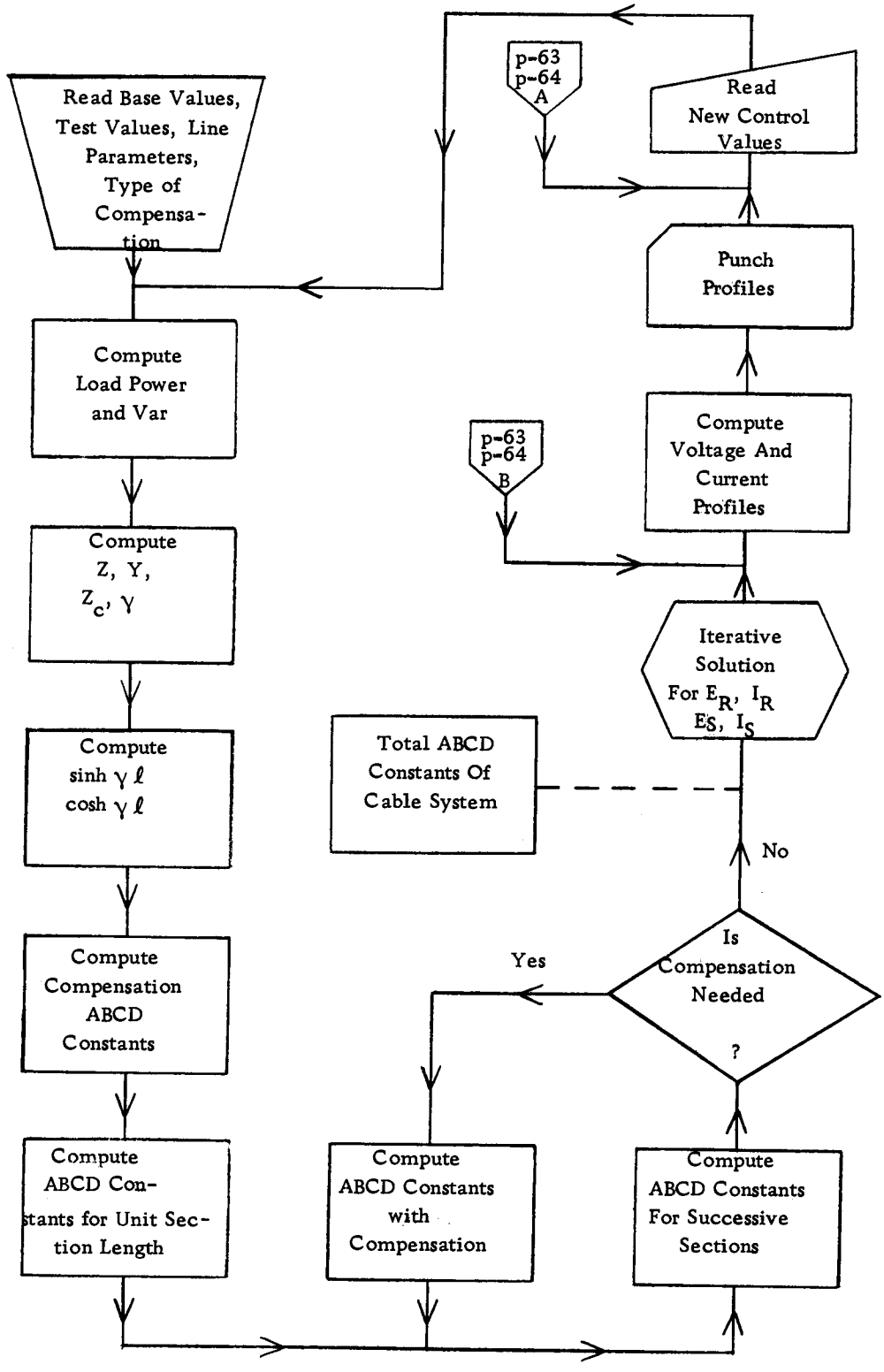

Figure 37. Flow chart of cable simulation program.

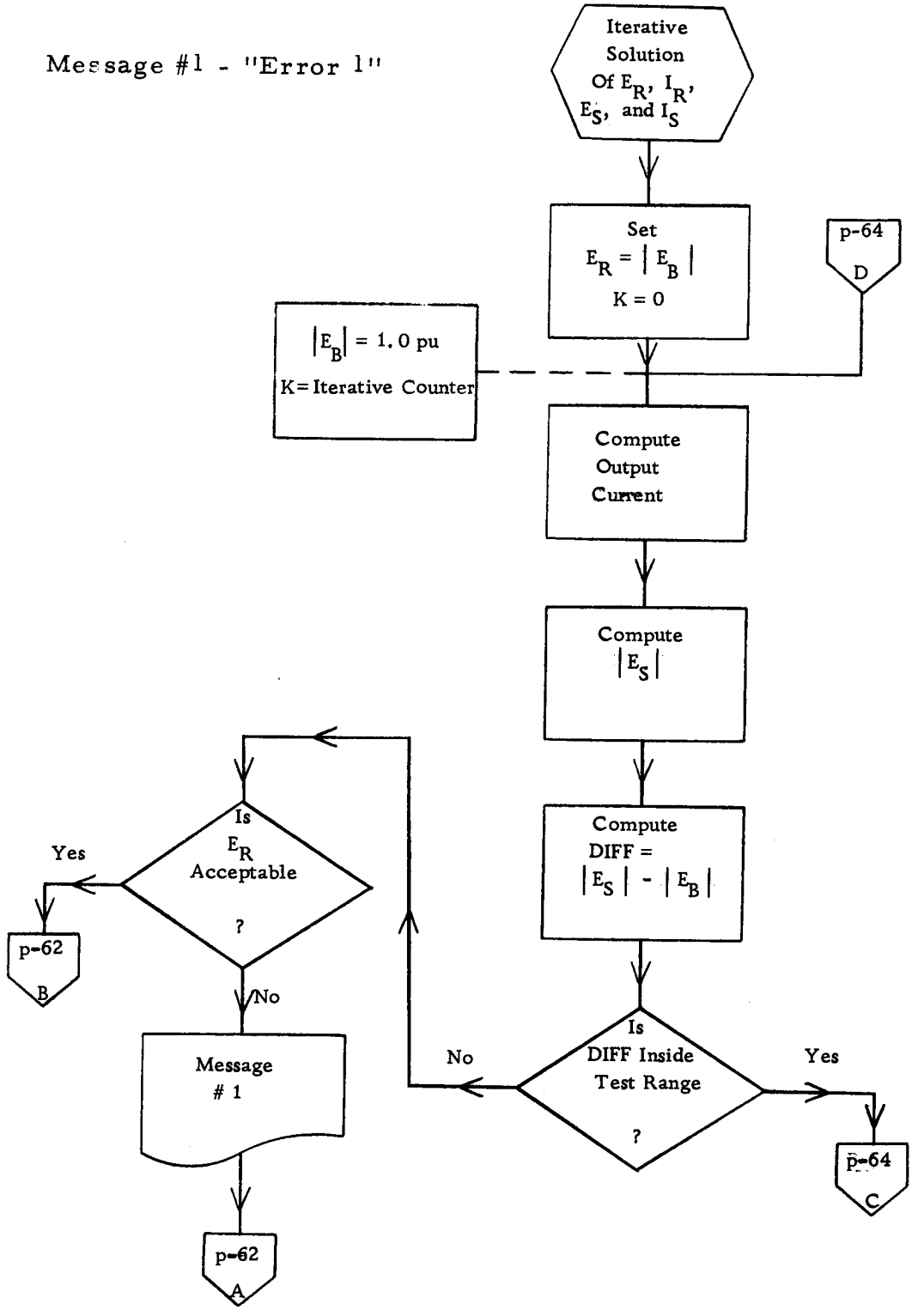

Figure 38. Flow chart of iterative subprogram.

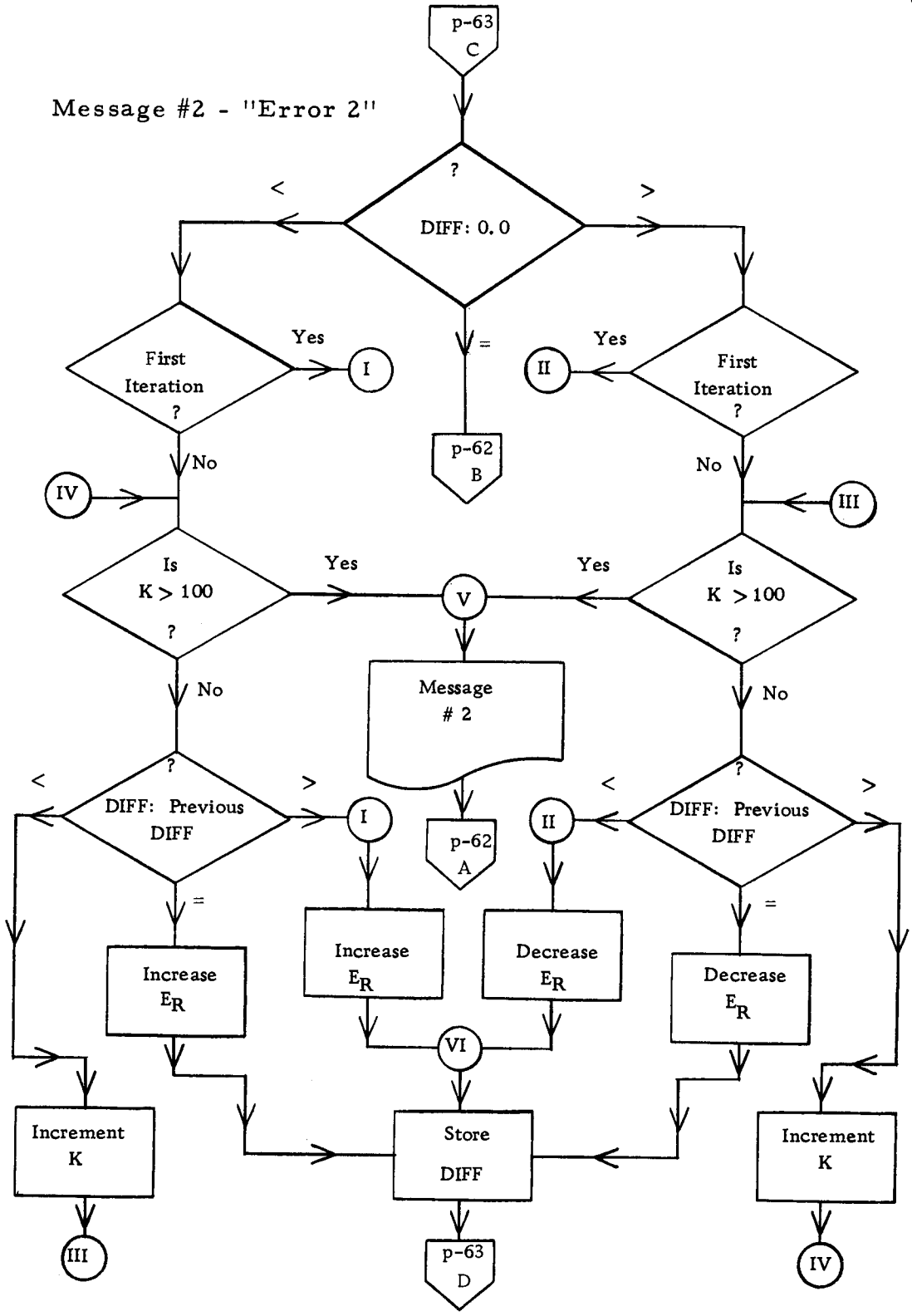

Figure 39. Flow chart of iterative subprogram.

APPENDIX VI

DATA AND COMPUTER RESULTS

Cable Data (3, p. 647)

Cable type: Oil filled, paper insulated single-conductor cable

Diameter of conductor: 1.835 inches

Insulation thickness: 925 mils

Area of conductor: 2, 000, 000 circular mils

Lead sheath thickness: 170 mils

GMR: 0.763 inches

Weight: 22, 990 pounds/1000 feet

60-cycle Characteristics

R_a = 0.038 ohms/phase/mile

X_a = 0.334 ohms/phase/mile

R_s = 0.315 ohms/phase/mile

X_s = 0.219 ohms/phase/mile

X_c = 5960 ohm-miles/phase

System voltage line-to-line: 230, 000 volts

Maximum current: 1004 amperes

The above cable data have been verified by the General Electric Company to be within an acceptable range.

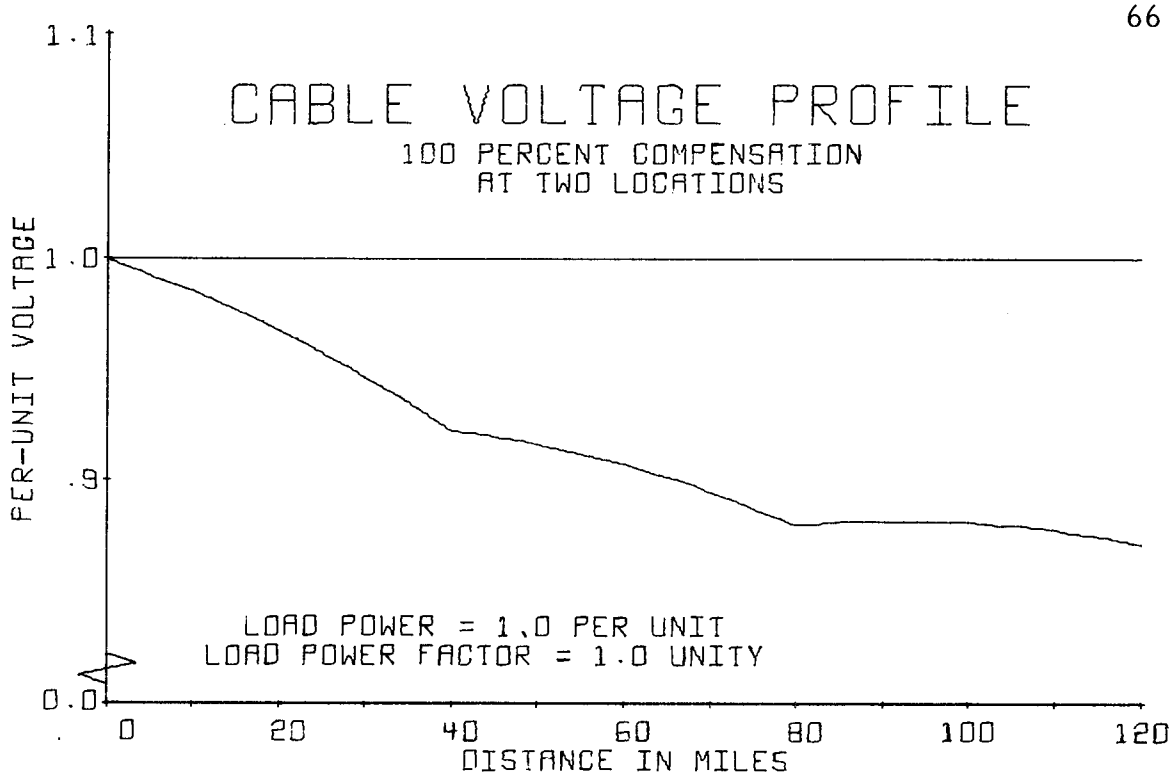

FIGURE 40. PER-UNIT VOLTAGE MAGNITUDE VERSUS DISTANCE FROM THE CABLE SENDING END.

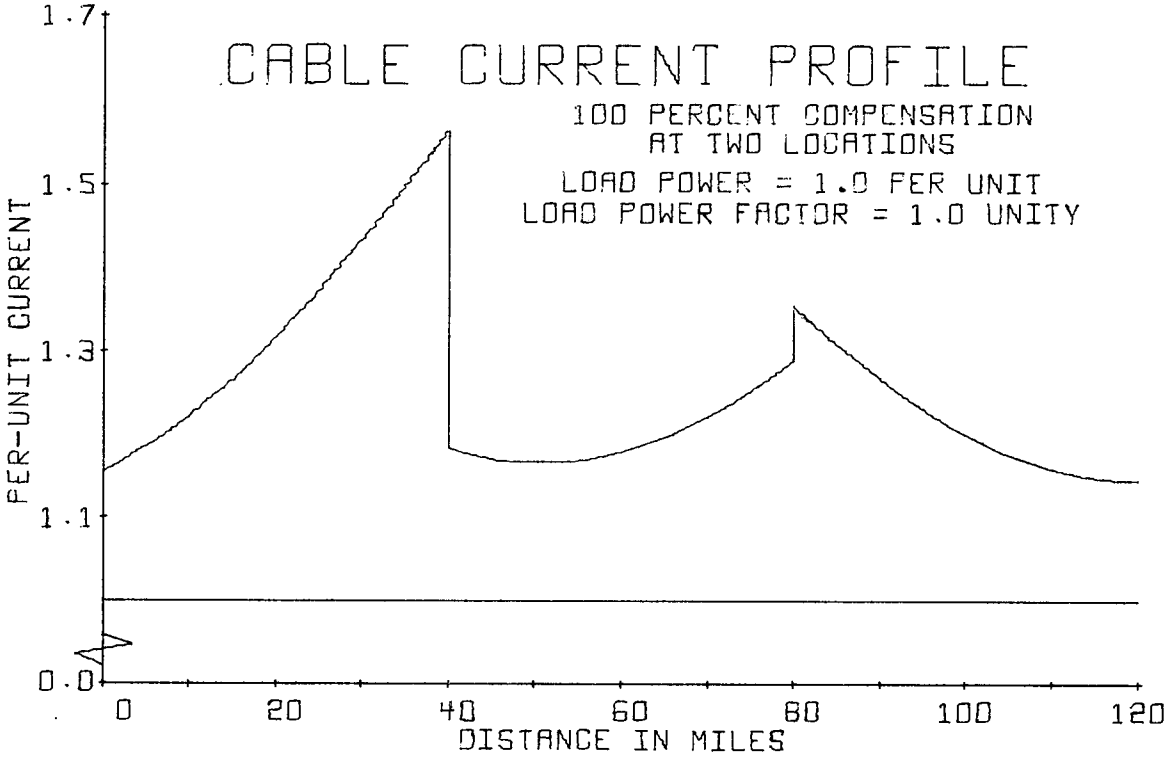

FIGURE 41. PER-UNIT CURRENT MAGNITUDE VERSUS DISTANCE FROM THE CABLE SENDING END.

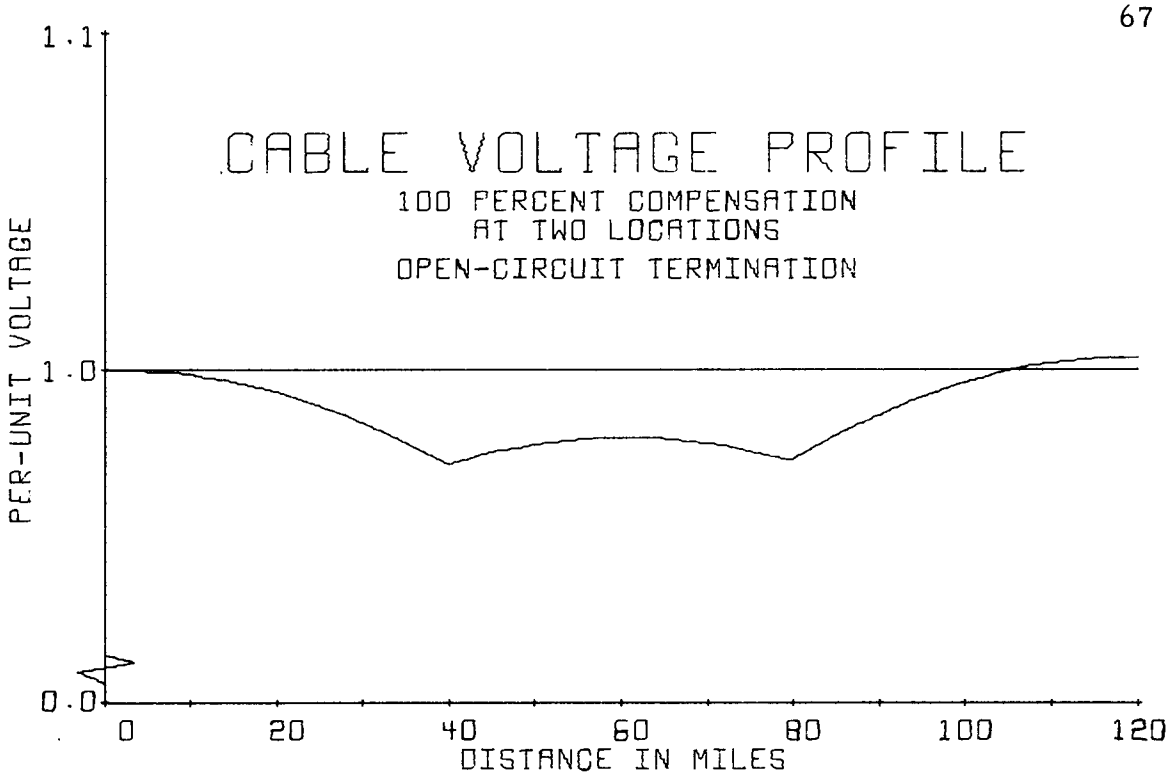

FIGURE 42. PER-UNIT VOLTAGE MAGNITUDE VERSUS DISTANCE FROM THE CABLE SENDING END.

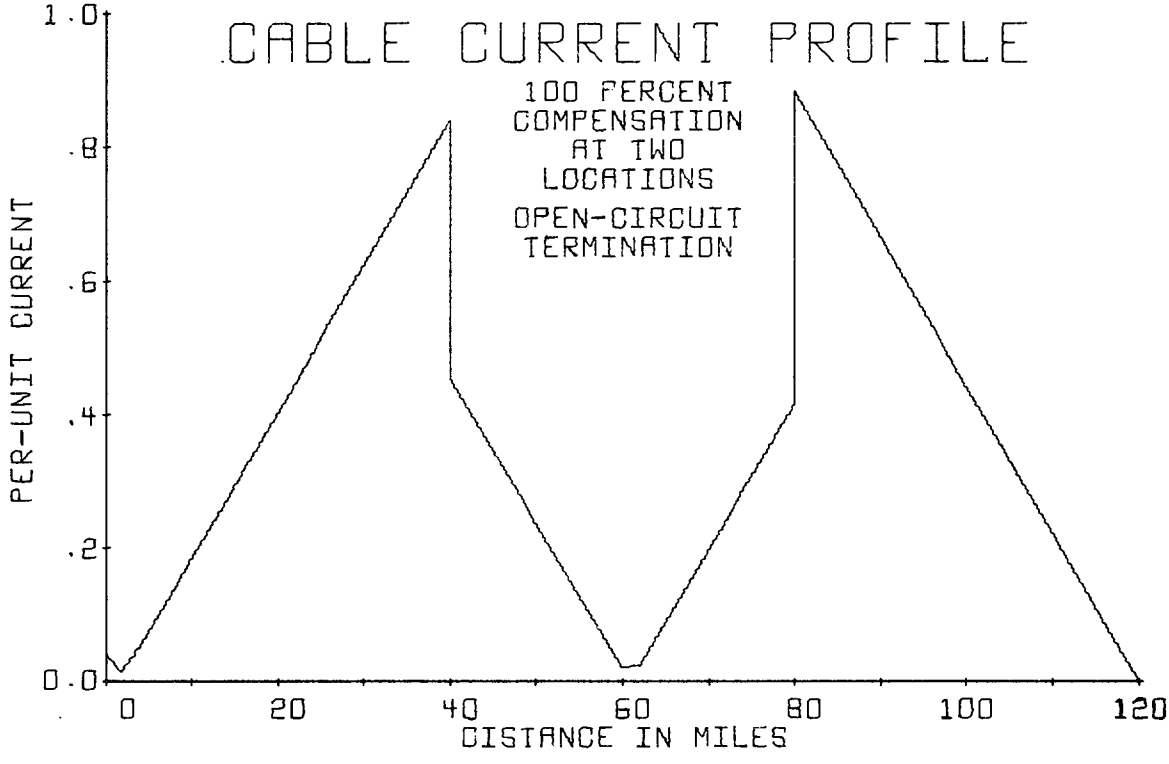

FIGURE 43. PER-UNIT CURRENT MAGNITUDE VERSUS DISTANCE FROM THE CABLE SENDING END.

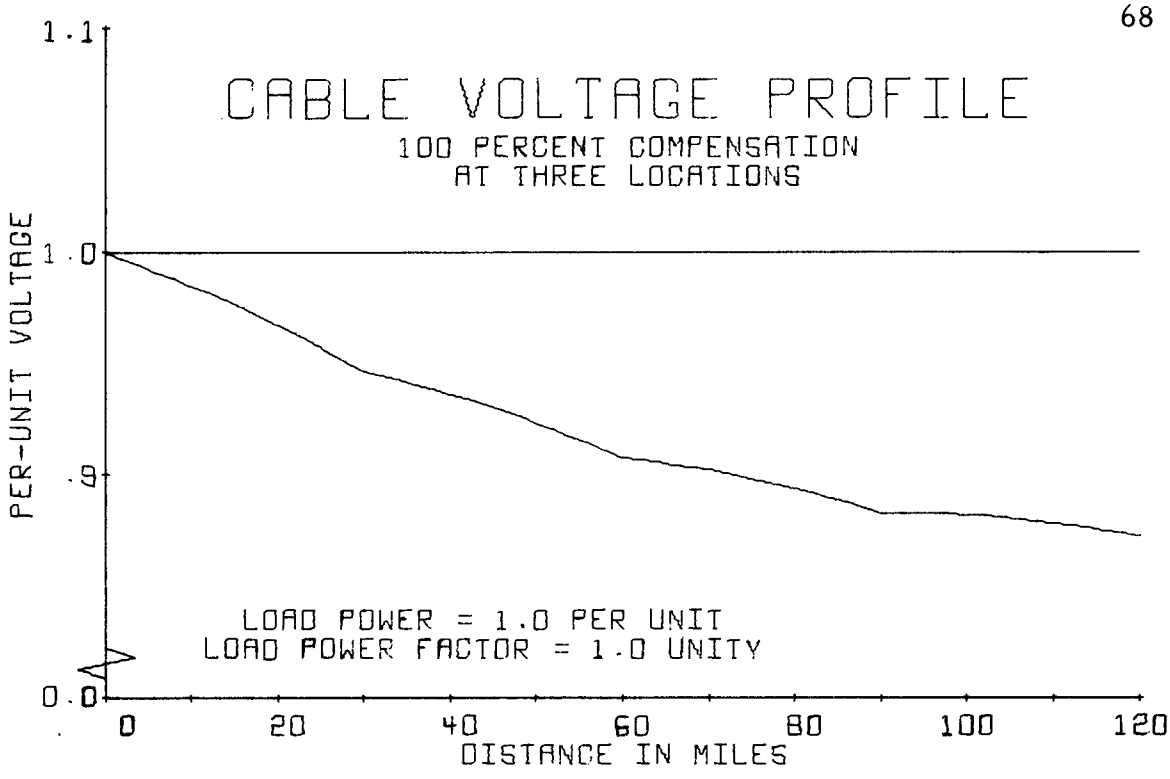

FIGURE 44. PER-UNIT VOLTAGE MAGNITUDE VERSUS DISTANCE FROM THE CABLE SENDING END.

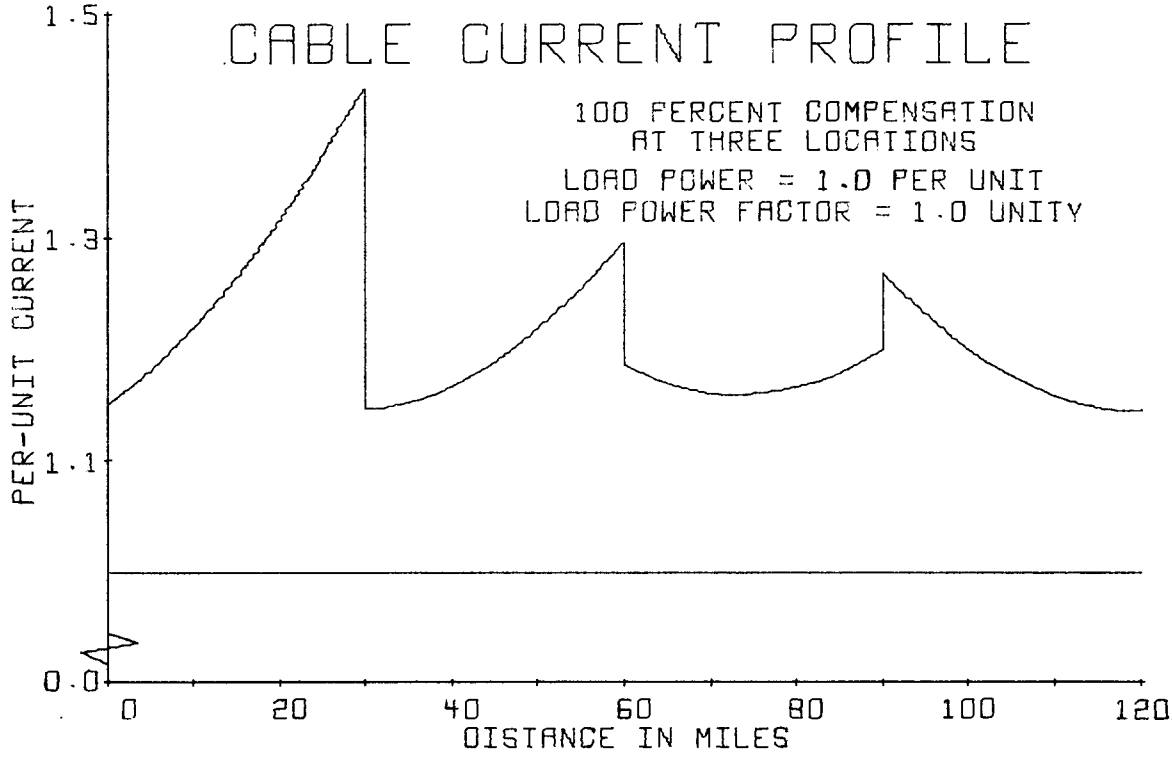

FIGURE 45. PER-UNIT CURRENT MAGNITUDE VERSUS DISTANCE FROM THE CABLE SENDING END.

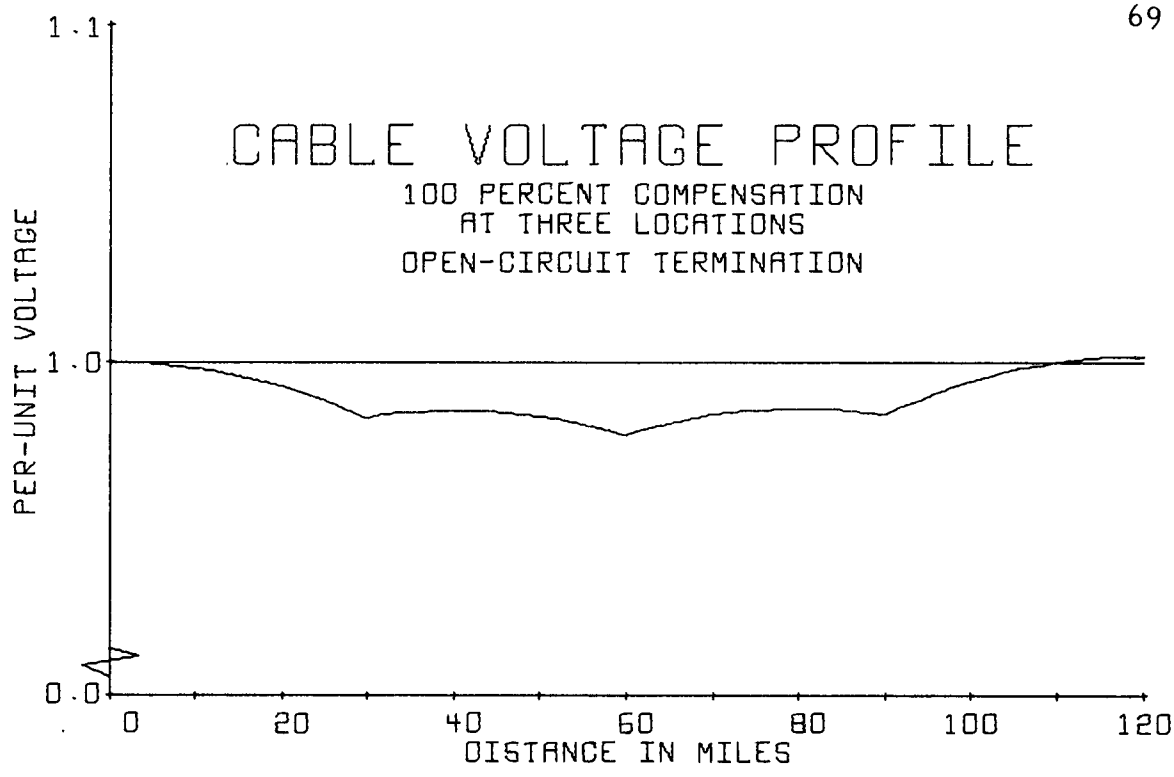

FIGURE 46. PER-UNIT VOLTAGE MAGNITUDE VERSUS DISTANCE FROM THE CABLE SENDING END.

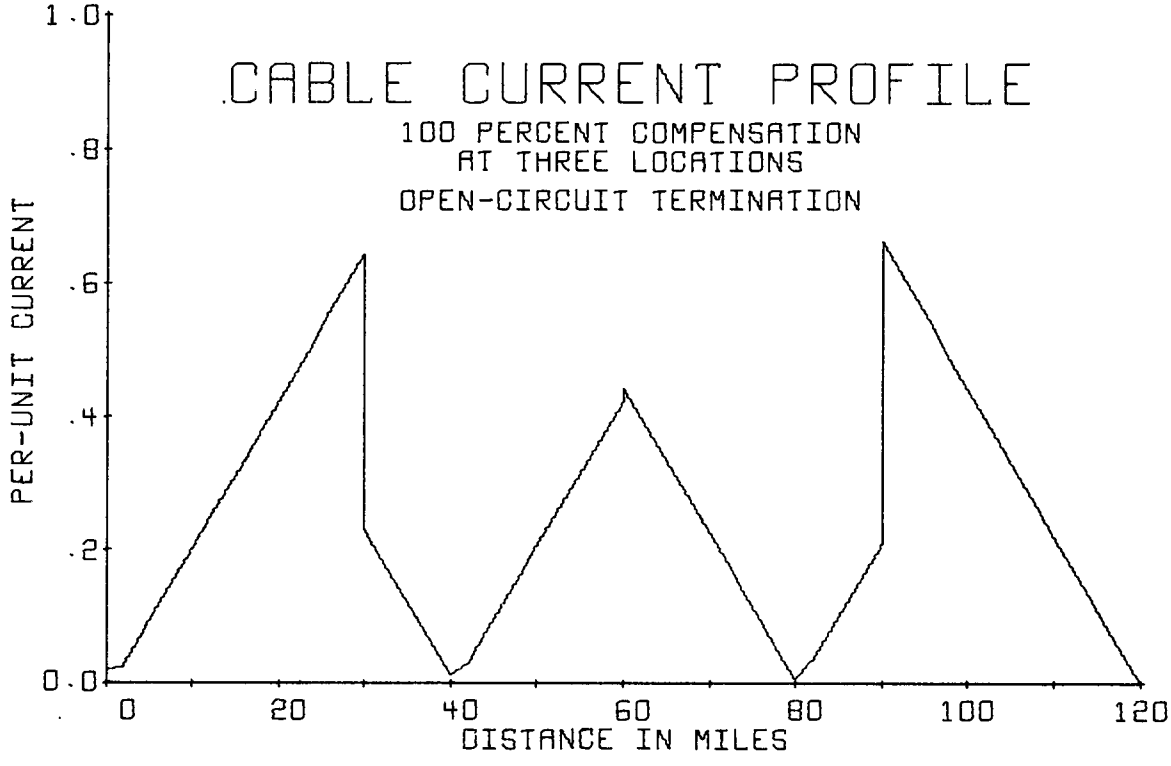

FIGURE 47. PER-UNIT CURRENT MAGNITUDE VERSUS DISTANCE FROM THE CABLE SENDING END.

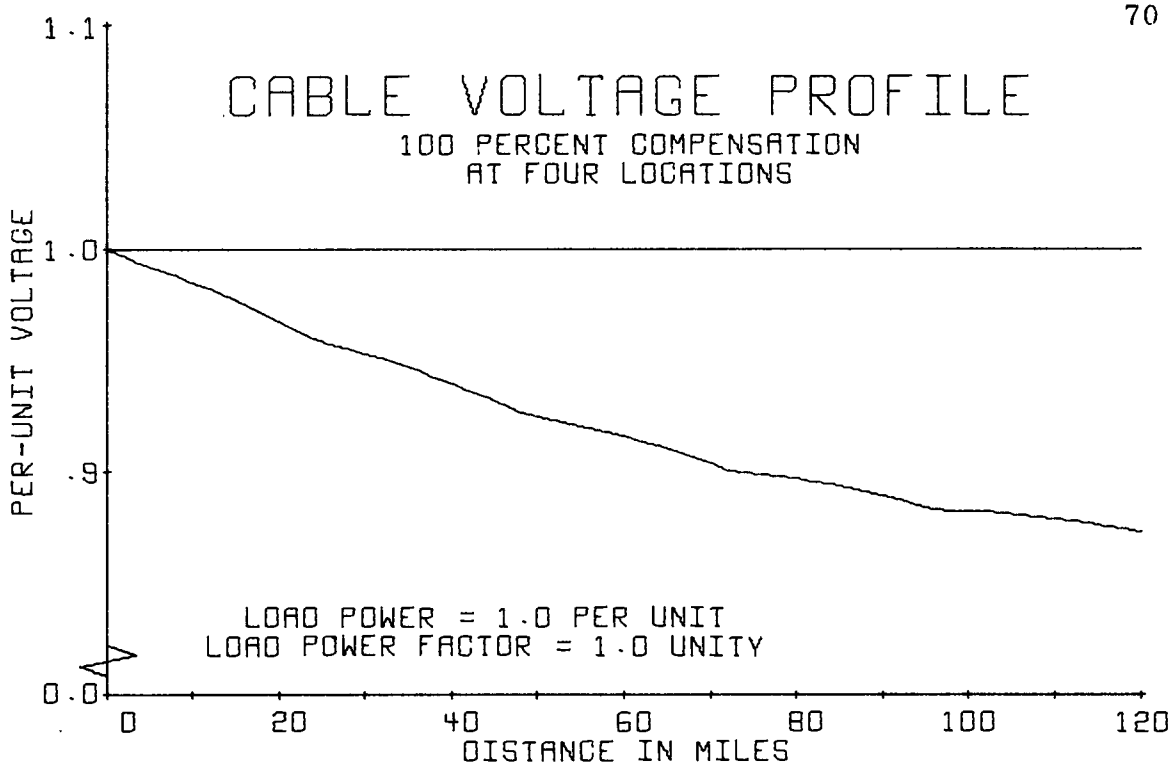

FIGURE 48. PER-UNIT VOLTAGE MAGNITUDE VERSUS DISTANCE FROM THE CABLE SENDING END.

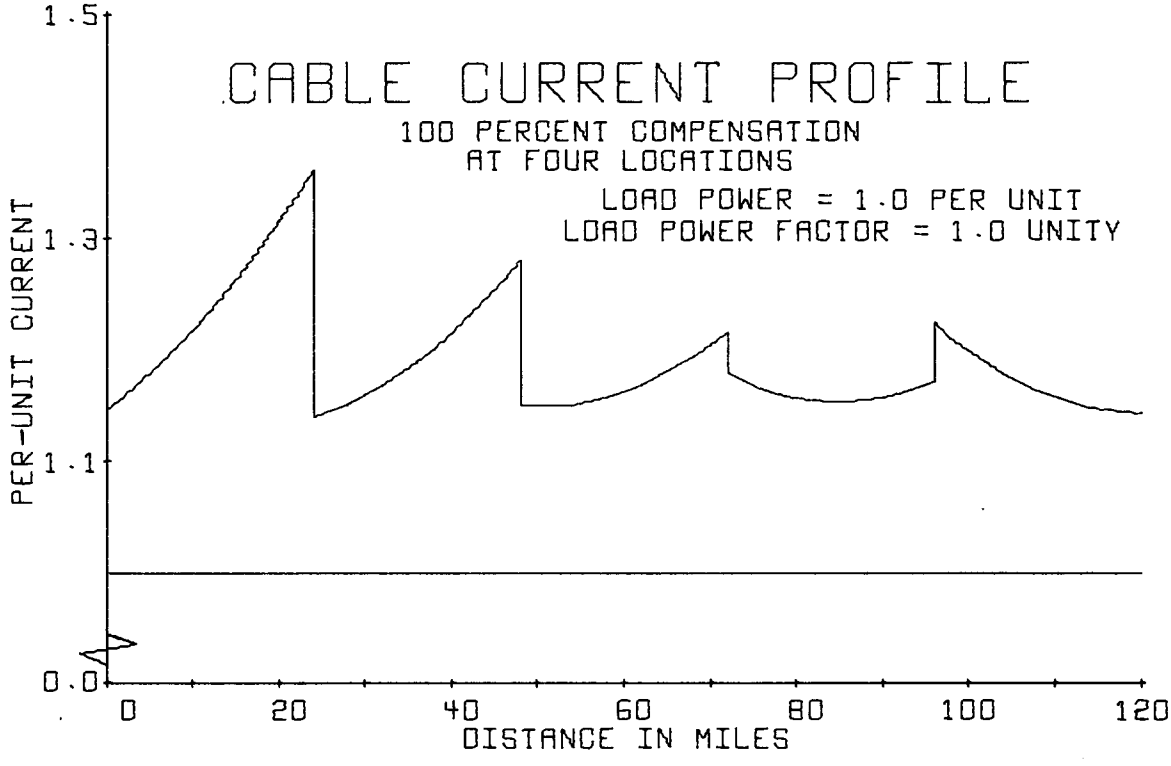

FIGURE 49. PER-UNIT CURRENT MAGNITUDE VERSUS DISTANCE FROM THE CABLE SENDING END.

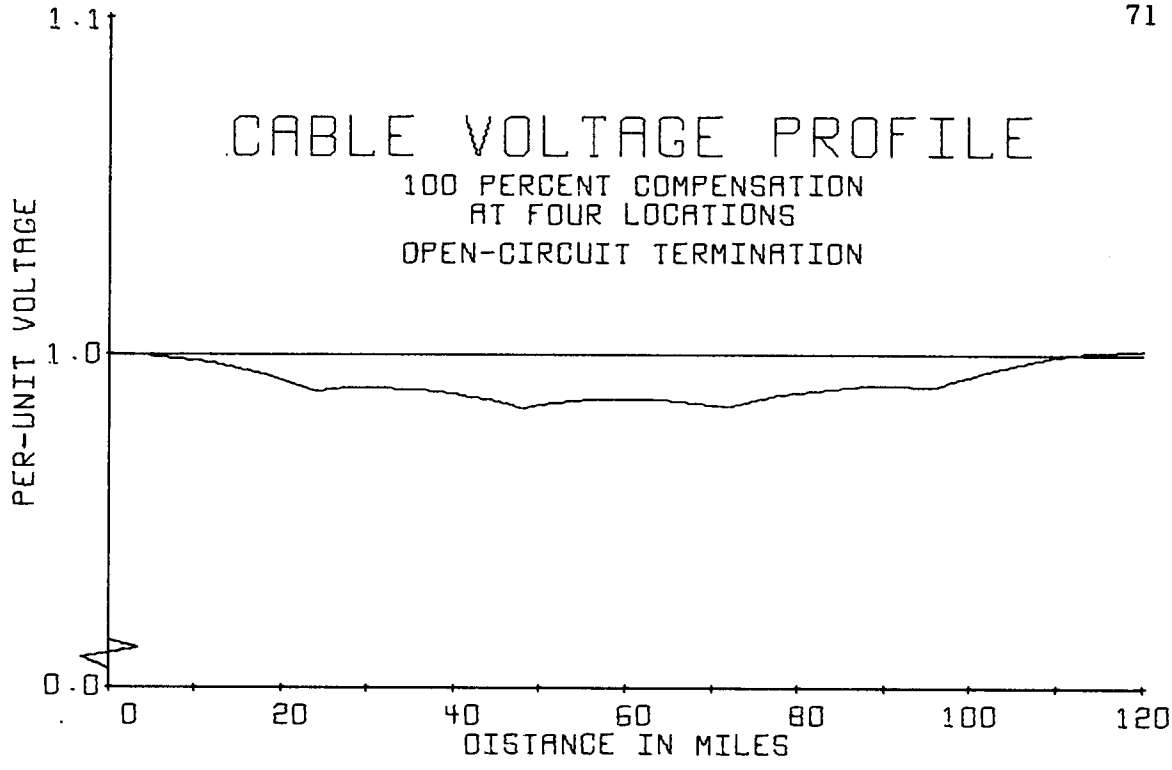

FIGURE 50. PER-UNIT VOLTAGE MAGNITUDE VERSUS DISTANCE FROM THE CABLE SENDING END.

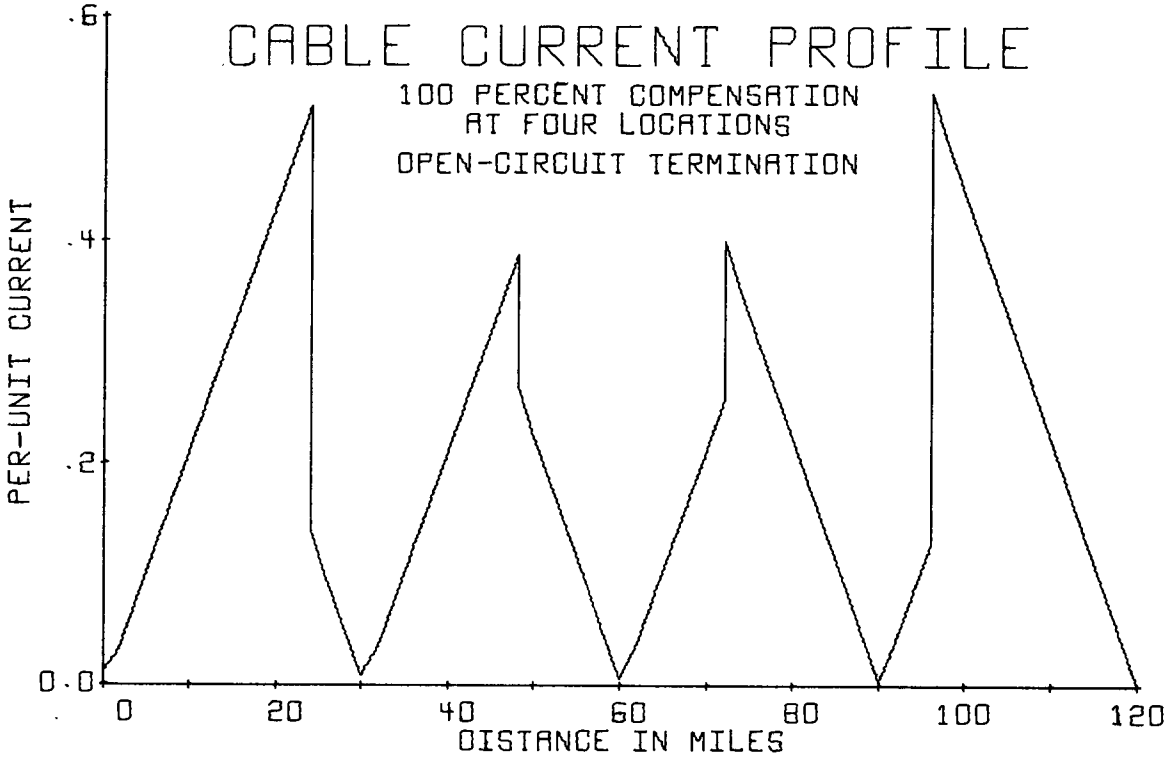

FIGURE 51. PER-UNIT CURRENT MAGNITUDE VERSUS DISTANCE FROM THE CABLE SENDING END.

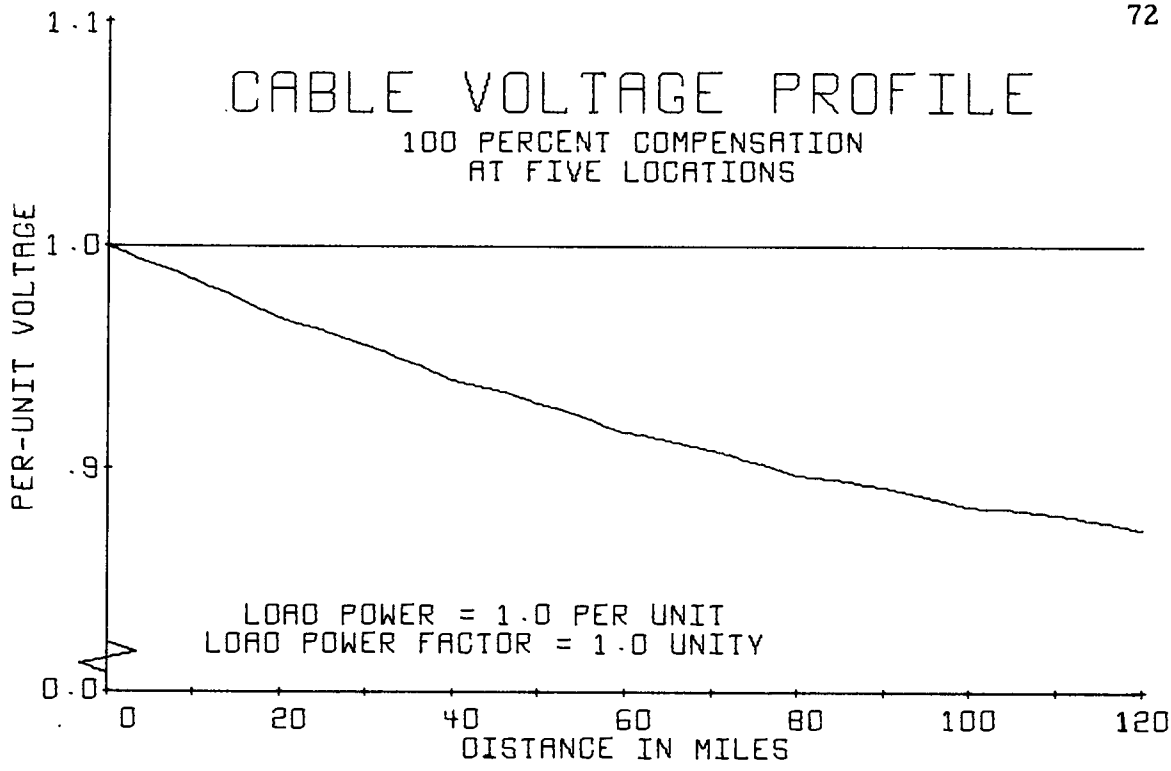

FIGURE 52. PER-UNIT VOLTAGE MAGNITUDE VERSUS DISTANCE FROM THE CABLE SENDING END.

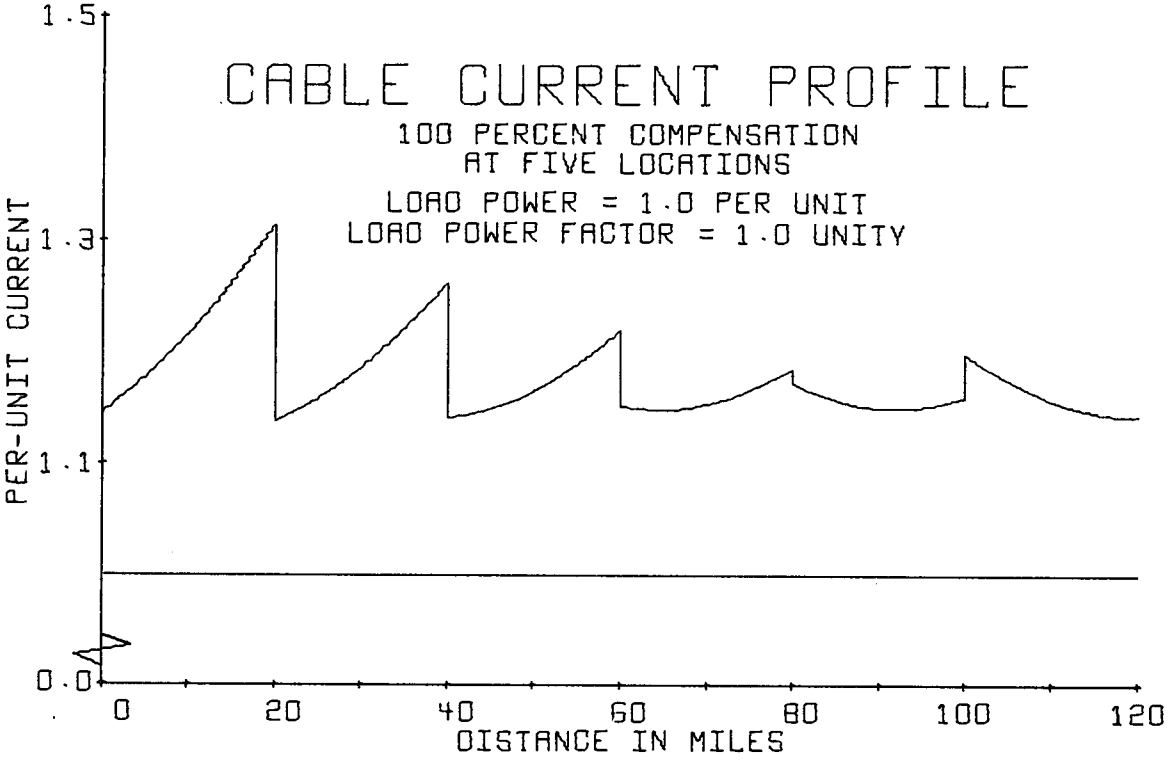

FIGURE 53. PER-UNIT CURRENT MAGNITUDE VERSUS DISTANCE FROM THE CABLE SENDING END.

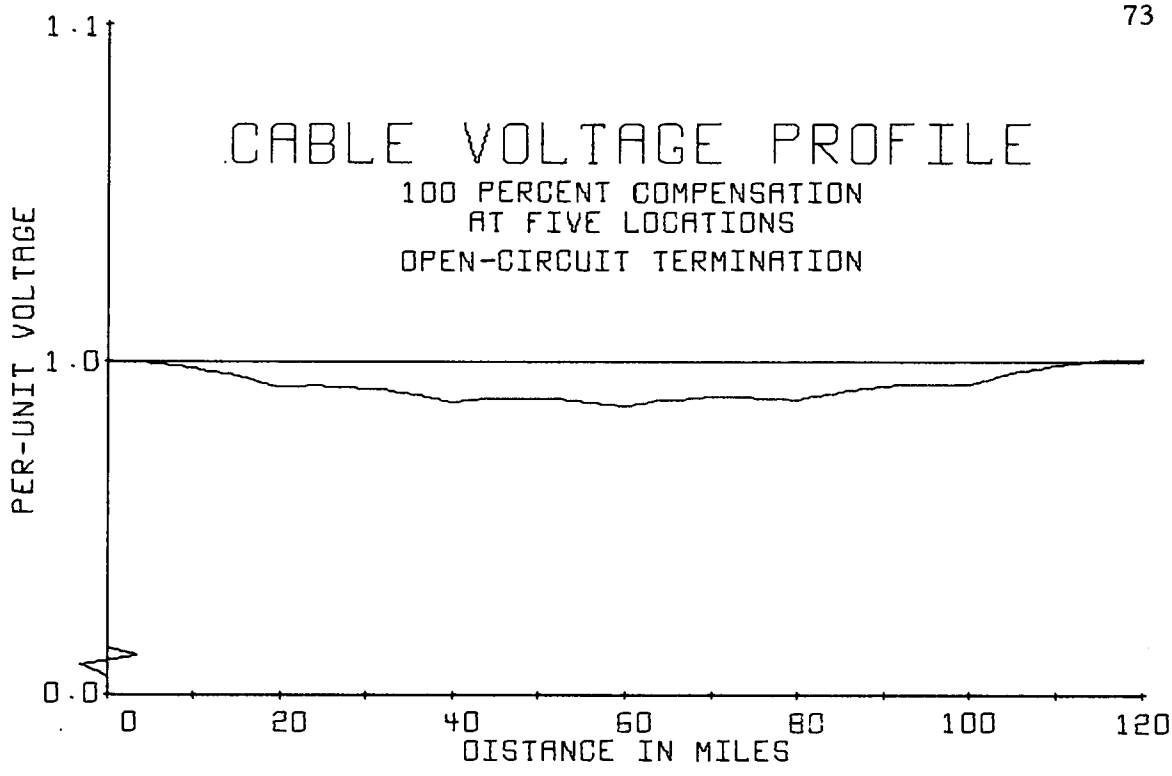

FIGURE 54. PER-UNIT VOLTAGE MAGNITUDE VERSUS DISTANCE FROM THE CABLE SENDING END.

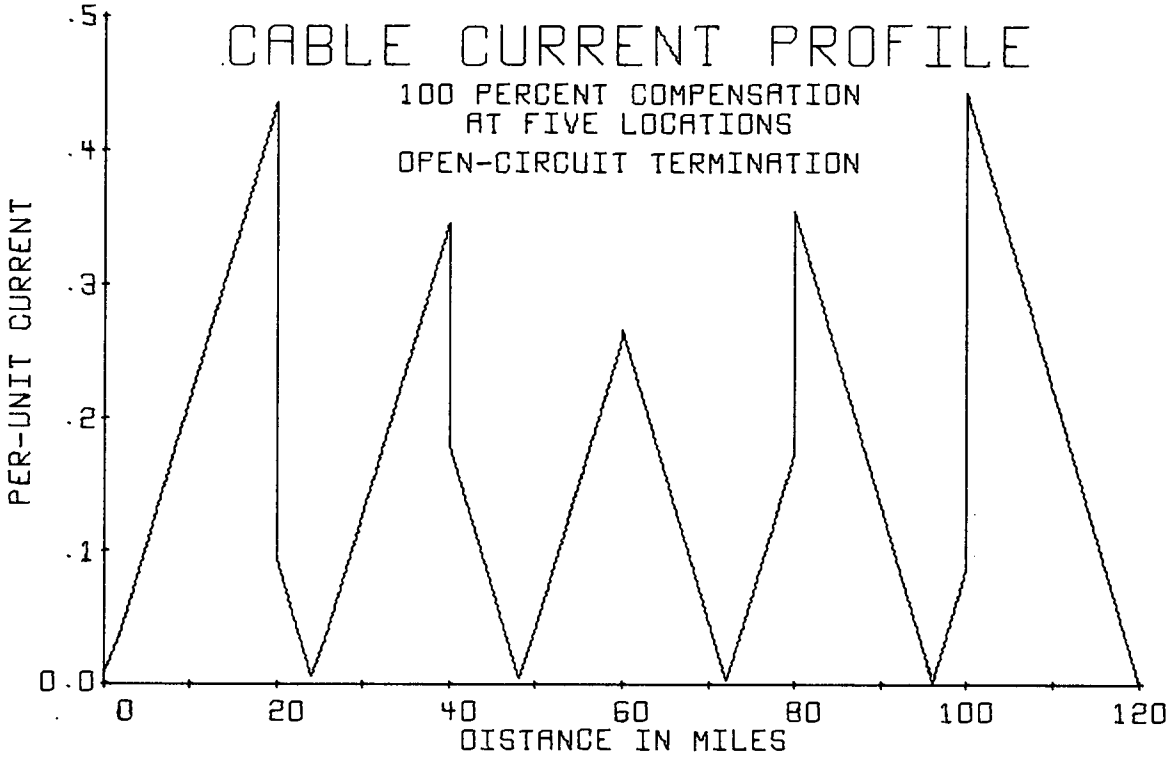

FIGURE 55. PER-UNIT CURRENT MAGNITUDE VERSUS DISTANCE FROM THE CABLE SENDING END.

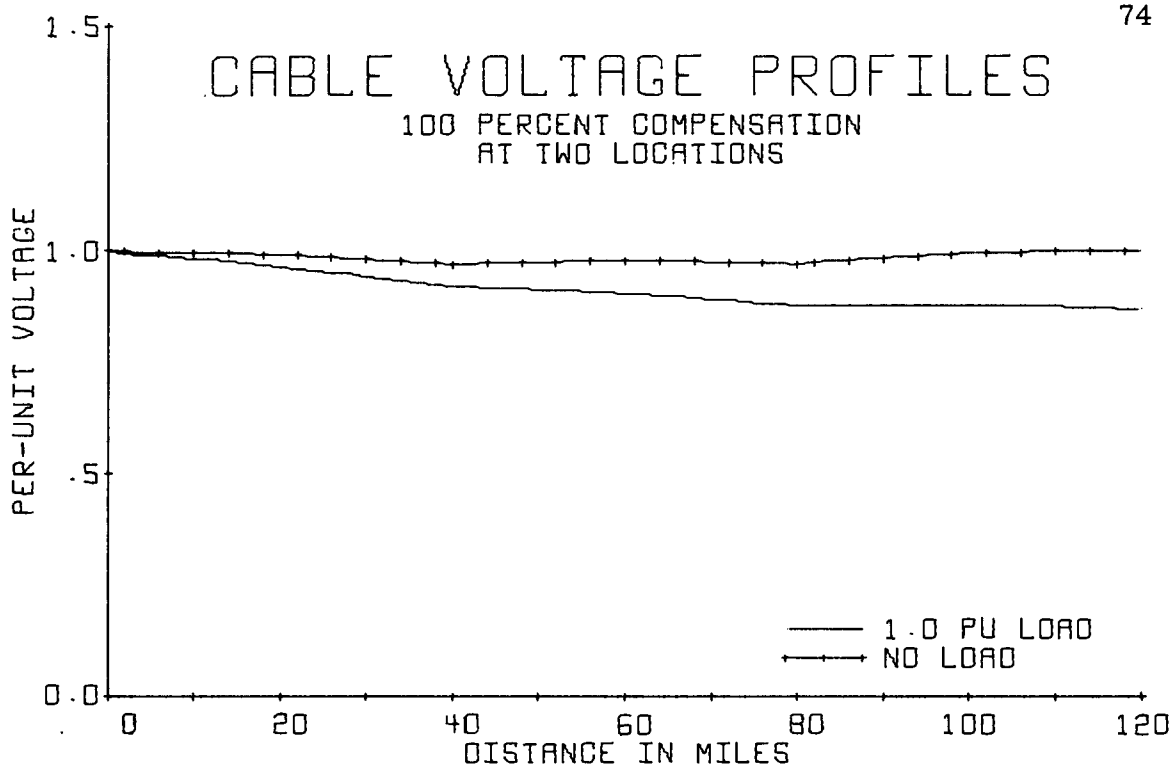

FIGURE 56. PER-UNIT VOLTAGE MAGNITUDES VERSUS DISTANCE FROM THE CABLE SENDING END FOR A UNITY PF LOAD.

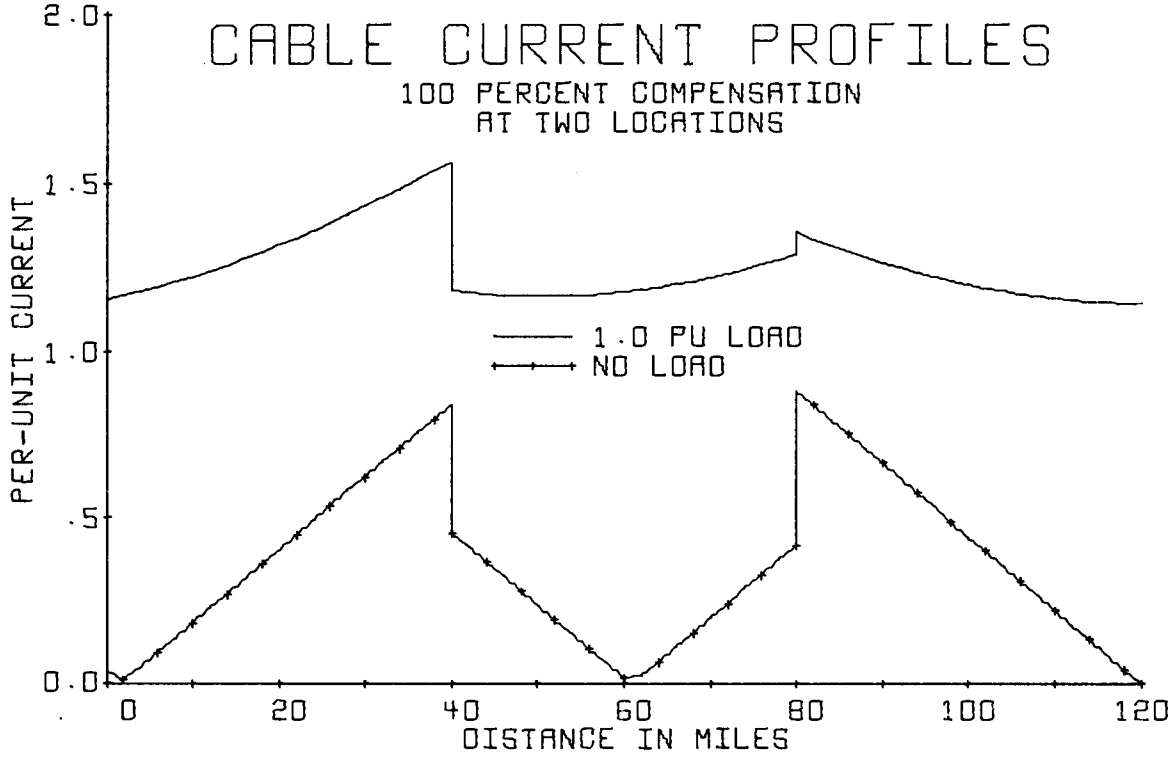

FIGURE 57. PER-UNIT CURRENT MAGNITUDES VERSUS DISTANCE FROM THE CABLE SENDING END FOR A UNITY PF LOAD.

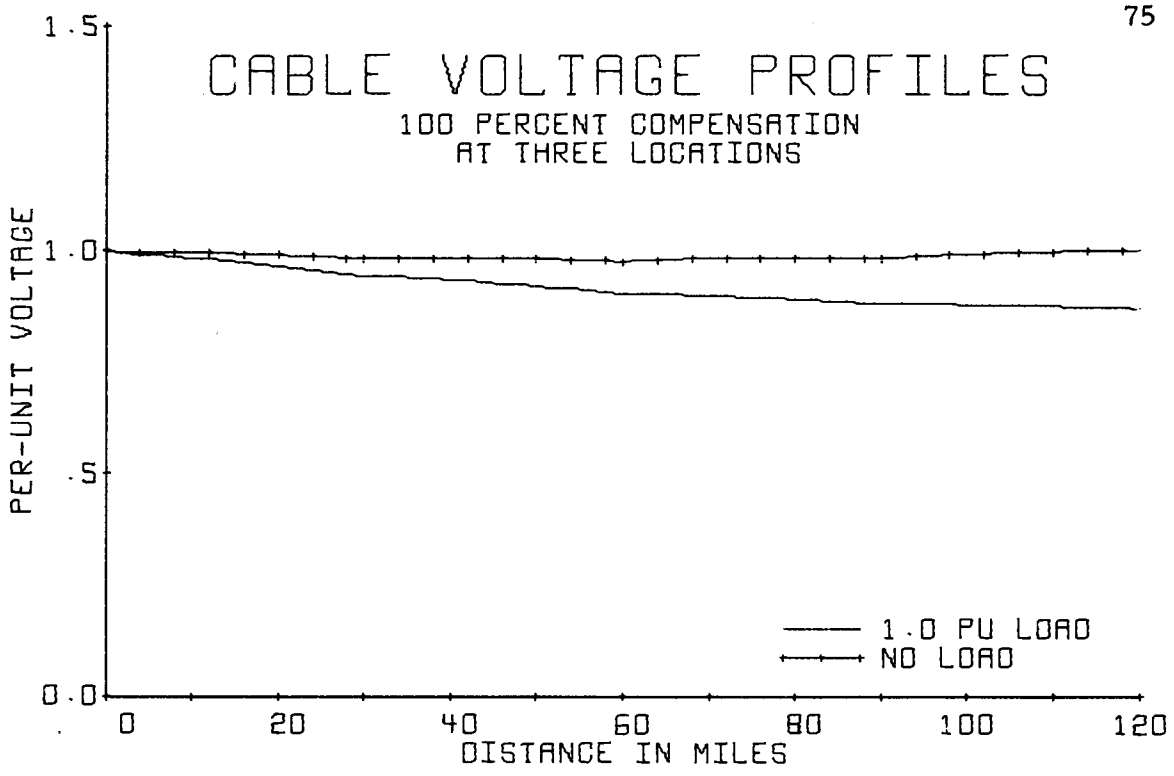

FIGURE 58. PER-UNIT VOLTAGE MAGNITUDES VERSUS DISTANCE FROM THE CABLE SENDING END FOR A UNITY PF LOAD.

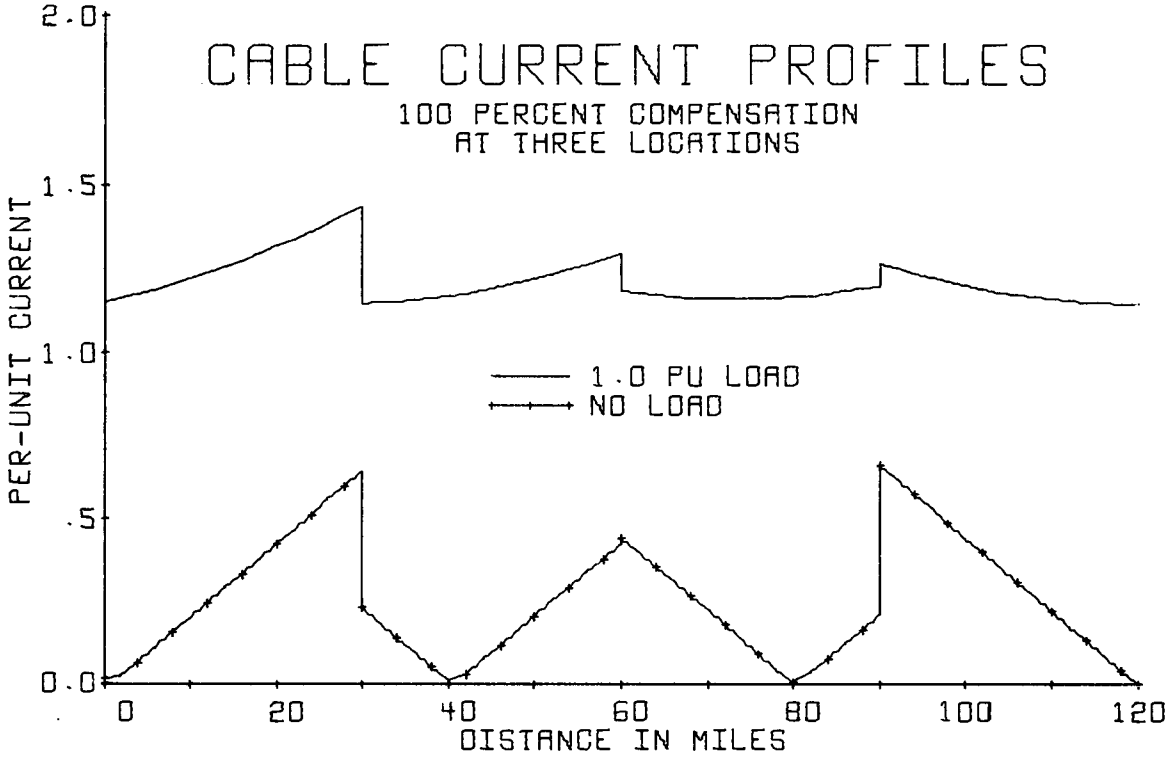

FIGURE 59. PER-UNIT CURRENT MAGNITUDES VERSUS DISTANCE FROM THE CABLE SENDING END FOR A UNITY PF LOAD.

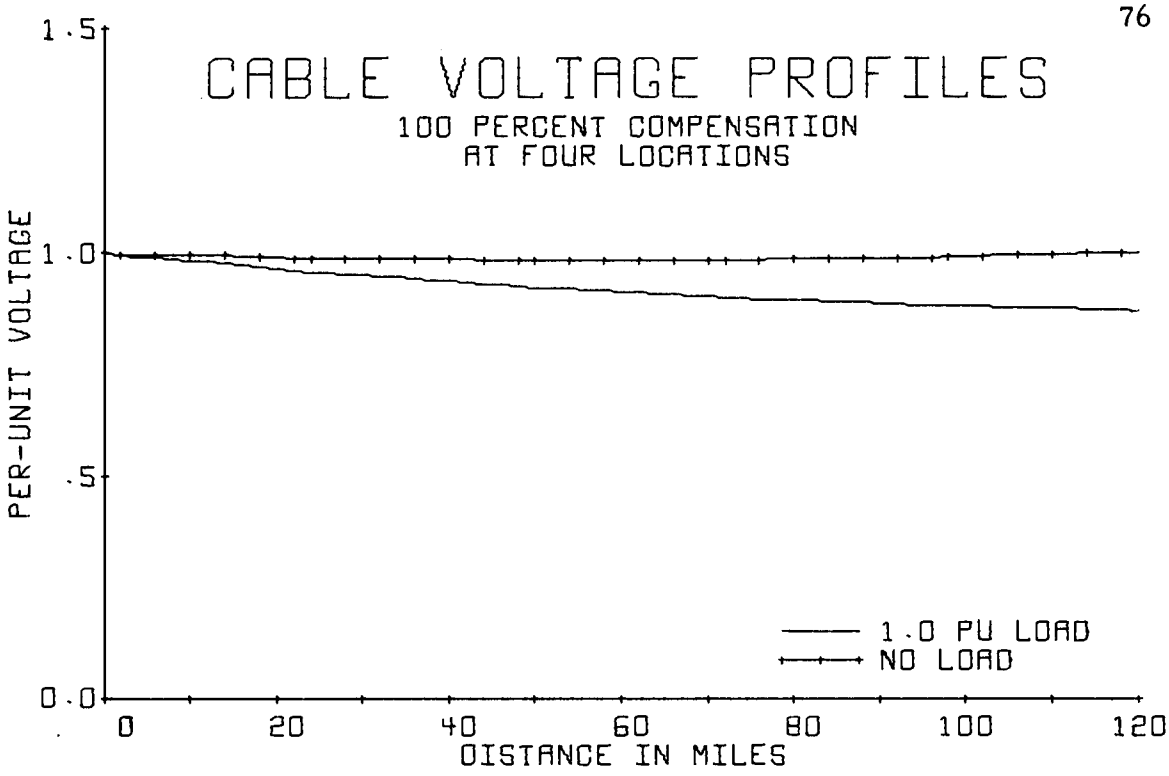

FIGURE 60. PER-UNIT VOLTAGE MAGNITUDES VERSUS DISTANCE FROM THE CABLE SENDING END FOR A UNITY PF LOAD.

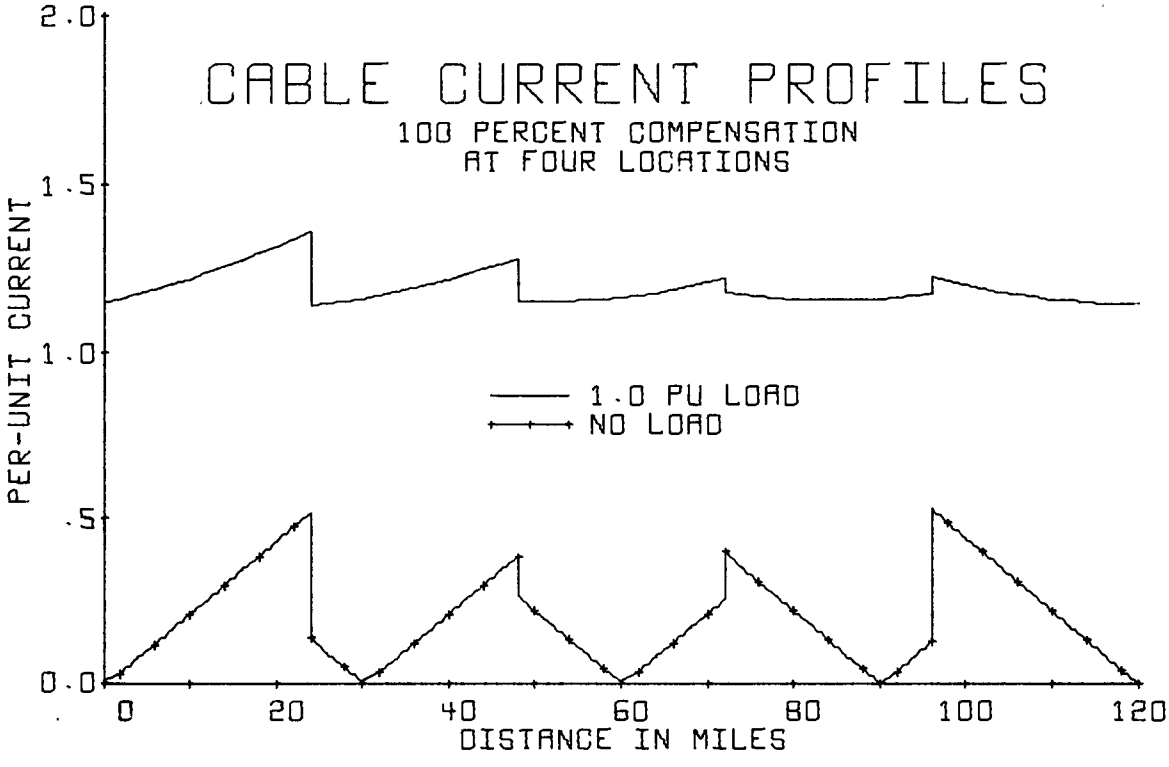

FIGURE 61. PER-UNIT CURRENT MAGNITUDES VERSUS DISTANCE FROM THE CABLE SENDING END FOR A UNITY PF LOAD.

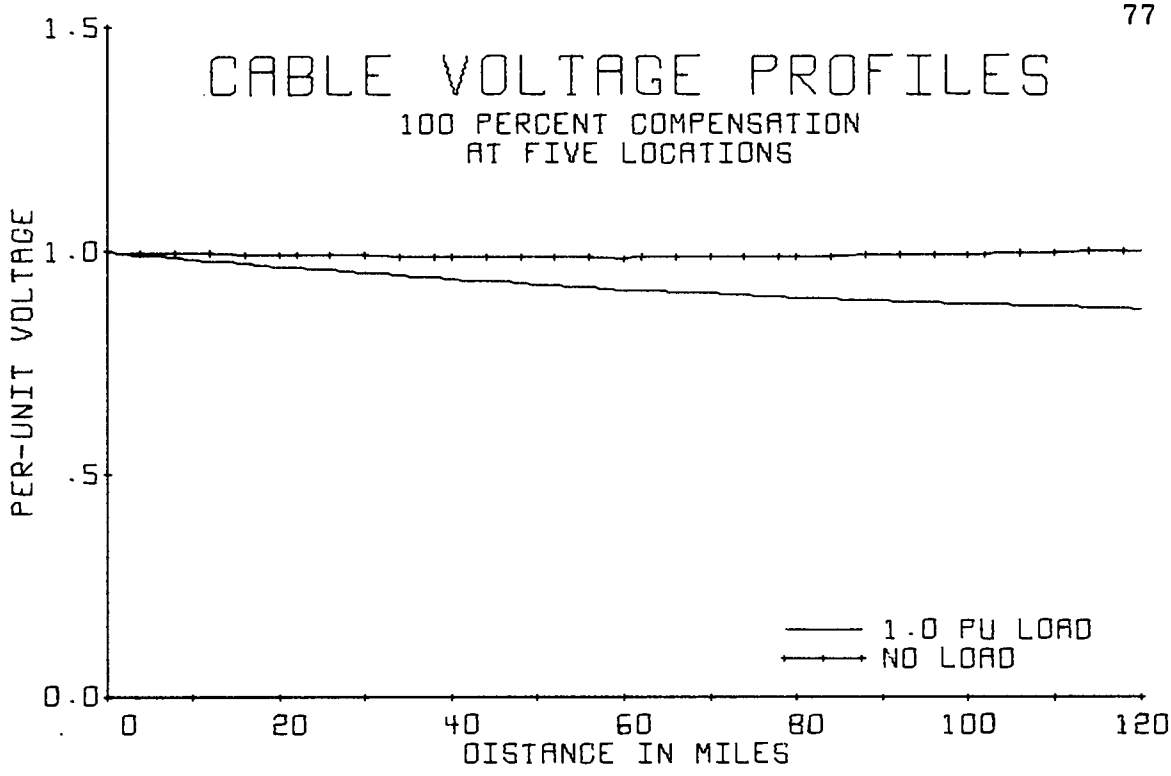

FIGURE 62. PER-UNIT VOLTAGE MAGNITUDES VERSUS DISTANCE FROM THE CABLE SENDING END FOR A UNITY PF LOAD.

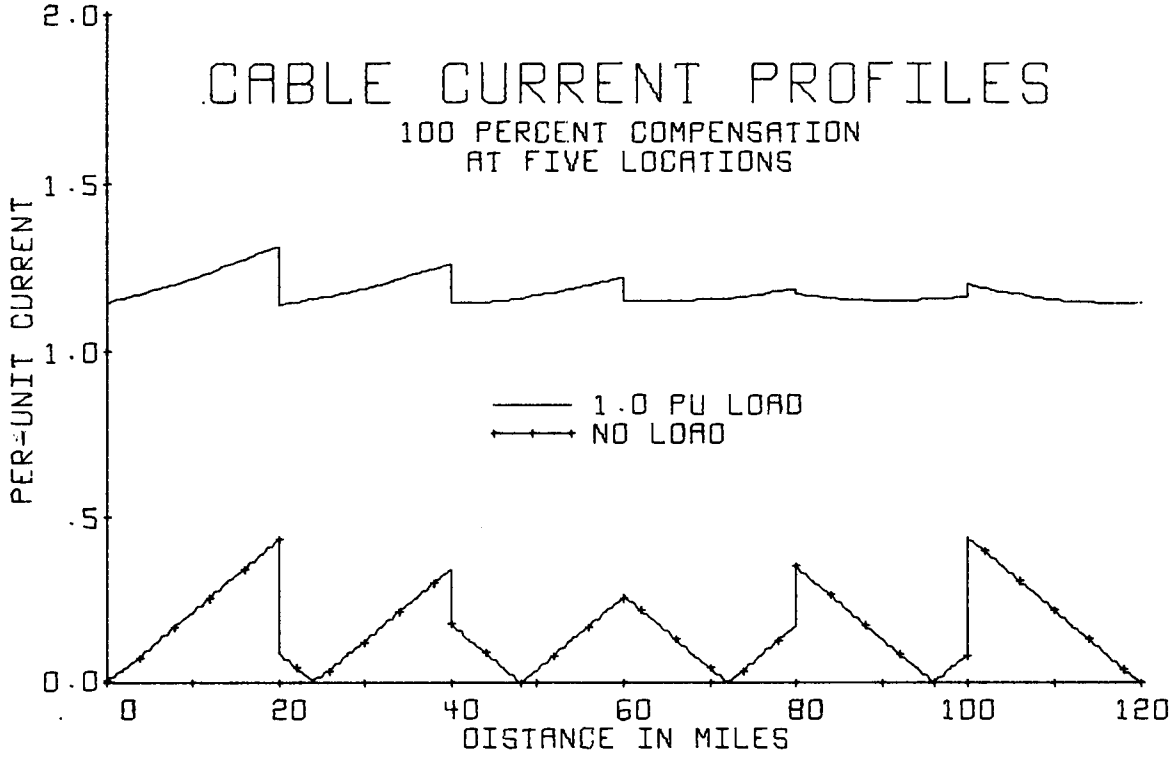

FIGURE 63. PER-UNIT CURRENT MAGNITUDES VERSUS DISTANCE FROM THE CABLE SENDING END FOR A UNITY PF LOAD.

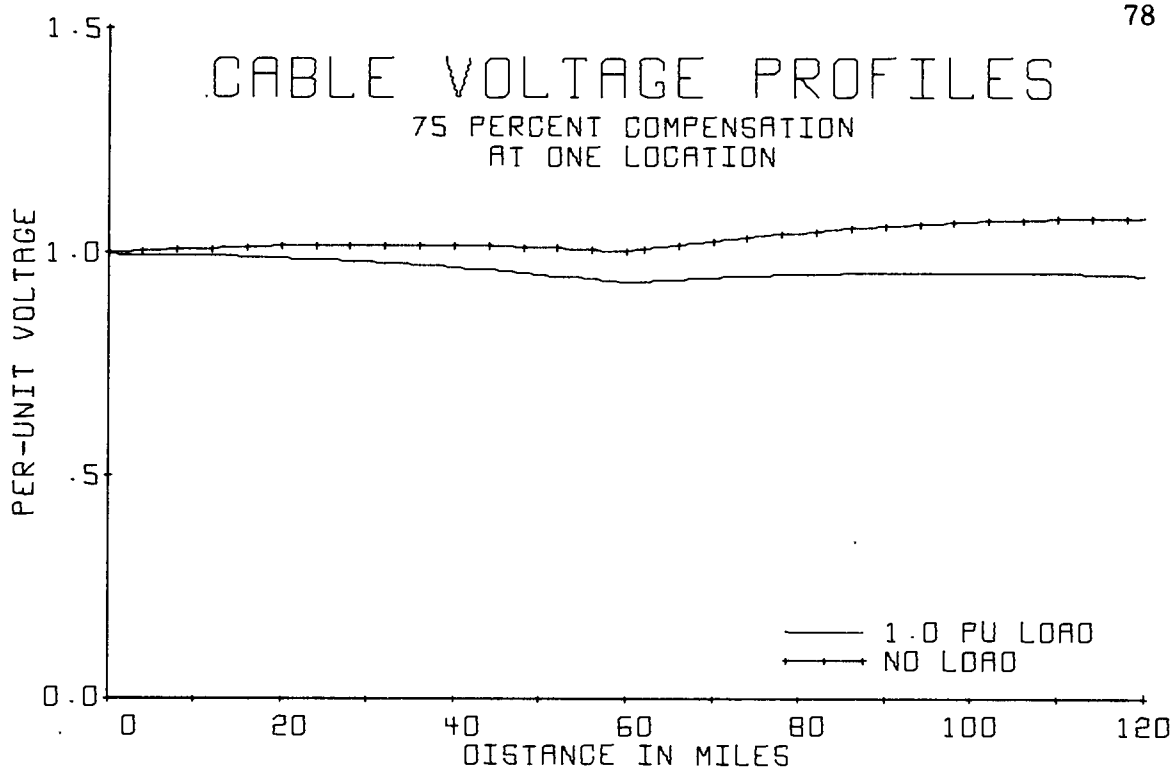

FIGURE 64. PER-UNIT VOLTAGE MAGNITUDES VERSUS DISTANCE FROM THE CABLE SENDING END FOR A UNITY PF LOAD.

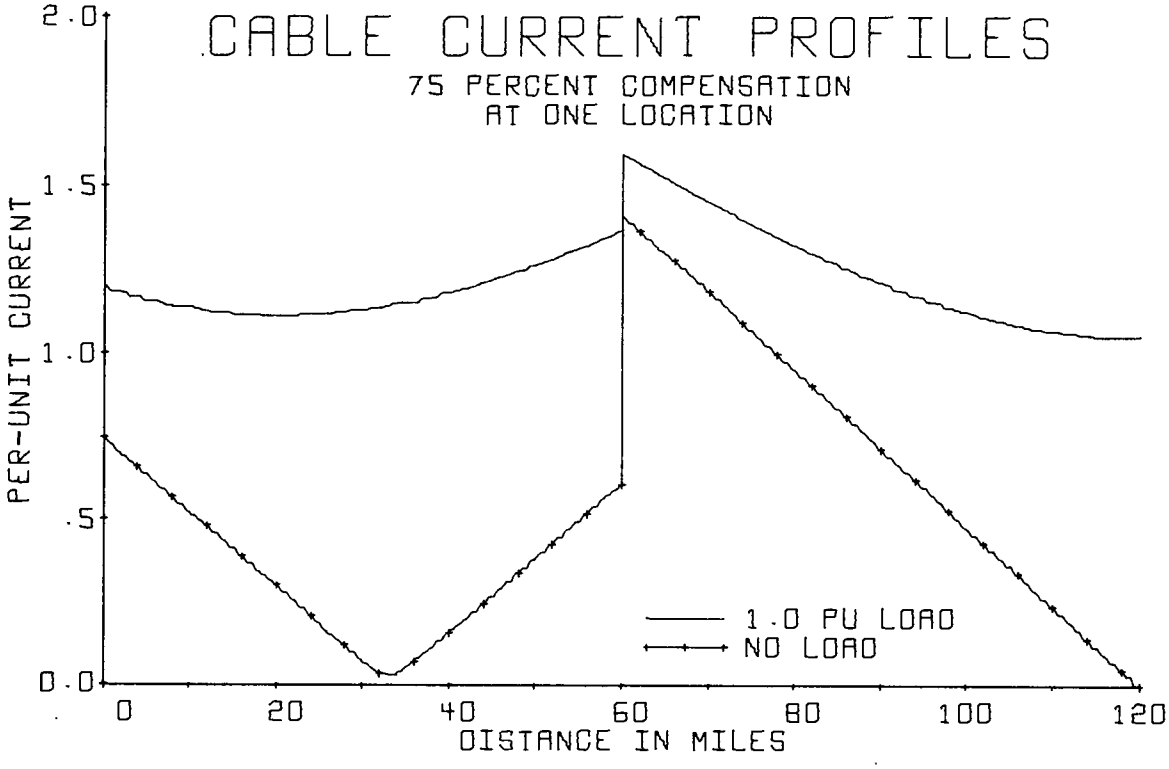

FIGURE 65. PER-UNIT CURRENT MAGNITUDES VERSUS DISTANCE FROM THE CABLE SENDING END FOR A UNITY PF LOAD.

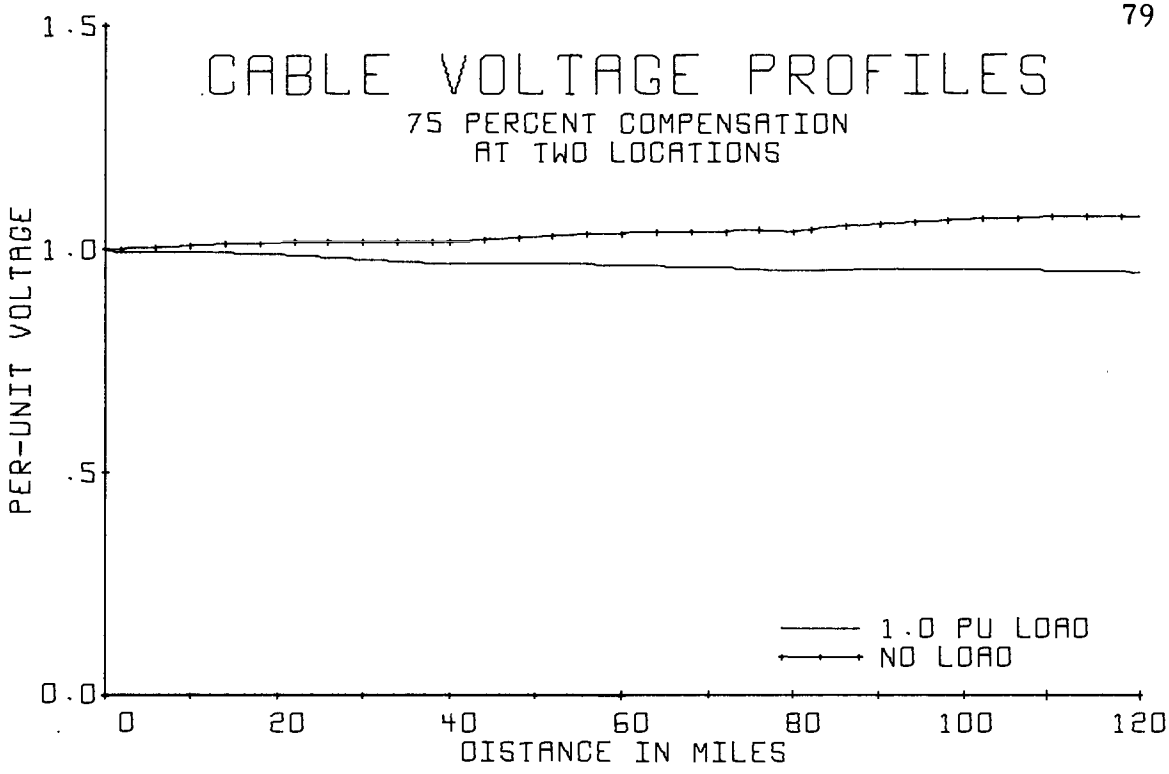

FIGURE 66. PER-UNIT VOLTAGE MAGNITUDES VERSUS DISTANCE FROM THE CABLE SENDING END FOR A UNITY PF LOAD.

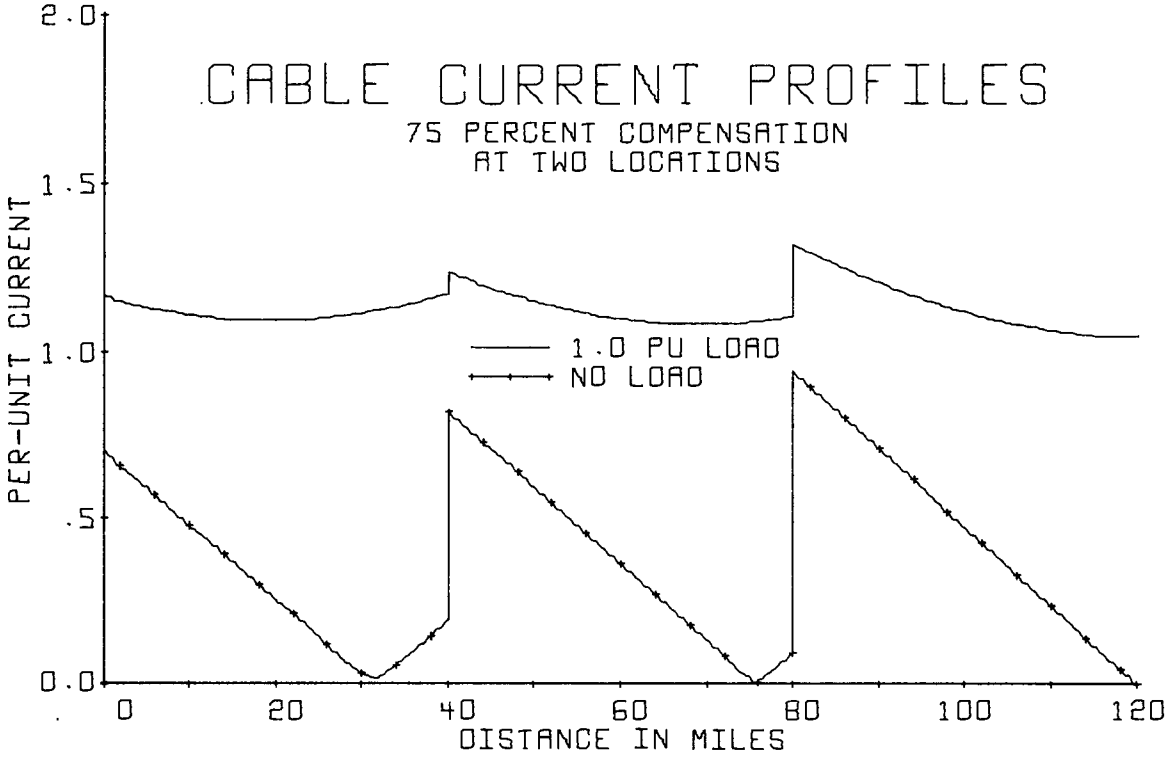

FIGURE 67. PER-UNIT CURRENT MAGNITUDES VERSUS DISTANCE FROM THE CABLE SENDING END FOR A UNITY PF LOAD.

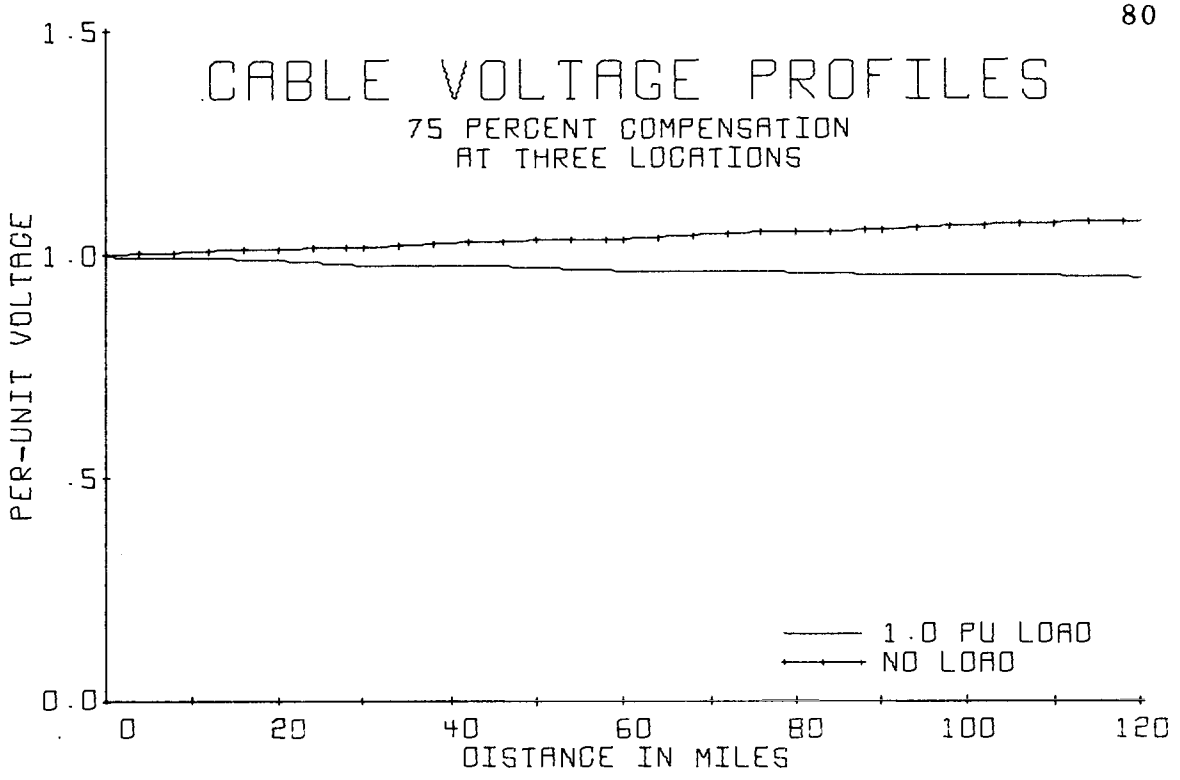

FIGURE 68. PER-UNIT VOLTAGE MAGNITUDES VERSUS DISTANCE FROM THE CABLE SENDING END FOR A UNITY PF LOAD.

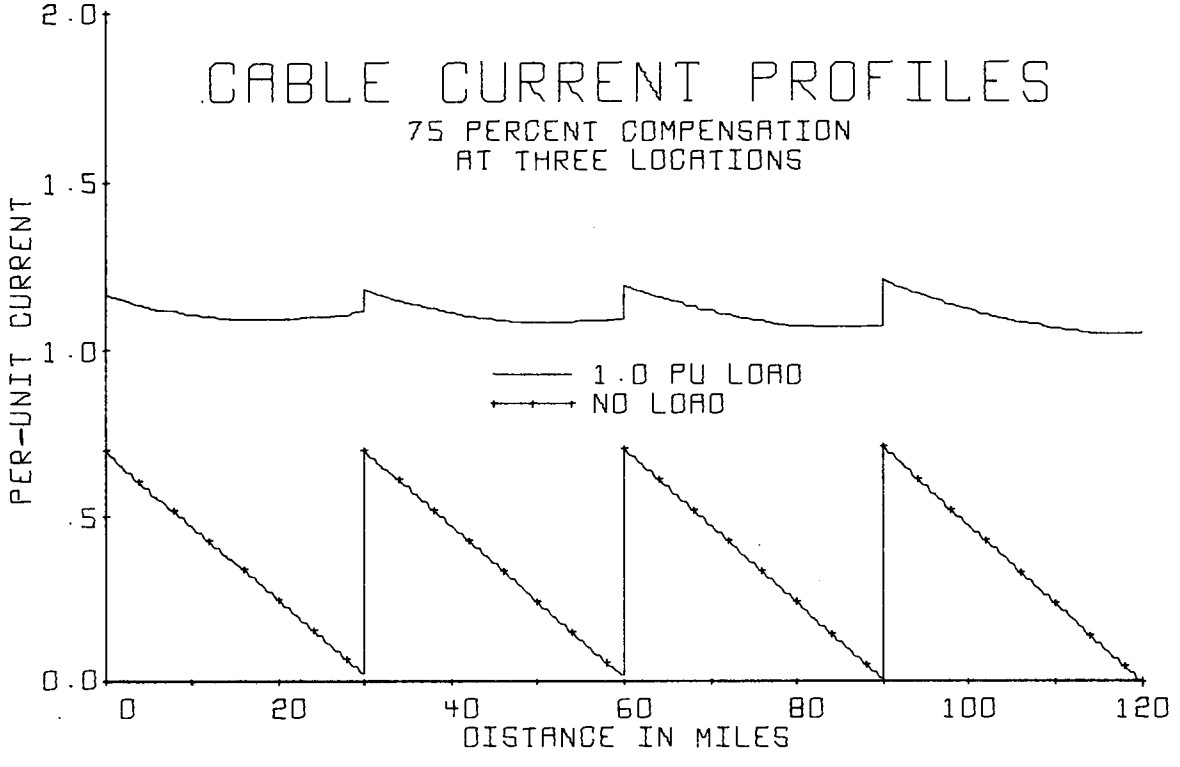

FIGURE 69. PER-UNIT CURRENT MAGNITUDES VERSUS DISTANCE FROM THE CABLE SENDING END FOR A UNITY PF LOAD.

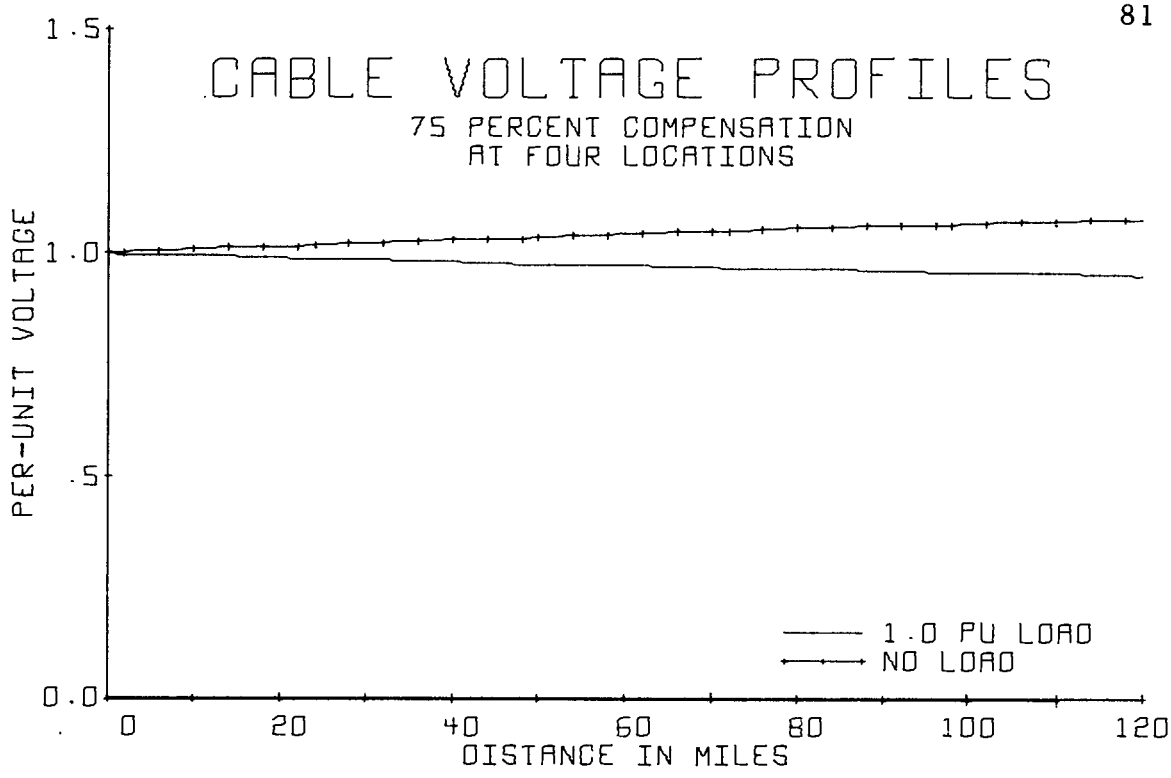

FIGURE 70. PER-UNIT VOLTAGE MAGNITUDES VERSUS DISTANCE FROM THE CABLE SENDING END FOR A UNITY PF LOAD.

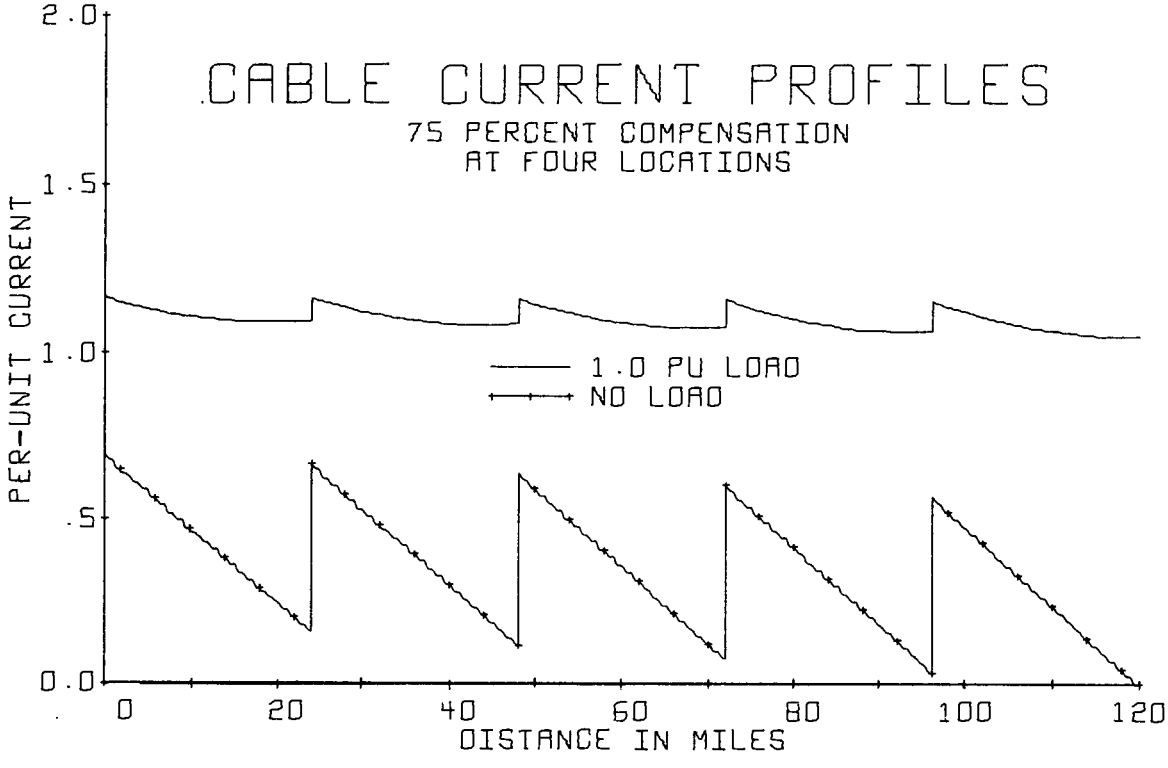

FIGURE 71. PER-UNIT CURRENT MAGNITUDES VERSUS DISTANCE FROM THE CABLE SENDING END FOR A UNITY PF LOAD.

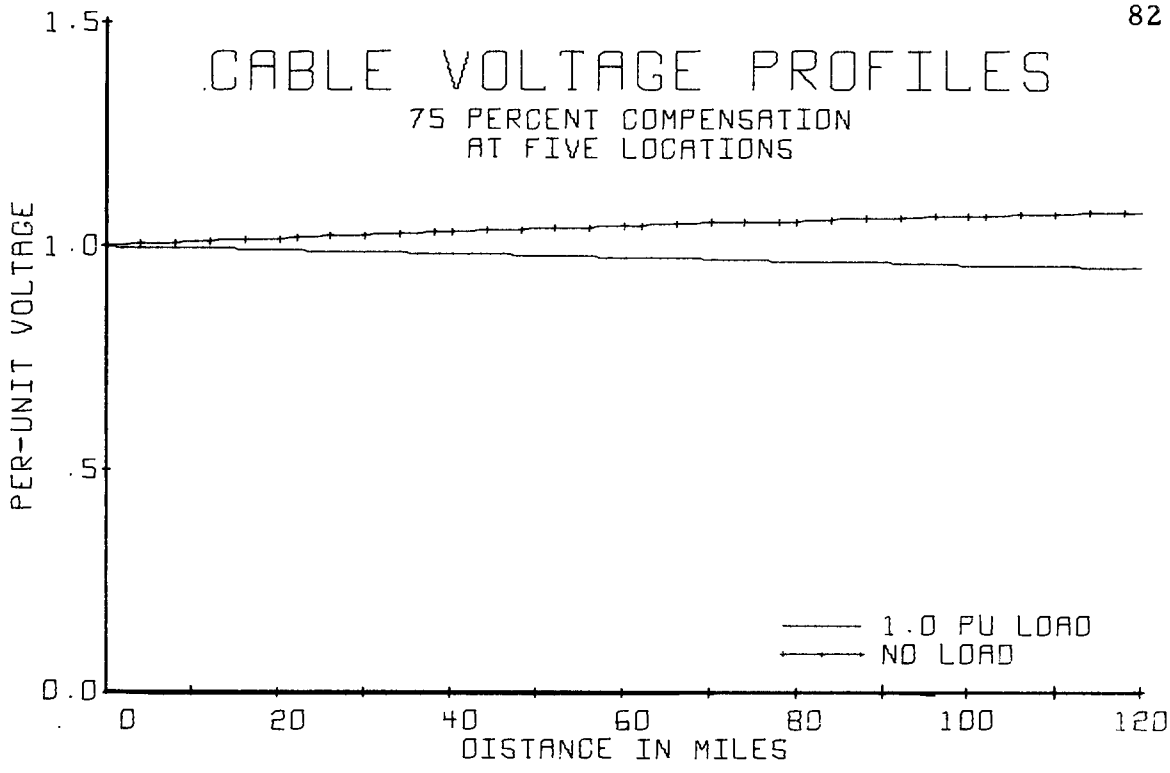

FIGURE 72. PER-UNIT VOLTAGE MAGNITUDES VERSUS DISTANCE FROM THE CABLE SENDING END FOR A UNITY PF LOAD.

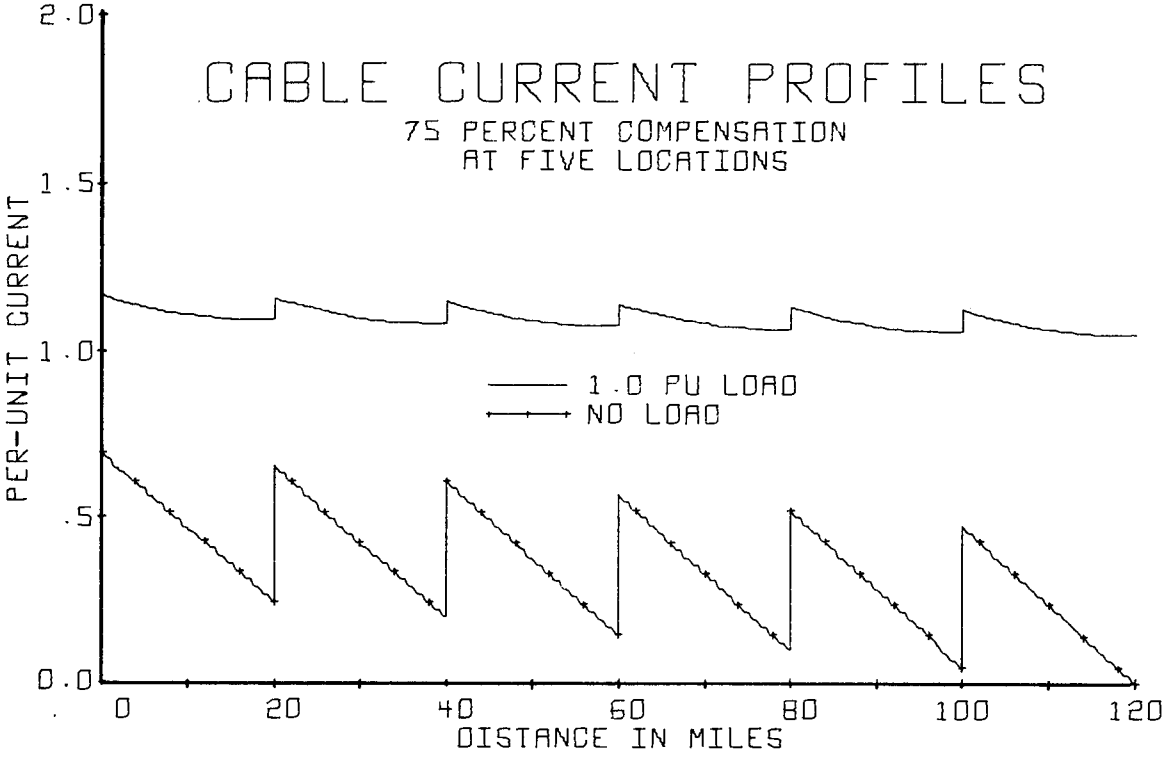

FIGURE 73. PER-UNIT CURRENT MAGNITUDES VERSUS DISTANCE FROM THE CABLE SENDING END FOR A UNITY PF LOAD.

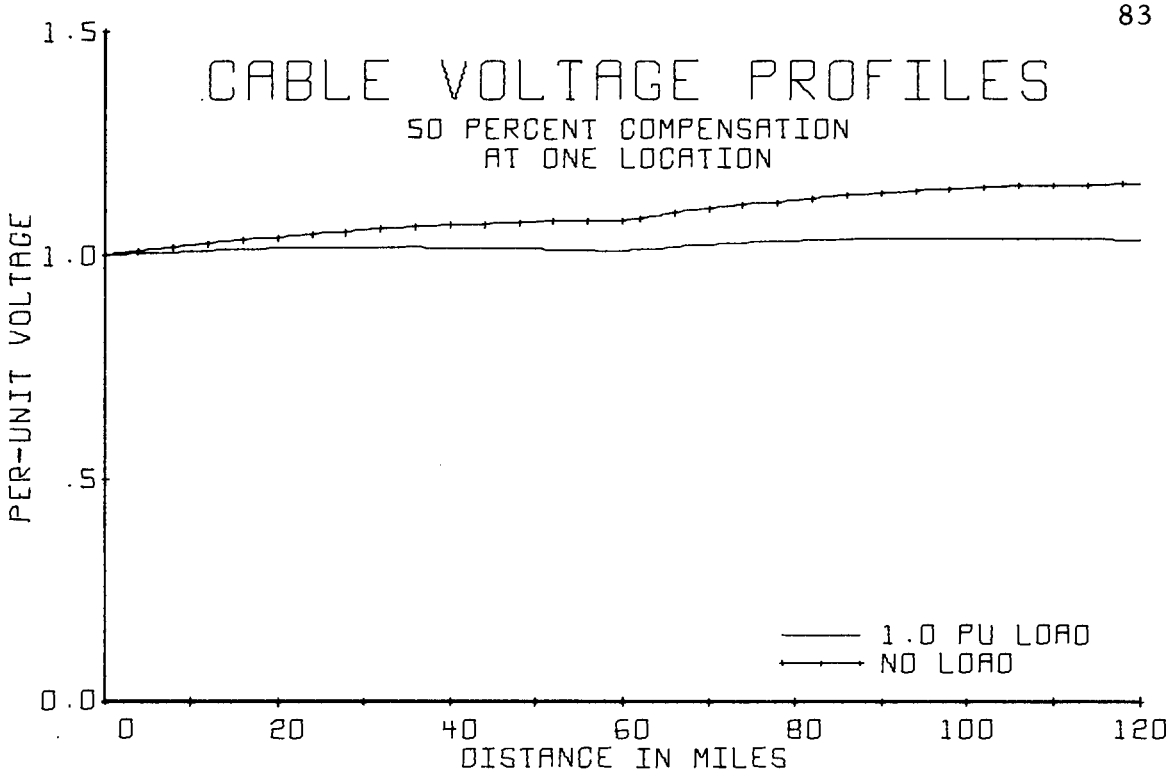

FIGURE 74. PER-UNIT VOLTAGE MAGNITUDES VERSUS DISTANCE FROM THE CABLE SENDING END FOR A UNITY PF LOAD.

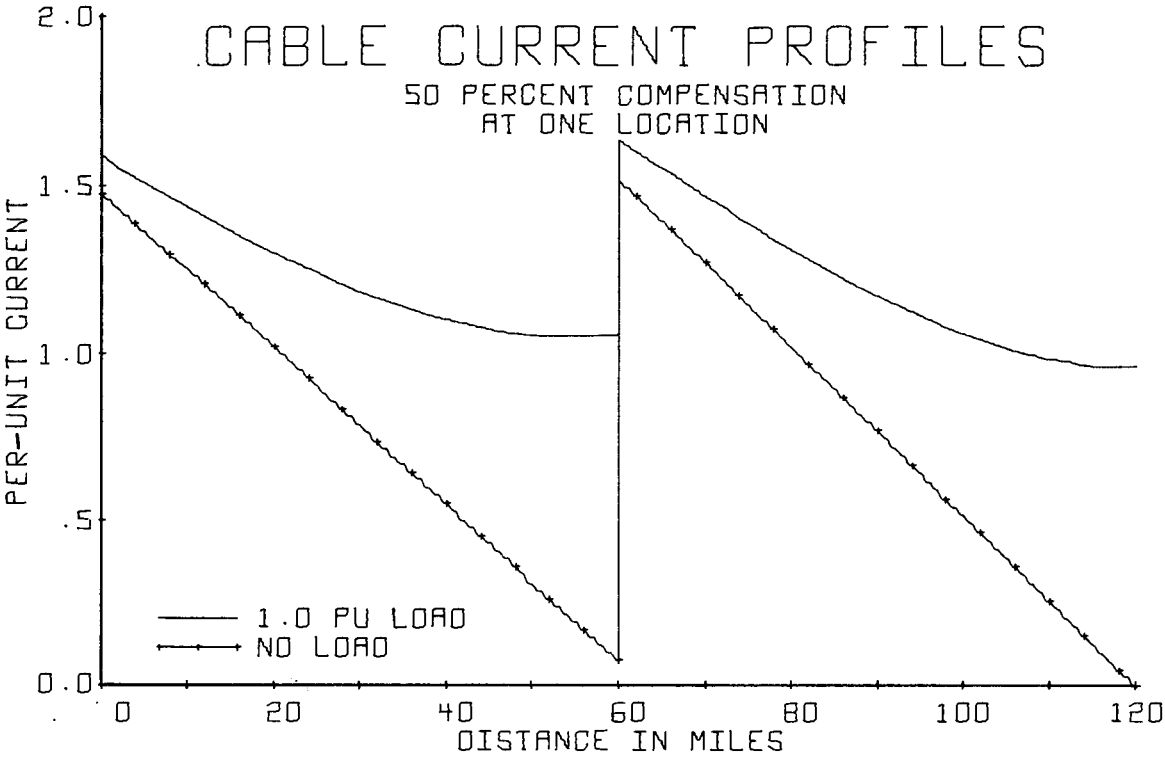

FIGURE 75. PER-UNIT CURRENT MAGNITUDES VERSUS DISTANCE FROM THE CABLE SENDING END FOR A UNITY PF LOAD.

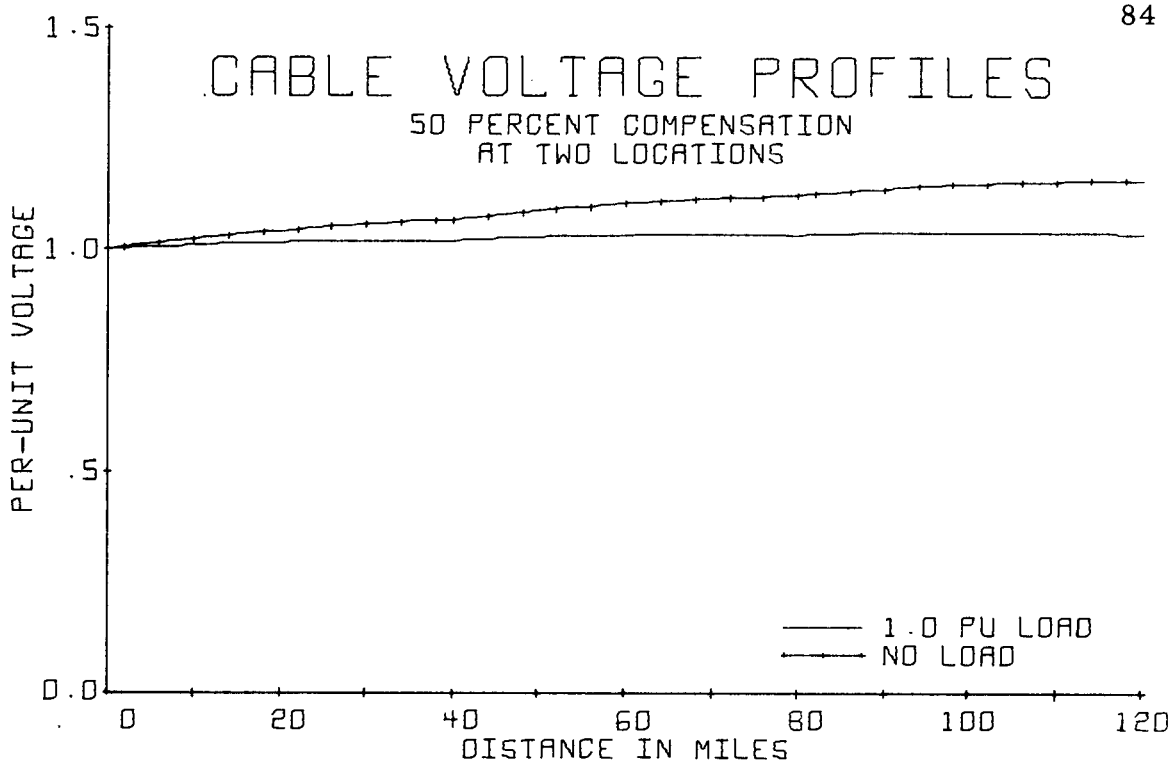

FIGURE 76. PER-UNIT VOLTAGE MAGNITUDES VERSUS DISTANCE FROM THE CABLE SENDING END FOR A UNITY PF LOAD.

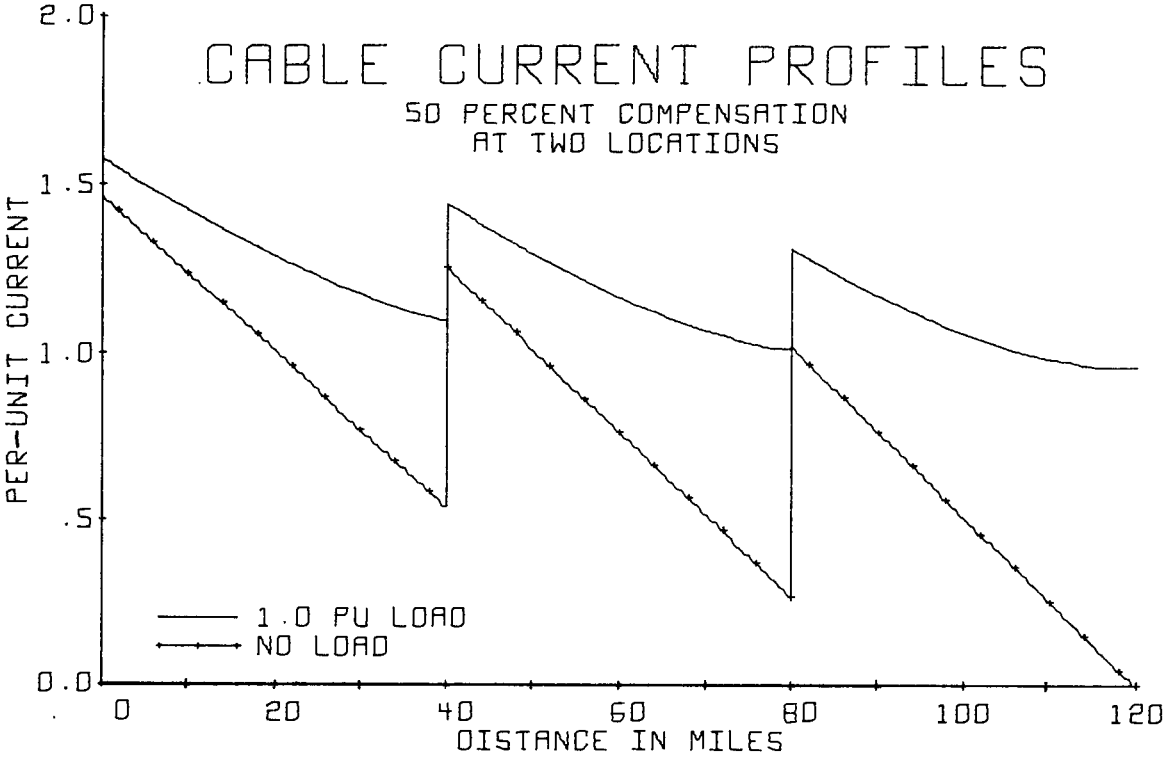

FIGURE 77. PER-UNIT CURRENT MAGNITUDES VERSUS DISTANCE FROM THE CABLE SENDING END FOR A UNITY PF LOAD.

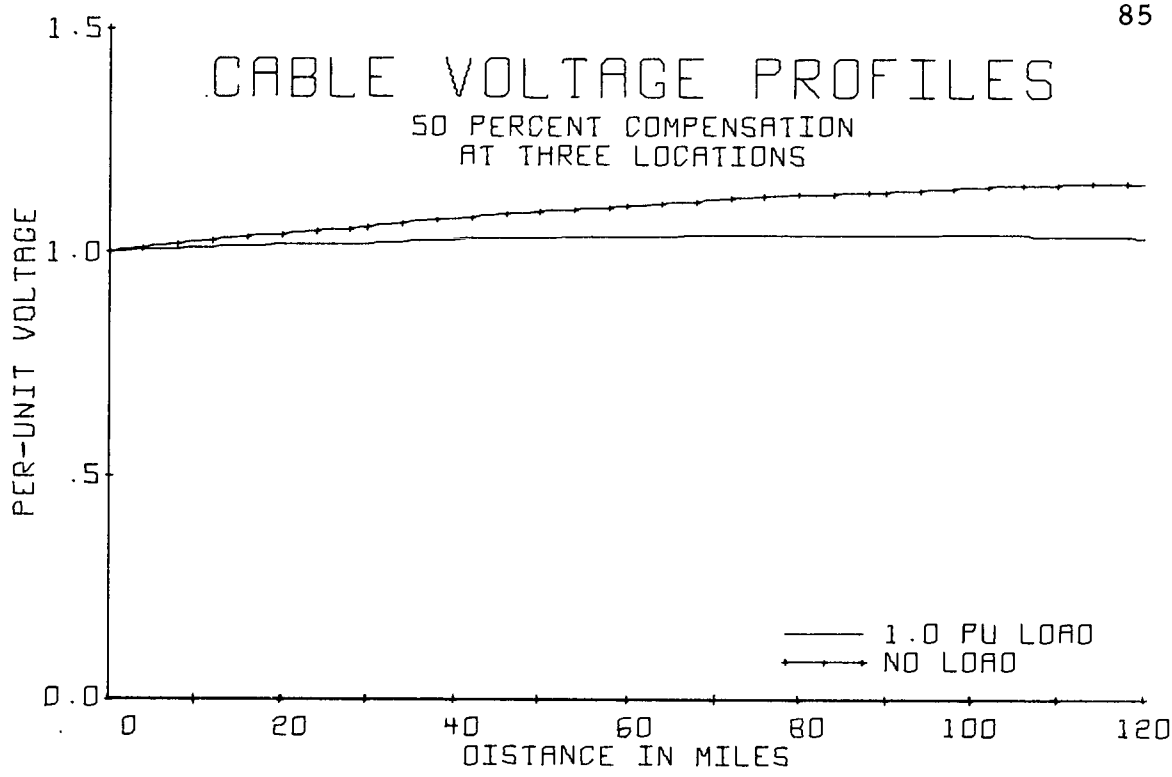

FIGURE 78. PER-UNIT VOLTAGE MAGNITUDES VERSUS DISTANCE FROM THE CABLE SENDING END FOR A UNITY PF LOAD.

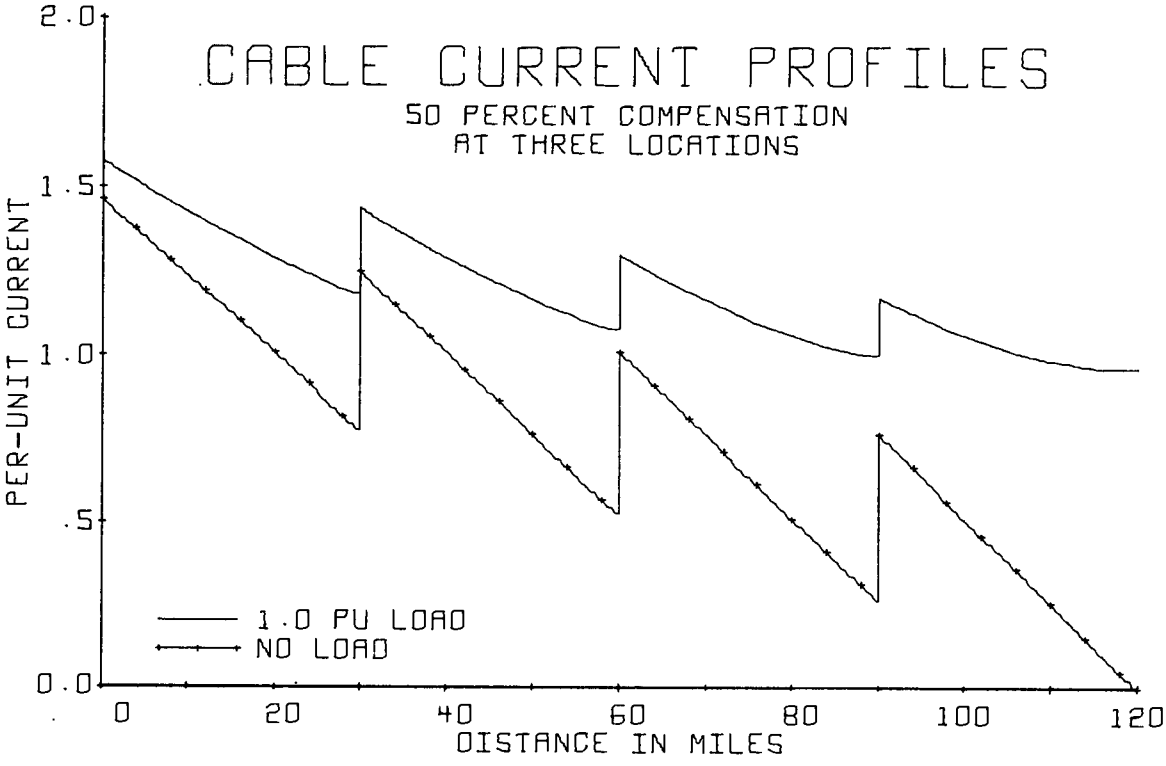

FIGURE 79. PER-UNIT CURRENT MAGNITUDES VERSUS DISTANCE FROM THE CABLE SENDING END FOR A UNITY PF LOAD.

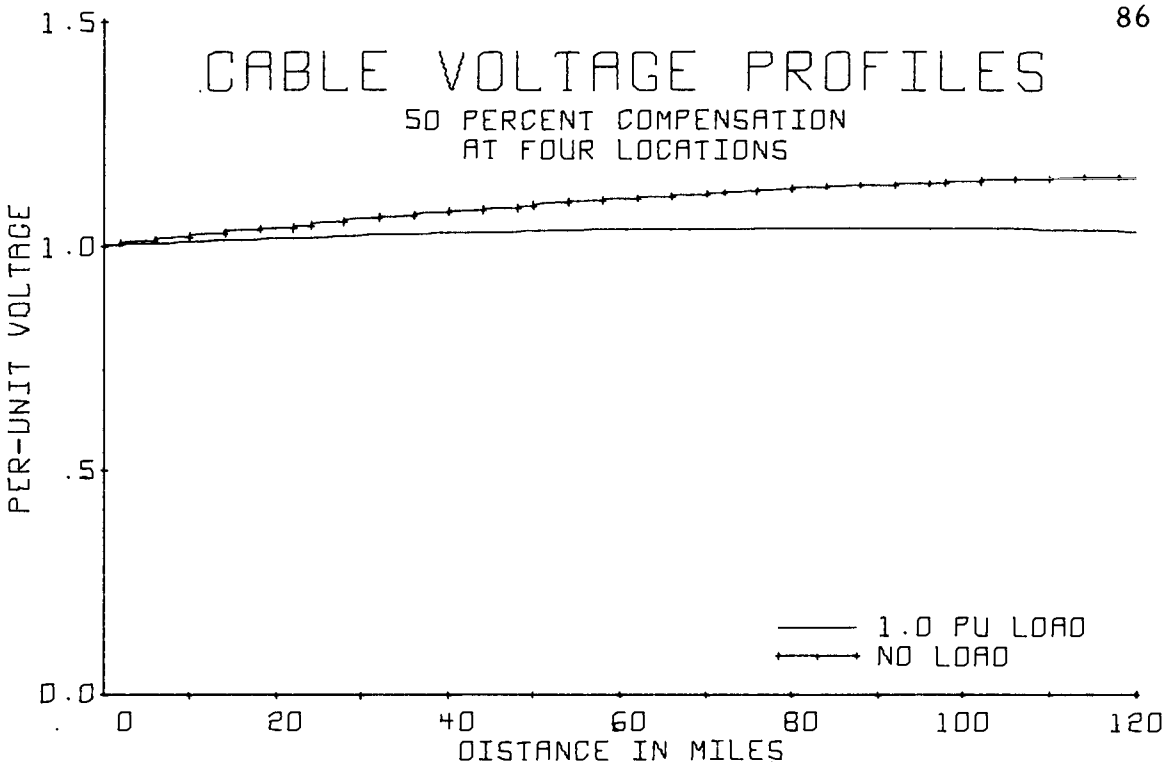

FIGURE 80. PER-UNIT VOLTAGE MAGNITUDES VERSUS DISTANCE FROM THE CABLE SENDING END FOR A UNITY PF LOAD.

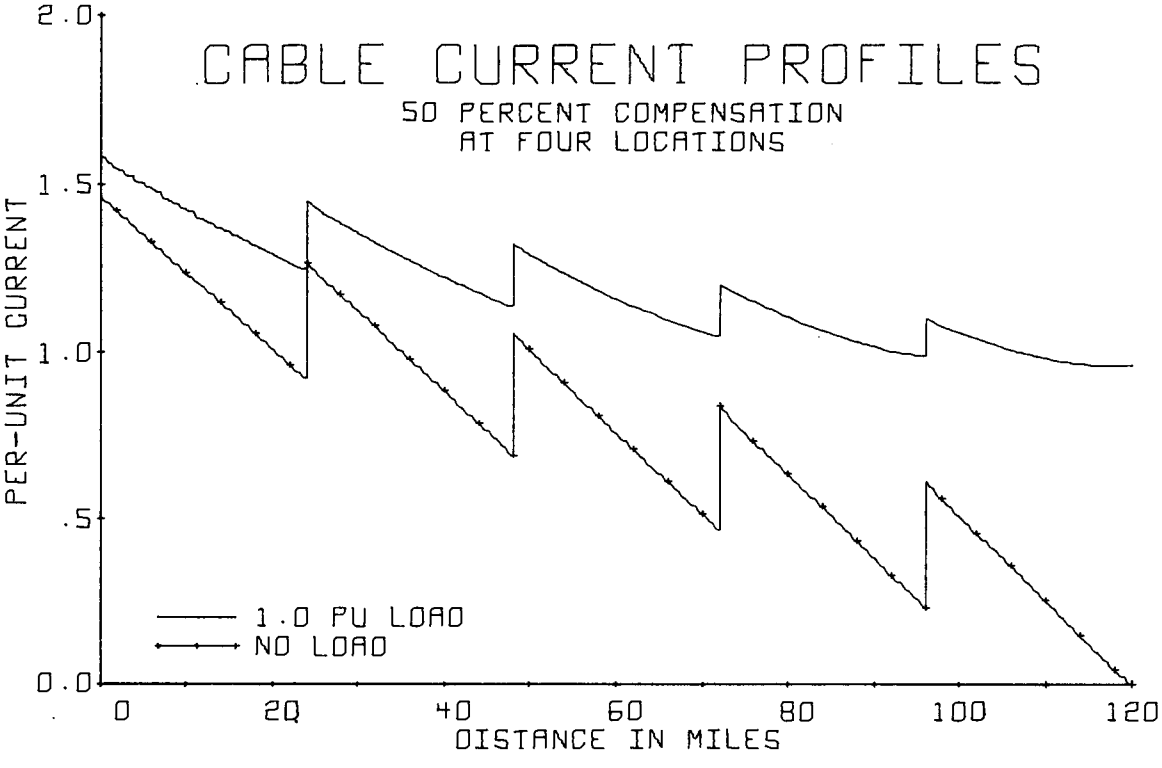

FIGURE 81. PER-UNIT CURRENT MAGNITUDES VERSUS DISTANCE FROM THE CABLE SENDING END FOR A UNITY PF LOAD.

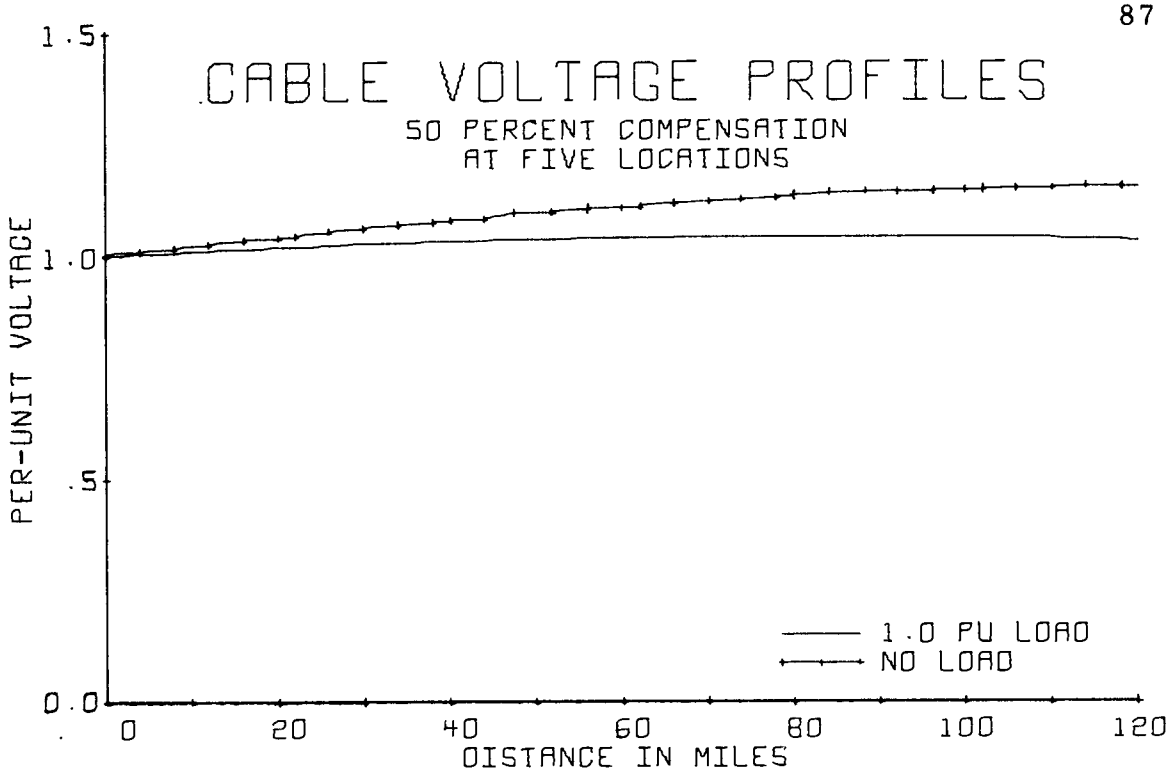

FIGURE 82. PER-UNIT VOLTAGE MAGNITUDES VERSUS DISTANCE FROM THE CABLE SENDING END FOR A UNITY PF LOAD.

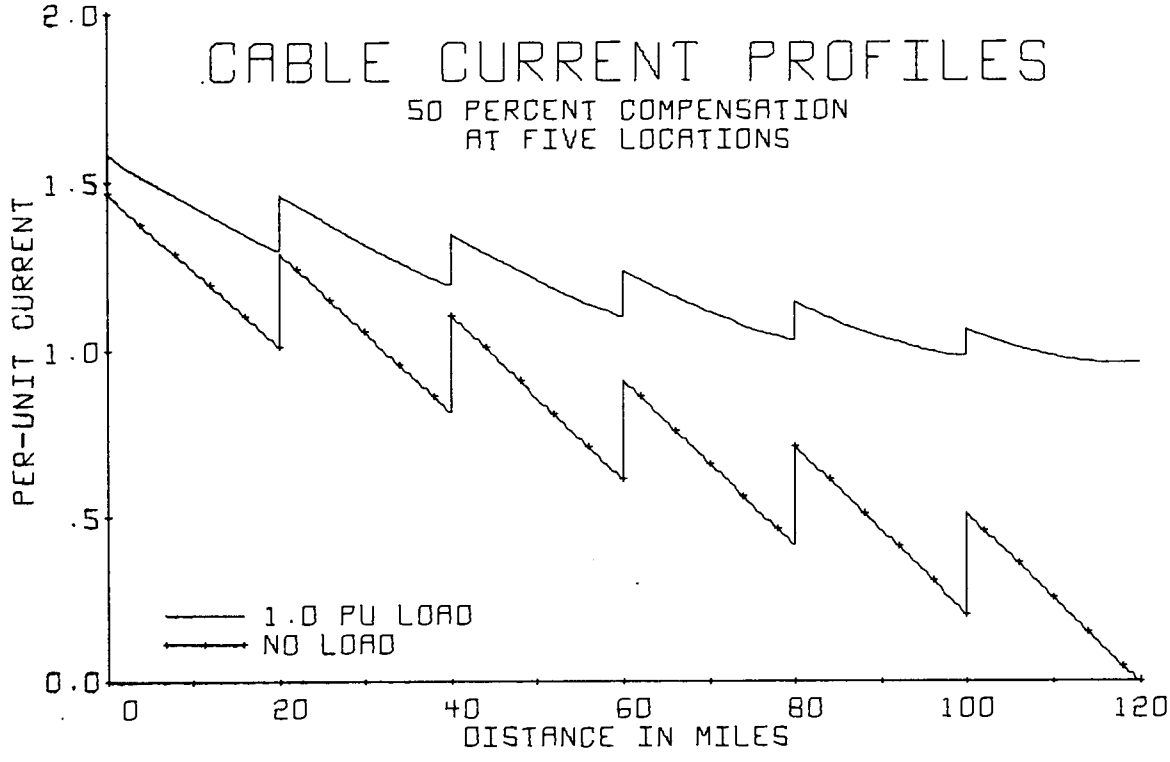

FIGURE 83. PER-UNIT CURRENT MAGNITUDES VERSUS DISTANCE FROM THE CABLE SENDING END FOR A UNITY PF LOAD.